Influence of Surgery on Musculoskeletal Mechanics in Children with Crouch Gait

By

Rachel L. Lenhart

A dissertation submitted in partial fulfillment of

the requirements for the degree of

Doctor of Philosophy

(Biomedical Engineering)

At the

UNIVERSITY OF WISCONSIN-MADISON

2015

Date of final oral examination: May 6, 2015

The dissertation is subject to approval by the following members of the Final Oral Committee:

Darryl G. Thelen, Professor, Mechanical Engineering

Matthew A. Halanski, Associate Professor, Orthopedics and Rehabilitation

Bryan Heiderscheit, Professor, Orthopedics and Rehabilitation

Ray Vanderby Jr, Professor, Biomedical Engineering

Scott Reeder, Professor, Radiology

Michael H. Schwartz, Associate Professor, Orthopedics, University of Minnesota

Robert Blank, Professor, Medicine, Medical College of Wisconsin

Dedication

I dedicate this thesis to my family, especially my mom, dad, and sister Abby, for their lifetime of support to me in all of my endeavors. I also dedicate this to Josh, who has shared in all of the day-to-day ups and downs these past seven years, and has provided constant love and encouragement.

Acknowledgements

The work in this thesis would not have been possible without the guidance and contributions of many others. First I would like to thank the members and alumni of the UW Neuromuscular Biomechanics Lab. I especially thank KneeMoS (Knee Modeling Subgroup) – particularly Colin Smith, Jarred Kaiser, and Mike Vignos. The discussions about my research were invaluable to its progression and success. Thanks to Colin with all of his help on the modeling work and Jarred for his help with everything MRI.

I also owe special thanks to those at the James R. Gage Center for Gait and Motion Analysis at Gillette Children's Specialty Healthcare. Your enthusiasm for treating children with gait disorders has been inspiring and has deepened my passion for the field. I particularly thank Mike Schwartz and Tom Novacheck for diving into this project with me, and giving me invaluable insights into my results. This project would have been much less fruitful if they had not regularly contributed their ideas and clinical expertise.

I would like to thank my committee – Bryan Heiderscheit, Ray Vanderby Jr., Robert Blank, Scott Reeder – for being involved with my research and their contributions to its direction and success.

I thank Matthew Halanski for being a continual clinical and research mentor. I've enjoyed all of our interactions, from time in the clinic to informal discussions of research ideas. You've been especially helpful as a sounding board for questions and concerns, both about research and life beyond graduate school.

I thank the members of the Motion Analysis Laboratory at Mayo Clinic, especially Kenton Kaufman and Melissa Morrow, for introducing me to gait analysis and sparking my interest in the field.

I also would like to thank the Medial Scientist Training Program at the University of Wisconsin-Madison, for their support as I travel along this journey to becoming a physician scientist. A special thanks to Deane Mosher for being a particular advocate for my passions and science.

Finally, I would like to thank my advisor, Darryl Thelen. I remember thinking after my interview with Darryl over seven years ago, that his was the lab I wanted to join, and I haven't once thought otherwise. Darryl has been a mentor to me in every sense of the word. He allowed me to explore and further my passions for clinical gait analysis and pediatric orthopedics. He has shared in my excitement for my project and its results. He has taught me techniques and skills that I hope to use in research for years to come. For all of this, I am supremely grateful.

Table of Contents

Introduction to the thesis

Cerebral palsy is the most common motor disability of childhood with approximately 1 in 323 affected (1). The disease arises due to a neurological lesion occurring before or during birth, or in infancy (2). This lesion is static, and the disease is non-progressive in its course (2-3). Cerebral palsy has a heterogeneous phenotype based on the extent of and where the lesion occurs (4-5). Spastic cerebral palsy usually is an injury to the cortex, and is the most common (5). This type is further broken down into categories that describe which limbs are involved (both legs = diplegia, one arm and leg = hemiplegia, both arms and legs = quadriplegia) (6). Besides spastic, the other types of cerebral palsy are dyskinetic (extrapyramidal system affected) and ataxic (lesion to the cerebellum) (5). While these subtypes are named distinctly, they can often present in the same patient (4). This thesis mostly deals with spastic cerebral palsy, but know that the other types can also be seen in children with spasticity.

The neurological lesion in cerebral palsy leads to motor abnormalities. In spastic cerebral palsy, motor abnormalities often arise due to spasticity and contractures of the muscles. Spasticity refers to increased velocity-dependent resistance to stretch (7), caused by decreased inhibitory signals from the brain leading to reduced ɣ-aminobutyric acid (GABA) in the spinal cord (8-9). The increased muscle activity and tone that results tends to affect the functional abilities of children with CP. Contractures refer to shortening of the muscle-tendon units, such that range of motion is reduced (10). The formation of these contractures can also lead to shortening of other tissues, such as nerves, blood vessels, and ligamentous structures like the posterior capsule (10-11). Contractures also limit functionality and tend to get worse as physical activity of the child declines (11).

Because of the problem with motor control and spasticity, many children with cerebral palsy develop abnormal walking patterns. Several common gait abnormalities have been described in cerebral palsy (6, 12-14). The one of the most common of those abnormalities is known as crouch gait (15). This walking pattern is characterized by excessive knee flexion during stance, but also tends to include hip

adduction, hip rotation, ankle dorsiflexion, and pes valgus (12, 14, 16-18). Other common abnormalities include true equinus (excessive ankle plantarflexion) and stiff knee gait among others (14). Crouch gait is the subject of this dissertation.

Crouch is incompletely understood. It is thought to be caused by a number of factors, including weak quadriceps, contracted hamstrings and/or psoas, lever-arm dysfunction, weak plantarflexors, and weak hip extensors (6, 12, 19-22). The crouched posture also reduces the ability of many muscles to generate extension (23), such that intrinsic weakness associated with cerebral palsy may contribute to its progression. Hence, crouch is also extremely fatiguing (24-25) with high levels of energy expenditure (often >3 times normal (26)), such that if untreated walking ability declines and is eventually lost (6, 11, 27). For this reason, surgical treatment is often sought to reverse this decline.

Crouch also has other associated issues, many of which involve the knee joint. Along with bony abnormalities and frequent anterior knee pain (28-29), patella alta is nearly a universal finding in those with crouch (28). Patella alta refers to an abnormally superior patellar position. It has long been speculated that this could contribute to lever-arm dysfunction, and hypothesized that alta should be corrected to help improve crouch gait (22). The correction of patella alta has also recently been motivated by findings that correlate patella alta with patellofemoral pain (30).

For many years, the human eye and then manually analyzed photography were the only ways we had to study cerebral palsy and the walking abnormalities that it caused. However, in the late 1970s and 1980s, computerized/automated 3D gait analysis was popularized as a way to better understand the abnormalities in CP, and to better characterize subtle differences that may arise in these children (31-32). Gait analysis has since been the gold standard and many labs around the country are focused on the clinical use of gait analysis for treatment planning and outcomes analysis of gait disorders in children with cerebral palsy.

While the use of gait analysis and patient case-studies remains a common way to study crouch and other gait abnormalities, other methods of analysis have arisen to help give more insights, both at the individual patient level, and on a larger more general scale. Full-body musculoskeletal modeling was popularized in the 1990s by Scott Delp and others through the creation of a computational framework for the simulation of movement (33), which later led to an open source version (OpenSim) now used by thousands of people around the world (34). Musculoskeletal modeling and simulation tools make it possible to examine quantities not directly measurable from gait analysis. It also allowed for predictive modeling allowing for simulating surgical procedures and determining sensitivity of certain parameters, such as musculoskeletal geometry, on functional measures, such as strength (19-20, 35-36). Other advances in imaging and big data have allowed for validation of models (37) and for more robust outcome prediction (38). Together, these modalities together have advanced our understanding of crouch gait and other gait abnormalities in cerebral palsy, as well as the surgical procedures used to treat them.

Treatment of crouch gait over the years has primarily focused on lengthening the hamstrings. Several specific methods exist, but the overarching goal is to overcome knee flexion contractures and allow the hamstrings to operate at a more normal length. There are several studies showing that hamstring lengthening can improve knee extension capacity, both passively and during gait (39-42). However, this procedure tends to have a high recurrence rate (22, 43-45). Further, musculoskeletal modeling tools have revealed that the hamstrings are not universally acting at shortened lengths in children with crouch gait (17, 46). Retrospective studies revealed that the length and velocity of the hamstrings were important discriminators of those patients who benefit from hamstring lengthening (46). The challenges of identifying appropriate candidates for hamstring lengthening and the high the recurrence rates have led many surgeons to seek other procedures to treat crouch gait.

More recently the distal femoral extension osteotomy and patellar tendon advancement (DFEO+PTA) has been re-introduced as a technique to treat crouch gait. The procedure was originally put forth in the early 1900s, but was abandoned in the 1960s, likely due to complications and difficulty

with the procedure (26). In the 2000s, this procedure was readopted and perfected by a group of surgeons at Gillette Children's Specialty Healthcare. In 2008/2009, the group published the procedure (47) as well as their initial outcomes (26). The procedure is a combination of two techniques. The distal femoral extension osteotomy (DFEO) is used to correct for static knee flexion contractures by creating an extension deformity of the distal femur. Patellar tendon advancement (PTA) is used to correct quadriceps insufficiency and tighten the quadriceps mechanism. In the process, it relocates the superiorly displaced patella by distalizing the patellar tendon insertion.

Much enthusiasm has surrounded this technique, because it seems to have better, more consistent short and medium term outcomes than traditional crouch correction procedures (e.g. hamstring lengthening) (26, 40, 43, 48). One year outcomes show improvement in knee flexion profile and overall normalcy of gait, moreso than either procedure alone (26). Additionally, patients also benefit from increased quadriceps strength and active knee extension capabilities (26). Because of these advantages, surgeons worldwide are beginning to adopt this technique.

Despite these observed benefits, concerns remain. Complication rates continue to be relatively high (~20%) (49), a subset of patients exhibit little to no improvement in knee flexion in gait, and some gait parameters (e.g. pelvic tilt) tend to worsen after surgery (26). Further, the long-term implications aren't well understood. For example, the PTA procedure tends to move the superiorly displaced patella into baja (26), a position that is more inferior that of typically developing children. Longitudinal data indicates that this position may continue to migrate distally with continued growth of the patient (50). Further, substantial changes in tibial slope have been observed at one year follow-up (51), raising questions about the impact of DFEO on skeletal growth and cartilage health. The radical alteration in the posture and load distribution on the tibial plateau is theorized to underlie this change. However, cartilage contact patterns and magnitudes in the treated and untreated knees of crouch patients have never been explored. There is continuing discussion on the appropriate technique for performing patellar tendon advancement. While Gillette prefers to advance the tendon insertion (47), other groups may shorten the

patellar tendon or imbricate it (51-53). Finally, the need for simultaneous procedures remains in question. Procedures are recommended (e.g. rectus femoris transfer (47)) or discouraged (e.g. hamstrings lengthening (54)) without appropriate scientific evidence regarding their impact. These problems highlight a need to further study the biomechanical consequences of DFEO+PTA to better understand the tradeoffs that the surgery represents and to attempt to optimize surgical parameters.

In this thesis, the overarching goal is to better understand crouch gait and patella alta, as well as the effects of DFEO+PTA on knee mechanics. In the first chapter, I will discuss the creation and validation of a novel 12 degree of freedom knee model used to better explore load-dependent kinematics that occur in many activities including gait. In the second chapter, I use this model to study the effect of patellar position on the patellar tendon moment arm and quadriceps forces during gait. I will also discuss what ramifications this has for crouch gait and PTA. Third, I'll discuss the impact of patellar position and crouch on tibiofemoral and patellofemoral pressures. The fourth chapter will detail the modeling of the DFEO, exploring the sensitivity of wedge angle to the change in muscles lengths. The next chapter will outline initial work using dynamic MRI to validate the modeling results. The final chapter will discuss the creation of a statistical model to predict which patients do well after DFEO+PTA. It will also explore whether the predictors created from one clinical database can be applied to another. The concluding section will summarize conclusions from all of the work, and discuss my future research plans.

References

1. Centers for Disease Control. Data and Statistics for Cerebral Palsy. Atlanta; 2012 [updated 2012 December 27, 2013; cited 2014 October 24]; Available from: http://www.cdc.gov/ncbddd/cp/data.html.

2. Rosenbaum P, Paneth N, Leviton A, Goldstein M, Bax M, Damiano D, et al. A report: the definition and classification of cerebral palsy April 2006. Dev Med Child Neurol Suppl. 2007;109(suppl 109):8-14.

3. Miller F. Cerebral Palsy. 1 ed. New York: Springer-Verlag; 2005.

4. Chan G, Miller F. Assessment and Treatment of Children with Cerebral Palsy. Orthopedic Clinics of North America. 2014;45(3):313-25.

5. Jones MW, Morgan E, Shelton JE, Thorogood C. Cerebral palsy: introduction and diagnosis (part I). Journal of Pediatric Health Care. 2007;21(3):146-52.

6. Gage J, Schwartz M, Koop S, Novacheck T. The Identification and Treatment of Gait Problems in Cerebral Palsy. 2 ed: John Wiley and Sons; 2009.

7. Young RR. Spasticity: a review. Neurology. 1994;44(11 Suppl 9):S12-20.

8. Albright AL. Spastic cerebral palsy. CNS drugs. 1995;4(1):17-27.

9. Selzer M, Clarke S, Cohen L, Duncan P, Gage F. Textbook of Neural Repair and Rehabilitation: Volume 2, Medical Neurorehabilitation: Cambridge University Press; 2006.

10. Elovic E, Brashear A. Spasticity: Diagnosis and Management: Demos Medical Publishing; 2010.

11. Flynn JM, Weisel SW. Operative Techniques in Pediatric Orthopaedics: LWW; 2010.

12. Sutherland DH, Davids JR. Common gait abnormalities of the knee in cerebral palsy. Clinical Orthopaedics and Related Research. 1993(288):139-47.

13. Davids JR, Bagley AM. Identification of common gait disruption patterns in children with cerebral palsy. Journal of the American Academy of Orthopaedic Surgeons. 2014;22(12):782-90.

14. Rodda J, Graham H. Classification of gait patterns in spastic hemiplegia and spastic diplegia: a basis for a management algorithm. European Journal of Neurology. 2001;8(s5):98-108.

15. Wren TAL, Rethlefsen S, Kay RM. Prevalence of specific gait abnormalities in children with cerebral palsy: influence of cerebral palsy subtype, age, and previous surgery. Journal of Pediatric Orthopaedics. 2005;25(1):79.

16. Steinwender G, Saraph V, Bernhard Zwick E, Steinwender C, Linhart W. Hip locomotion mechanisms in cerebral palsy crouch gait. Gait & Posture. 2001;13(2):78-85.

17. Delp SL, Arnold AS, Speers RA, Moore CA. Hamstrings and psoas lengths during normal and crouch gait: Implications for muscle-tendon surgery. Journal of Orthopaedic Research. 1996;14(1):144-51.

18. Novacheck TF, Gage JR. Orthopedic management of spasticity in cerebral palsy. Child's Nervous System. 2007;23(9):1015-31.

19. Hicks J, Arnold A, Anderson F, Schwartz M, Delp S. The effect of excessive tibial torsion on the capacity of muscles to extend the hip and knee during single-limb stance. Gait & Posture. 2007;26(4):546-52.

20. Schwartz M, Lakin G. The effect of tibial torsion on the dynamic function of the soleus during gait. Gait & Posture. 2003;17(2):113-8.

21. Arnold AS, Anderson FC, Pandy MG, Delp SL. Muscular contributions to hip and knee extension during the single limb stance phase of normal gait: a framework for investigating the causes of crouch gait. Journal of biomechanics. 2005;38(11):2181-9.

22. Lotman DB. Knee flexion deformity and patella alta in spastic cerebral palsy. Developmental Medicine & Child Neurology. 1976;18(3):315-9.

23. Hicks JL, Schwartz MH, Arnold AS, Delp SL. Crouched postures reduce the capacity of muscles to extend the hip and knee during the single-limb stance phase of gait. Journal of Biomechanics. 2008;41(5):960-7.

24. Winter DA. Knee flexion during stance as a determinant of inefficient walking. Physical Therapy. 1983;63(3):331-3.

25. Waters RL, Mulroy S. The energy expenditure of normal and pathologic gait. Gait & Posture. 1999;9(3):207-31.

26. Stout JL, Gage JR, Schwartz MH, Novacheck TF. Distal femoral extension osteotomy and patellar tendon advancement to treat persistent crouch gait in cerebral palsy. The Journal of Bone and Joint Surgery (American). 2008;90(11):2470-84.

27. Bell KJ, Ounpuu S, DeLuca PA, Romness MJ. Natural progression of gait in children with cerebral palsy. Journal of Pediatric Orthopaedics. 2002;22(5):677-82.

28. Topoleski TA, Kurtz CA, Grogan DP. Radiographic abnormalities and clinical symptoms associated with patella alta in ambulatory children with cerebral palsy. Journal of Pediatric Orthopaedics. 2000;20(5):636.

29. Senaran H, Holden C, Dabney KW, Miller F. Anterior knee pain in children with cerebral palsy. Journal of Pediatric Orthopaedics. 2007;27(1):12-6.

30. Sheehan FT, Babushkina A, Alter KE. Kinematic Determinants Of Anterior Knee Pain In Cerebral Palsy, A Case-Control Study. Archives of Physical Medicine and Rehabilitation. 2012;93(8):1431-40.

31. Sutherland DH. The evolution of clinical gait analysis: Part II Kinematics. Gait & Posture. 2002;16(2):159-79.

32. Whittle MW. Clinical gait analysis: A review. Human Movement Science. 1996;15(3):369-87.

33. Delp SL, Loan JP. A computational framework for simulating and analyzing human and animal movement. Computing in Science & Engineering. 2000;2(5):46-55.

34. Delp SL, Anderson FC, Arnold AS, Loan P, Habib A, John CT, et al. OpenSim: open-source software to create and analyze dynamic simulations of movement. IEEE Transactions on Biomedical Engineering. 2007;54(11):1940-50.

35. Arnold AS, Delp SL. Rotational moment arms of the medial hamstrings and adductors vary with femoral geometry and limb position: implications for the treatment of internally rotated gait. Journal of biomechanics. 2001;34(4):437-47.

36. Delp SL, Statler K, Carroll NC. Preserving plantar flexion strength after surgical treatment for contracture of the triceps surae: a computer simulation study. Journal of orthopaedic research. 1995;13(1):96-104.

37. Arnold AS, Salinas S, Asakawa DJ, Delp SL. Accuracy of muscle moment arms estimated from MRI-based musculoskeletal models of the lower extremity. Computer Aided Surgery. 2000;5(2):108-19.

38. Schwartz MH, Rozumalski A, Truong W, Novacheck TF. Predicting the outcome of intramuscular psoas lengthening in children with cerebral palsy using preoperative gait data and the random forest algorithm. Gait & Posture. 2012.

39. Chang WN, Tsirikos AI, Miller F, Lennon N, Schuyler J, Kerstetter L, et al. Distal hamstring lengthening in ambulatory children with cerebral palsy: primary versus revision procedures. Gait & Posture. 2004;19(3):298-304.

40. Kay RM, Rethlefsen SA, Skaggs D, Leet A. Outcome of medial versus combined medial and lateral hamstring lengthening surgery in cerebral palsy. Journal of Pediatric Orthopaedics. 2002;22(2):169-72.

41. Baumann J, Ruetsch H, Schürmann K. Distal hamstring lengthening in cerebral palsy. International orthopaedics. 1980;3(4):305-9.

42. Park MS, Chung CY, Lee SH, Choi IH, Cho T-J, Yoo WJ, et al. Effects of distal hamstring lengthening on sagittal motion in patients with diplegia: hamstring length and its clinical use. Gait & Posture. 2009;30(4):487-91.

43. Rethlefsen SA, Yasmeh S, Wren TA, Kay RM. Repeat hamstring lengthening for crouch gait in children with cerebral palsy. Journal of Pediatric Orthopaedics. 2013;33(5):501-4.

44. Dhawlikar S, Root L, Mann R. Distal lengthening of the hamstrings in patients who have cerebral palsy. Long-term retrospective analysis. The Journal of Bone and Joint Surgery (American). 1992;74(9):1385-91.

45. Dreher T, Vegvari D, Wolf SI, Geisbüsch A, Gantz S, Wenz W, et al. Development of knee function after hamstring lengthening as a part of multilevel surgery in children with spastic diplegia. The Journal of Bone & Joint Surgery. 2012;94(2):121-30.

46. Arnold AS, Liu MQ, Schwartz MH, Ounpuu S, Delp SL. The role of estimating muscle-tendon lengths and velocities of the hamstrings in the evaluation and treatment of crouch gait. Gait & Posture. 2006;23(3):273-81.

47. Novacheck TF, Stout JL, Gage JR, Schwartz MH. Distal Femoral Extension Osteotomy and Patellar Tendon Advancement to Treat Persistent Crouch Gait in Cerebral Palsy: Surgical Technique. The Journal of Bone and Joint Surgery (American). 2009;91-A(Supplement 2):271-86.

48. Das S, Pradhan S, Ganesh S, Sahu P, Mohanty R, Das S. Supracondylar femoral extension osteotomy and patellar tendon advancement in the management of persistent crouch gait in cerebral palsy Indian Journal of Orthopedics. 2012;46(2):221-8.

49. Novacheck T, Stout J, Gage J. Distal Femoral Extension Osteotomy and Patellar Tendon Advancement in the Treatment of Crouch Gait: A Review of Complications. Proceedings of the Gait and Clinical Movement Analysis Society Annual Conference. 2011.

50. Novacheck TF, Varghese RA, Stout JL, Schwartz MH. Does Patellar Position Change with Subsequent Growth after Patellar Tendon Advancement in Children with Cerebral Palsy? Proceedings of the Gait and Clinical Movement Analysis Society; Grand Rapids, MI2012.

51. Patthanacharoenphon C, Maples D, Saad C, Forness M, Halanski M. The Effects of Patellar Tendon Advancement on the Proximal Tibia. Journal of Children's Orthopaedics. 2013;7(2):139-46.

52. Joseph B, Reddy K, Varghese RA, Shah H, Doddabasappa SN. Management of severe crouch gait in children and adolescents with cerebral palsy. Journal of Pediatric Orthopaedics. 2010;30(8):832-9.

53. Roberts W, Adams JP. The patellar-advancement operation in cerebral palsy. The Journal of Bone & Joint Surgery. 1953;35(4):958-79.

54. Healy M, Schwartz M, Stout J, Gage J, Novacheck T. Is simultaneous hamstring lengthening necessary when performing distal femoral extension osteotomy and patellar tendon advancement? Gait and Posture. 2011;33(1):1-5.

Chapter 1

Prediction and validation of load-dependent behavior of the tibiofemoral and patellofemoral joints during movement

Rachel L. Lenhart, Jarred Kaiser, Colin R. Smith, Darryl G. Thelen

(Note that this chapter is currently in press in the Annals of Biomedical Engineering)

Abstract

The study objective was to construct and validate a subject-specific knee model that can simulate full six degree-of-freedom tibiofemoral and patellofemoral joint behavior in the context of full body movement. Segmented MR images were used to reconstruct the geometry of 14 ligament bundles and articular cartilage surfaces. The knee was incorporated into a lower extremity musculoskeletal model, which was then used to simulate laxity tests, passive knee flexion, active knee flexion, and human walking. Simulated passive and active knee kinematics were shown to be consistent with subject-specific measures obtained via dynamic MRI. Anterior tibial translation and internal tibial rotation exhibited the greatest variability when uncertainties in ligament properties were considered. When used to simulate walking, the model predicted knee kinematic patterns that differed substantially from passive joint behavior. Predictions of knee cartilage contact pressures during normal gait reached 6.2 and 2.8 MPa on the medial tibial plateau and patellar facets, respectively. Thus, the dynamic modeling framework can be used to simulate the interaction of soft tissue loads and cartilage contact during locomotion activities, and therefore provides a basis to simulate the effects of soft tissue injury and surgical treatment on functional knee mechanics.

Key Terms: knee mechanics; gait; computational biomechanics; elastic foundation model

Introduction

Dynamic musculoskeletal models provide a consistent framework to simulate soft tissue loads and joint kinematics in locomotor activities. For example, prior studies have used dynamic simulations to investigate muscular contributions to tibiofemoral loads in walking,[47] and the influence of quadriceps

coordination on patellofemoral joint force in running.[38] However, most current gait models use a highly simplified representation of the knee. Specifically, the knee is often represented as a one degree of freedom joint, in which patellofemoral kinematics and secondary tibiofemoral kinematics are constrained functions of knee flexion.[4, 16] There are two fundamental limitations with this approach. First, a one degree-of-freedom knee joint does not provide estimates of the ligament and cartilage loading patterns that act to constrain secondary joint motion. Second, joint motion constraints are often assumed based on the passive behavior of cadaveric joints,[4, 16, 49-50, 52] which intrinsically ignores load-dependent variations in joint kinematics.[9, 18, 26, 30, 33, 51] Loading effects are likely very relevant during locomotion activities, where secondary tibiofemoral kinematics vary substantially over the gait cycle.[18, 30]

Anatomically detailed knee models have been introduced that allow for full six degree of freedom (DOF) kinematics at the tibiofemoral and patellofemoral joints. Finite element (FE) formulations are attractive since they provide for estimates of internal tissue stresses and strains.[17] However, FE models remain computationally challenging to solve within the context of a multibody simulation of gait.[24] Dynamic multi-body knee models provide a viable alternative for simulating gait, where elastic ligament bundles can capture overall joint laxity[11, 44-45, 48] and elastic foundation models can provide estimates of cartilage contact pressure that are comparable to FE predictions.[25] However, computing coordinated muscle actions needed to control six DOF joints remains challenging. We recently introduced a modified computed muscle control (CMC) algorithm that can modulate muscle excitations to track knee flexion, while secondary knee motions evolve naturally due to muscle, ligament, cartilage contact, and external loading.[48] While we have shown that the modified CMC framework can accurately simulate tibiofemoral contact loads in a total knee replacement,[48] the capacity to simulate natural knee behavior has not yet been demonstrated.

The purpose of this study was to develop and validate a subject-specific, multi-body knee model that allows for 6 DOF motion at both the tibiofemoral and patellofemoral joints. We first used high resolution magnetic resonance (MR) images to create a knee model that included ligamentous constraints and articular cartilage contact. We then compared model predictions of tibiofemoral and patellofemoral

kinematics with dynamic MRI measures obtained under passive and active loading conditions.[3, 28] Probabilistic simulations were performed to assess the propagation of uncertain ligament properties onto knee kinematics. Finally, we used the model to simulate secondary knee kinematics in walking, and compared the results to those obtained via conventional gait models.

Materials and Methods

Participant Information:

MR imaging and gait analysis were performed on a 23 year old female subject (height=1.65 m, mass=61 kg) with no history of chronic knee pain, injury, or surgery. The study was approved by the University of Wisconsin-Madison's Health Sciences Institutional Review Board, and appropriate written informed consent was obtained prior to testing.

MR Imaging:

The subject underwent a MR examination in a clinical 3.0-T MR scanner (MR750, General Electric Healthcare, Waukesha, WI). An eight-channel phased-array extremity coil (Precision Eight TX/pulse repetition time (TR) High Resolution Knee Array; Invivo, Orlando, FL) was positioned about her dominant (right) knee in an extended posture. Two high-resolution static scans were performed, which included a 3D IDEAL[19] spoiled gradient-echo (SPGR) sequence (256 x 256 x 108 cubic voxels with 0.78 mm spacing) and a fast-spin echo (FSE) cube sequence (512 x 512 x 392 cubic voxels with 0.30 mm spacing).

We manually segmented (MIMICS, Materialise Group, Leuven, Belgium) the bone geometries from the static IDEAL-SPGR images, and the articular cartilage surfaces and knee ligaments from the FSE Cube images. Bone geometries were smoothed (<0.1 mm average deviation from original, unsmoothed model) and decimated to 7000 triangles for the femur and tibia and to 2000 triangles for the patella (Geomagic, Research Triangle Park, NC). Cartilage surface geometries were likewise smoothed (<0.02 mm average deviation from original, unsmoothed model) and decimated to 4000, 2000, and 2000 triangles for the femoral, tibial, and patellar cartilages, respectively.

Anatomical reference frame orientations were established for each bone using a automatic algorithm based on geometric and inertial properties of the 3D segments.[37, 41] The medial-lateral axis of femur was aligned with the centerline of a best-fit cylinder to the condyles and the superior-inferior axis is based off the smallest inertial axis of the diaphysis. The tibial axes were defined as the first, second, and third inertial axes of the plateaus. The anterior-posterior axis of the patella was defined as the principal axis corresponding with the smallest mass moment of inertia. The superior-inferior axis was aligned with the median ridge. The origins of the femoral and tibial reference frames were both placed at the center of the best-fit cylinder of the femoral condyles. The origin of the patellar reference frame was placed at the center of mass.

The subject was next positioned supine on a MR-compatible loading device[46] with her dominant knee centered in a 16-channel flex coil (GEM Flex, NeoCoil, Pewaukee, WI) coil. The knee was cyclically flexed and extended under three conditions: voluntary motion against an inertial load which induced quadriceps loading with the knee flexed,[28, 51] voluntary motion against an elastic load which induced quadriceps loading with the knee extended,[51] and a passive case in which a researcher cyclically flexed the subject's relaxed leg. Inertial loading was applied via rotating disks and elastic loading was applied via a torsion spring as described in Westphal et al.[51] Knee range of motion was limited by the MRI bore size (60 cm diameter), ranging from 36 deg in the passive task to 45 deg in the active tasks. Cyclic task rates (0.5 Hz) were maintained via an audible metronome, with repeatability enhanced by

having the subjects practice the tasks prior to the MR examination. A dynamic SPGR sequence in conjunction with vastly-undersampled isotropic projections (SPGR-VIPR, 160 x 160 x 160 cubic voxels with 1.5 mm spacing, 75,000 unique lines, 5 min scan time) was used to continuously acquire volumetric image data over 150 motion cycles of each motion task.[28]

The dynamic images were used to track tibiofemoral and patellofemoral kinematics using methods that have been described previously.[28] Briefly, an encoder measurement of knee angle was used to retrospectively sort SPGR-VIPR projections into 60 bins over the motion cycle. Sorted projections were used to reconstruct 60 volumetric image sets. Femur, tibia, and patella bone model geometries were then registered to each image set using numerical optimization.[40] This resulted in 3D trajectories of the translations and rotation angles for the femur, tibia, and patella over the motion cycle, which were subsequently low-pass filtered (5 Hz cutoff frequency). Tibiofemoral kinematics were described by three translations and three successive body-fixed rotations (flexion, adduction, and internal rotation) of the tibia relative to the femur.[22] Similarly, patellofemoral orientation was defined by successive body-fixed rotations consisting of flexion, lateral rotation, and medial tilt of the patella relative to the femur.

Knee Model:

Twelve ligament volumes were segmented from the FSE Cube images: superficial and deep medial collateral ligament (sMCL, dMCL), lateral collateral ligament (LCL), anteriomedial and posteriolateral anterior cruciate ligament (aACL, pACL), anteriolateral and posteriomedial posterior cruciate ligament (aPCL, pPCL), patellar tendon (PT), medial and lateral patellofemoral ligaments (MPFL, LPFL), popliteofibular ligament (PFL), posteriomedial capsule (pmCAP), the posterior capsule (CAP), and the iliotibial band (ITB). Ligaments were smoothed and centerlines were calculated using the MIMICS Medcad module. Each ligament was represented by a bundle of nonlinear springs spanning from the ligament origin footprint to its insertion footprint. Wrap objects were defined for the medial collateral ligament, posterior capsule, and patellar tendon so that they wrapped appropriately around the tibia, femur, and patella respectively.

Each ligament bundle was represented by a discrete number of strands. Tensile forces were computed assuming each strand behaved as a nonlinear stiffening spring at low strains ($\varepsilon<0.06$), and having a linear stiffness at higher strains.[10] The linear stiffness of each ligament were estimated as the product of the average ligament cross-sectional area and an assumed ligament elastic modulus of 125 MPa.[13] Ligament cross-sectional areas for the MPFL, LPFL, PFL, ITB, pmCAP, and CAP could not be well estimated from the images, such that the values for cross-sectional area or stiffness were adapted from other modeling and cadaveric studies.[1, 6, 27, 36, 39, 43, 48] Ligament stiffness was equally portioned to all strands included in the bundle. The reference strains of each ligament strand in an extended knee posture were adapted from the literature.[43, 45, 48] See Appendix A for ligament properties used in this model.

Tibiofemoral and patellofemoral cartilage contact pressures were computed using an elastic foundation model in which pressure is assumed to be a function of the depth of penetration between contacting cartilage surfaces. Regions of cartilage contact were determined at each time step using ray-casting techniques together with hierarchical bounding boxes.[48] At each triangle of the tibia plateau, the contact pressure was computed using a nonlinear elastic foundation formulation,[8] with cartilage assumed to have an elastic modulus of 5 MPa,[10, 12] a Poisson's ratio of 0.45,[5, 10, 12] and a uniform cartilage thickness of 3 mm over each surface (i.e. 6 mm total thickness).[42]

The knee model was incorporated into a generic lower extremity musculoskeletal model with a 6 DOF pelvis, a three DOF ball-in-socket representation of the hip, and a one DOF ankle allowing for dorsi/plantarflexion (Fig. 1).[4] The model included 44 musculotendon units acting about the right hip, knee and ankle. To incorporate the knee model, the femoral skeletal and cartilage geometries were positioned to closely align with the femoral geometry in the generic lower extremity model. Tibial and patellar geometries were then positioned to just contact the femoral surfaces in an upright posture. The full model was implemented in SIMM,[15] with the Dynamics Pipeline (Musculographics Inc., Santa Rosa, CA) and SD/Fast (Parametric Technology Corp., Needham, MA) used to generate code describing muscle-tendon dynamics and the multibody equations of motion.

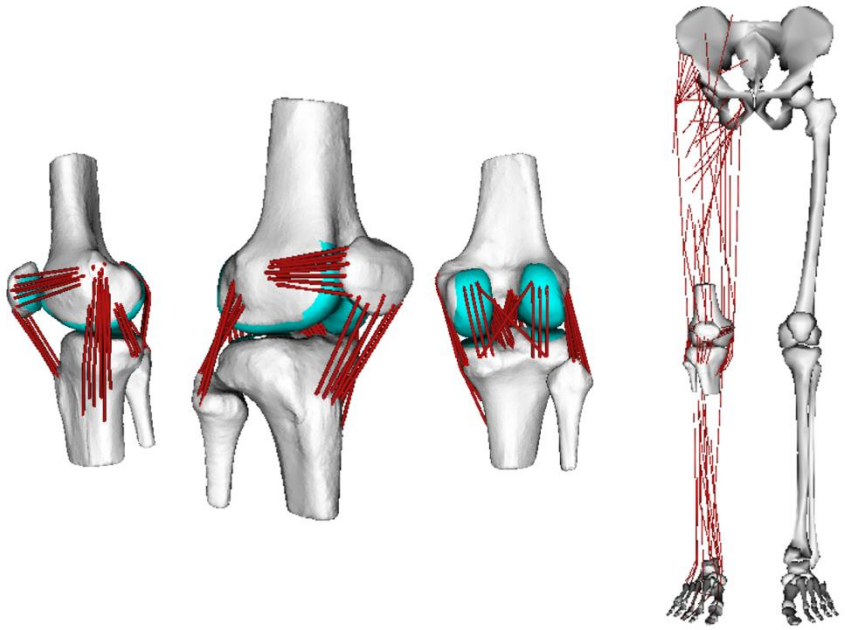

Figure 1: (Left) Ligament, skeletal and cartilage geometries were reconstructed from segmented MR images. The 12 degree of freedom knee model included 14 ligament bundles (76 elements) acting across the tibiofemoral and patellofemoral joints. (Right) The knee model was included into a generic lower extremity musculoskeletal model[4] for simulating functional movement.

Dynamic Simulations:

As a first assessment of veracity of the model, we simulated laxity tests and compared the resulting knee kinematics to those measured in cadaveric studies.[2, 20-21, 35] In these tests, the femur was fixed and muscle activations were set to 0. Anterior-posterior (A-P) laxity was assessed by applying a +/- 100 N force on the tibia at a position 10 cm inferior to the tibial reference frame origin. Forward dynamics was used to simulate the resulting tibial and patellar motion. Rotational laxity was assessed by applying a +/- 5 Nm torque about the long axis of the tibia and using dynamic simulation to predict the resulting tibiofemoral rotations. Both A-P and rotational laxity was assessed at 10 degree increments of knee flexion between 0 and 90 degrees.

Simulations were then performed to compare model predictions against the *in vivo* tibiofemoral and patellofemoral kinematic measured from the dynamic MRI experiments. For these simulations, we emulated the dynamic MRI setup by prescribing posterior pelvic tilt to 90 degrees and hip flexion to 20 deg. The passive knee flexion task was then simulated by setting muscle activations to a low level (activation a=0.01) and prescribing knee flexion to cycle between 0 and 50 deg of knee flexion at 0.5 Hz. The active loading cases were simulated by using a modified computed muscle control algorithm[48] to compute muscle excitations needed to drive cyclic knee flexion against simulated inertial and elastic loads applied to the tibia. Applied tibia load magnitudes were set such that peak knee extensor moments of 30 Nm were generated, as was measured previously in the comparison dynamic MRI experiments.[51] Ankle plantarflexion was also actively controlled to track a fixed value of 20 degrees. The resulting tibiofemoral and patellofemoral kinematics were compared to both subject-specific and population[51] measures obtained with dynamic MRI.

We performed Monte Carlo simulations (n=2000) to evaluate the effects of uncertainty in ligament stiffness and reference strains on passive knee kinematics. For each simulation, ligament stiffness and reference strains were selected from a normal distribution with mean value set to the nominal model value. The standard deviation chosen for reference strain was 0.02 and for stiffness was 30% of the nominal ligament stiffness.[7] Perturbations to reference strain and stiffness were independently assigned for each ligament bundle, but all strands within a bundle were prescribed the same parametric variations.

The subject underwent gait analysis during overground walking at a preferred speed. Whole body kinematics were recorded using an eight-camera, passive motion capture system (Motion Analysis, Santa Rosa, CA) to track 44 retroreflective markers, which included 25 markers on anatomical landmarks and 14 markers on rigid plates attached to the thigh and shank segments. The lower extremity model was scaled to the subject based on segment lengths determined in a standing upright posture. Pelvis, thigh, and shank reference frames were set using anatomical markers placed over the anterior superior iliac spine, posterior superior iliac spine, and the medial and lateral epicondyles and malleoli. A functional calibration

routine was used to determine hip joint centers in the pelvis reference frame.[31] During walking, marker kinematics were collected at 100 Hz and then low-pass filtered at 12 Hz. Ground reaction forces were simultaneously collected at 2000 Hz (forceplate model BP400600, AMTI, Watertown, MA) and then low-pass filtered at 50 Hz.

A global optimization inverse kinematics routine determined pelvis translations, pelvis rotations, hip angles, knee flexion and ankle dorsiflexion that best agreed with marker positions measured during gait.[34] At this stage, secondary tibiofemoral and all patellofemoral DOF were assumed to be a constrained function of knee flexion, with these functions based on our simulated passive knee behavior.[4] We then used a modified CMC algorithm to compute muscle excitations that drove the dynamic multi-body model to track measured hip kinematics, knee flexion and ankle dorsiflexion trajectories over a gait cycle.[48] The pelvis coordinates were prescribed to reproduce measured values, and measured ground reaction forces were applied directly to the feet. It should be explicitly noted that only knee flexion was tracked in the gait simulation, with all other tibiofemoral and patellofemoral DOFs being allowed to evolve as a function of muscle and ligament forces and cartilage contact. We then compared simulated tibiofemoral and patellofemoral kinematics during gait to our passive knee joint behavior to better understand the importance of load-dependent effects.

Results

Knee Laxity:

The nominal model-predicted patterns of translational and rotational laxity were consistent with measures obtained on cadaveric specimens (Fig. 2). A 100 N anterior force induced tibial translations of 1-7 mm with a peak at 30 deg knee flexion, while a 100 N posterior force induced translations of 1-7 mm with a peak at 10 deg knee flexion. A 5 Nm internal rotation moment induced internal tibial rotation angles ranging from 10-22 deg across the 90 deg of knee flexion considered, while external rotation moments induced rotations of 9-18 deg.

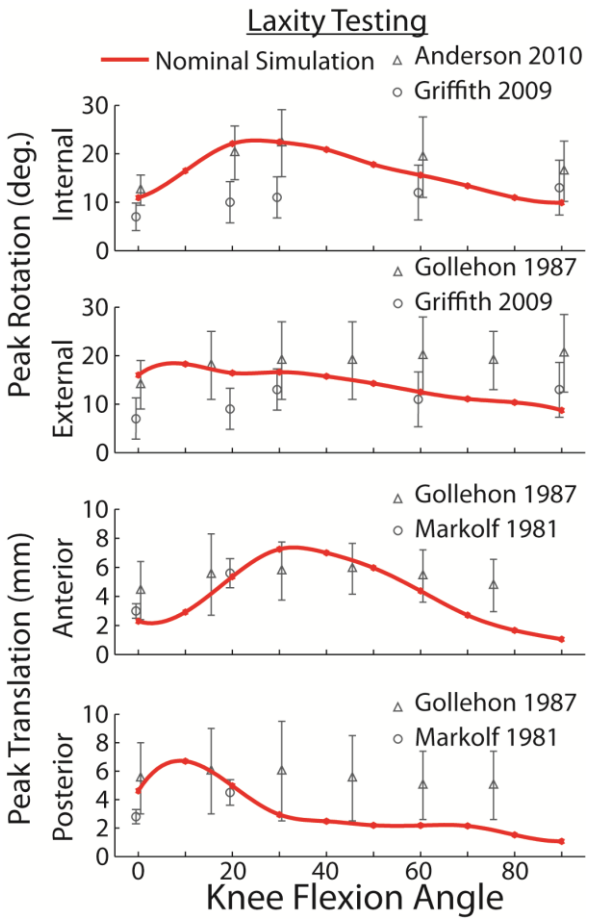

Figure 2**:** The passive knee model exhibited anterior-posterior translational laxity and internal-external rotation laxity that was consistent with prior cadaveric studies (symbols = mean, error bars = one standard deviation).[2, 20-21, 35]

Passive Knee Flexion-Extension:

Dynamic MRI measurements of tibiofemoral and patellofemoral kinematics in the passive flexion-extension tasks were consistent with model predictions, generally falling within the simulated uncertainty range (Fig. 3). One exception was patellofemoral tilt, with the model predicting a small amount of medial tilt (1.8 deg on average) with tibiofemoral flexion, while the MRI results showed approximately 3.0 deg of lateral tilt. In addition, anterior patellar translation was slightly underpredicted relative to MRI measures. The nominal model did exhibit some kinematic hysteresis, with the kinematics

being predicted during flexion and extension being slightly disparate for anterior tibial translation, internal tibial rotation and patellar flexion. Tibiofemoral translations, internal tibial rotation, superior patellar translation, and patellar flexion exhibited the greatest sensitivity to ligament properties. For example, one standard deviation in internal tibiofemoral rotation ranged from 1.5 to 5.8 degrees over the knee flexion range of motion, while adduction varied only 0.6 to 1.1 degrees.

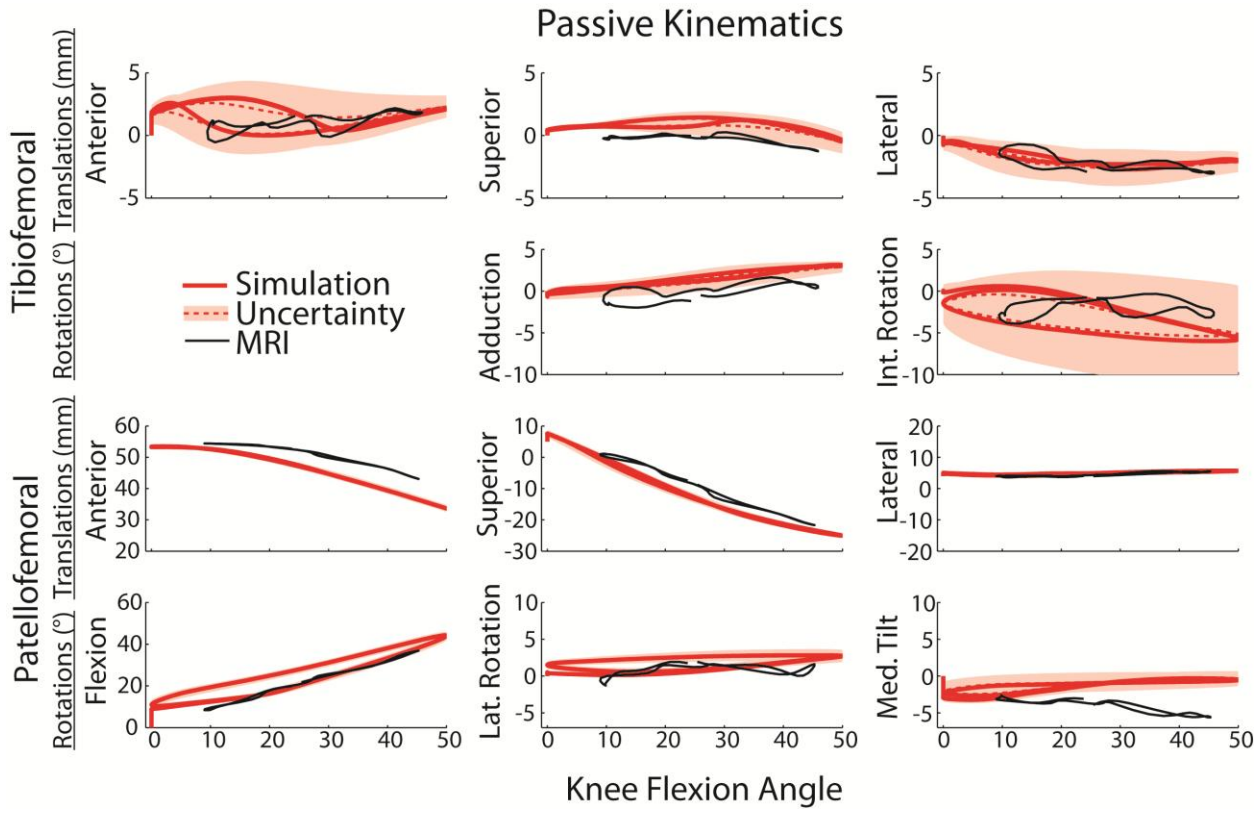

Figure 3: Forward dynamic simulations of passive knee flexion-extension (solid red line) compared with subject-specific dynamic MRI measurements (solid black line). Shaded regions represent Monte Carlo simulation results (red dotted line = mean; shaded region = one standard deviation) obtained by accounting for uncertainty in ligament stiffnesses and reference strains. The effect of ligament uncertainty was directionally dependent, with the greatest variability seen in tibiofemoral translations, internal tibial rotation and medial patellar tilt.

Inertial and Elastic Loading Conditions:

Simulations of the elastic and inertial loading conditions produced distinct tibiofemoral and patellofemoral kinematic patterns (Fig. 4). For example, when quadriceps activity occurred at extended knee postures (i.e. in the elastic case), greater anterior tibial translation (2.2 mm), internal tibial rotation (5.1 deg) and superior patellar translation (5.2 mm) were predicted in the extended position. Inertial loading (i.e. quadriceps active when knee was flexed) induced greater anterior (6.2 mm) and inferior (3.3 mm) tibial translation, and a more anterior (4.0 mm) and extended (7.2 deg) patella in a flexed knee posture. At the patellofemoral joint, there was increased superior (5.2 mm) and lateral (1.0 mm) translation of the patella in the elastic case at maximum extension. In addition, there was patella flexion (7.2 deg), and increased anterior (4.0 mm) and superior (4.2 mm) translation at maximum knee flexion during the inertial case. These load-dependent kinematic differences generally agreed with both subject-specific and population-average[51] dynamic MRI measurements. For example, average difference between our subject-specific MRI and simulated results over a similar range of motion were 0.6 mm of superior translation, 0.7 mm of lateral translation, and 1.5 degrees of adduction.

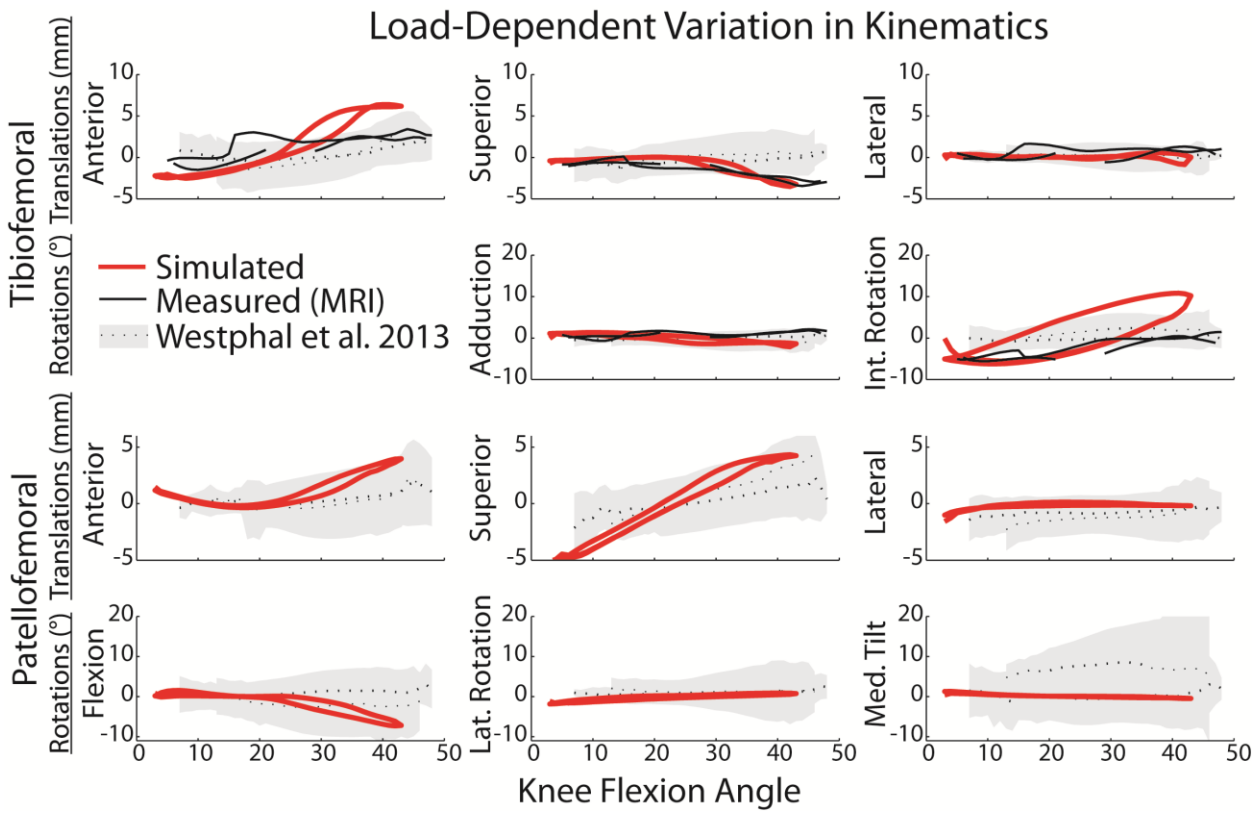

Figure 4: Tibiofemoral and patellofemoral kinematics were simulated and measured under inertial (peak quadriceps activity with flexion) and elastic (peak quadriceps activity with extension) loading conditions. Shown are the differences in kinematics observed between the inertial and elastic loading conditions, as predicted by the nominal simulation (red line) and measured with dynamic MRI (black line=subject-specific, shaded region represents +/- 1 s.d. reported in Westphal et al.[51]). Non-zero values represent phases where load-dependent behavior is evident, with the load-dependent effects most prominent in anterior tibial translation, tibial rotation, superior patellar translation, and patellar flexion.

Gait Simulations:

The gait simulation predicted secondary tibiofemoral and patellofemoral kinematics that differed considerably from what would be assumed based a constrained 1 DOF knee model created from the passive motion results (Fig. 5-6). In particular, the largest load-dependent effects occurred in tibial rotation and anterior tibial translation (Fig. 5). The gait simulation predicted external rotation through

load acceptance, internal rotation through toe-off, followed by external tibia rotation during much of swing. In stance, the tibia was also substantially more anteriorly and laterally translated than a knee model based on passive behavior would predict (Fig. 6).

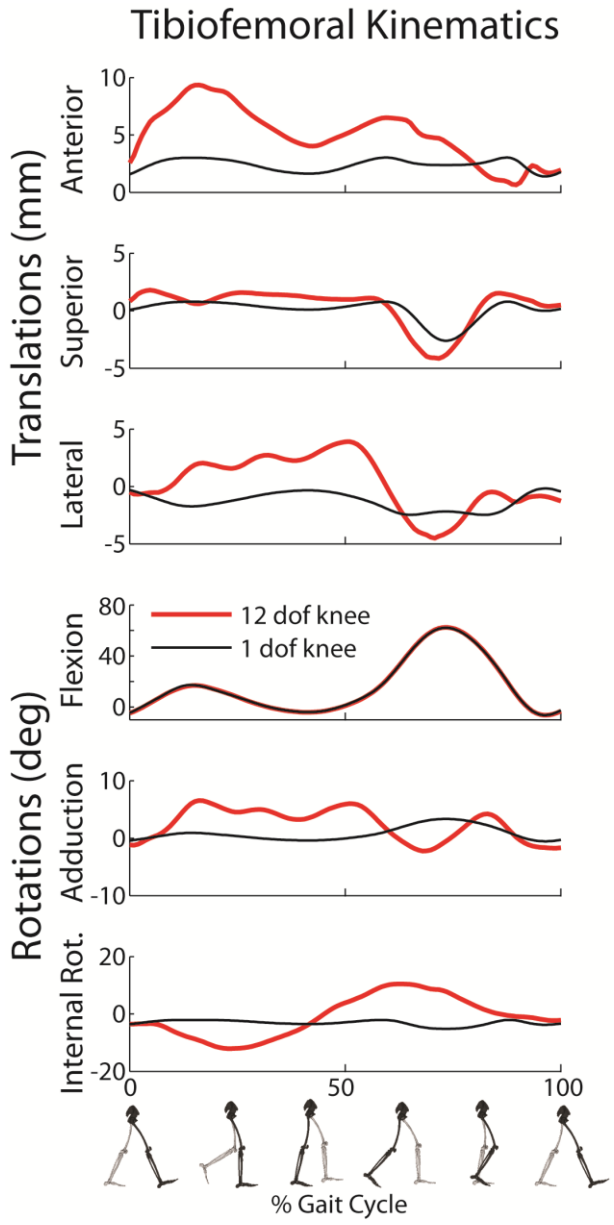

Figure 5: Simulation of tibiofemoral kinematics during a normal gait cycle. The simulation results (red line) differ substantially from what would be assumed via passive joint behavior.

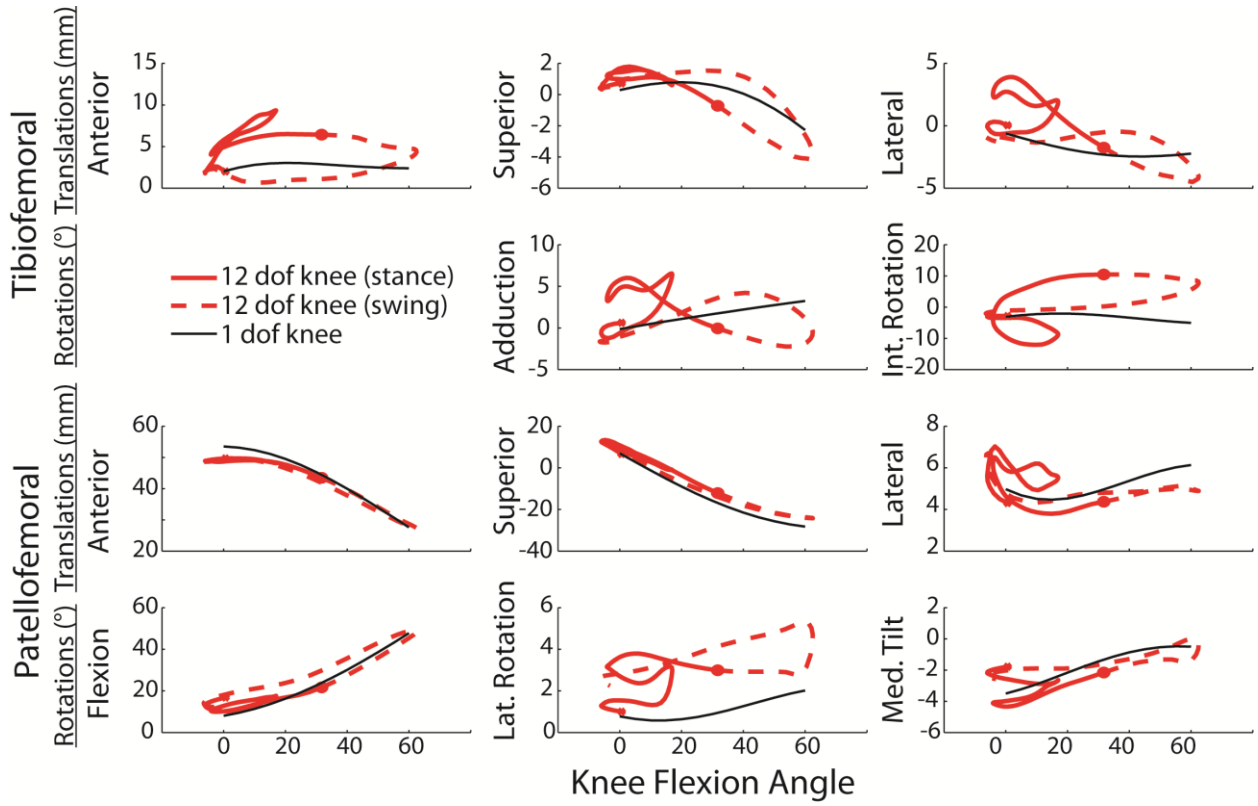

Figure 6: Plots of the predicted tibiofemoral and patellofemoral kinematics (solid red=stance, dashed red=swing) vs. knee flexion over a walking gait cycle. For many of the degrees of freedom (e.g. anterior tibial translation, internal tibial rotation), there are substantial variations in the predicted kinematics and that assumed when describing secondary tibiofemoral kinematics and patellofemoral kinematics as a constrained function of knee flexion (solid black line).

Model predictions of tibiofemoral contact pressures on the medial plateau were higher than those on the lateral plateau through the majority of stance. Medial tibial plateau contact pressures averaged 6.2 and 5.7 MPa at the first (15% gait cycle) and second (50% gait cycle) peaks of tibiofemoral loading, respectively (Fig. 7). Contact pressure on the patellar facets reached an average of 2.8 MPa at the first peak of tibiofemoral loading.

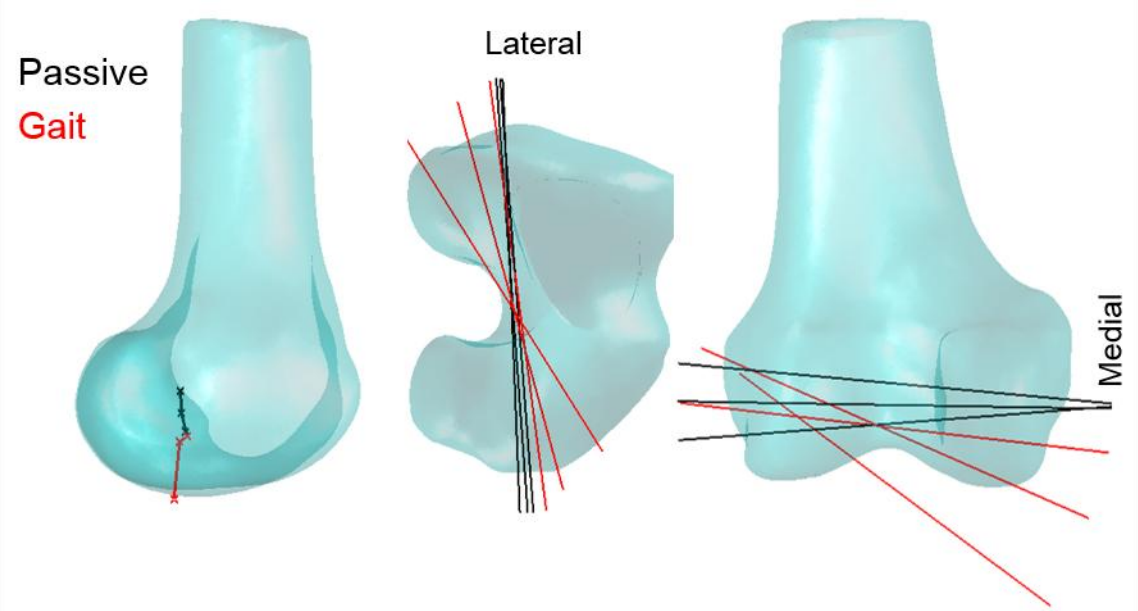

Figure 7: Predicted patellar and tibial plateau contact pressures at different percentages of the gait cycle during normal walking.

Discussion

We have introduced and validated a 12 DOF multi-body, dynamic knee model suitable for simulating load-dependent knee behavior during locomotor activities. A key feature of the model is the capacity to predict the tibiofemoral and patellofemoral mechanics that arise from the interaction of muscle, ligament, and contact forces, instead of relying on pre-assumed behavior based on cadaveric studies.[4, 16] We showed that the knee model produced kinematics that were consistent with *in vivo* measures obtained with dynamic MRI. When extended to gait, the framework predicted secondary knee kinematics that differ substantially from that is assumed based on traditional knee models used in gait analysis.[4, 16] Thus, multi-scale interactions that occur between internal joint mechanics and movement dynamics seem important to consider in simulations of human locomotion. Further, as demonstrated by our stochastic simulations, the new knee model may be extremely relevant in simulating movement in cases of altered ligament properties due to injury or disease.

Our knee model validation efforts were perhaps the most extensive ever performed, with model predictions directly compared to *in vivo* measures obtained under both passive and active conditions. We found that passive kinematic behavior of the model compared very well to that observed experimentally, but that specific degrees of freedom (notably tibiofemoral translations and internal tibial rotation) are highly dependent on ligament properties (Fig. 3). In contrast, tibiofemoral adduction and patellofemoral behavior were much less dependent on ligament properties, suggesting that cartilage geometries assume a more major role in guiding those movements. Inherent laxity in the knee model allowed for the prediction of load-dependent knee behavior that has been measured experimentally (Fig. 4).[9, 18, 30, 51] The model predicted an increase in anterior tibial translation and internal rotation with quadriceps loading in a flexed knee posture (i.e. in the inertial loading case), a result that was seen in the dynamic MRI (Fig. 4) and has been recorded previously in cadaveric studies.[26, 33] Such predictive capabilities are important when using knee models to investigate the influence of soft tissue injury and treatment on internal joint behavior.

When used to simulate gait, the co-simulation framework predicted variations in secondary knee kinematics that differed substantially from what is assumed based on passive behavior of cadaveric knees.[4, 50, 53] In particular, phase plots clearly show that secondary kinematics are not simple functions of knee flexion, but also depend on the current internal and external loading state (Fig. 6). Notably, internal tibial rotation occurred with knee extension during the second half of stance, motion that is opposite of the classically defined screw home mechanism but is consistent with empirical studies of gait.[9, 18, 30] Anterior tibial translation arises during the early stance phases of gait, an effect likely attributable to the quadriceps loading. An important feature of the knee model is the capacity to simultaneously estimate muscle forces and cartilage contact pressure patterns that arise during locomotion. In the nominal gait simulation, medial tibial plateau pressure was larger than the lateral tibial plateau pressure through much of stance and approximately two times greater than the patellar pressures through mid-stance (Fig. 7).

What is the clinical relevance of being able to simulate load-dependent knee behavior? There are two potentially important considerations. First is the recognition that slight variations in secondary knee kinematics can have a substantial impact on both the magnitude and location of cartilage contact pressure.

It has been suggested that sudden shifts in the location of cartilage contact, due to ligament injury or surgical repair, may be a precipitator to tissue degeneration and osteoarthritis.[14] Hence, the proposed knee model provides a systematic way of predicting how variations in treatment factors may influence cartilage tissue loading. Second, variations in knee kinematics can affect the capacity of soft tissues to induce joint motion. We began to assess this effect by computing the tibiofemoral finite helical axis during stance. This analysis shows that the tibiofemoral adduction and rotation during gait resulted in a skewing of the finite helical axis (FHA) and a distal migration of location of the FHA in the mid-sagittal plane (Fig. 8). Load-dependent shifts in the FHA alter the effective moment arms of the muscles and ligaments crossing the knee, such as has been previously observed for the patellar tendon.[51] Variations in muscle moment arms are not currently considered in standard gait knee models, but would appear relevant in an intact knee and likely become an even more important consideration when joint laxity exists.

While our knee model has improved prediction of load-dependent kinematics, we must acknowledge some of its inherent limitations. We represented the ligaments as spring elements, rather than deformable 3D representations that account for spatial variations in strain. We were able to include some wrap objects to improve wrapping around the bony structures. However, these wrapping surfaces were simple geometric representations (e.g. cylinder, ellipse) and ligament-ligament interactions were not incorporated. Ligament reference strains are not measurable *in vivo*, so these parameters were estimated from the literature. We followed the approach of Baldwin et al. of using stochastic simulations to assess the influence of this uncertainty has on our model predictions.[7] Our cartilage surface was represented as a constant thickness, an approximation which has been used by other groups.[10, 42] We believe that inclusion of variable cartilage thickness, as can be determined from MR images,[29] will be straightforward to implement in the future. Further, the knee model does not currently have a meniscus. While the meniscus is not considered a primary constraint in low load conditions,[32] incorporating a meniscus model[23] will become important as the model is used for large-load tasks or in cases of ligamentous deficiency. Finally, our gait simulations applied measured ground reactions directly to the feet. Future improvements include adding a ground contact model that can simulate reaction forces arising from foot-floor interactions.

In conclusion, this study introduced a new, multi-body dynamic knee model that includes 6 DOF tibiofemoral and patellofemoral joints. The model provides simultaneous prediction of the ligament, muscle, and articular contact loads underlying human motion. We showed that model predictions compare well with load-dependent knee kinematic behavior measured *in vivo*. When extended to walking, the model predicted knee kinematic patterns that differ markedly from that traditionally assumed in gait analysis models. Thus, the modeling framework provides a powerful new approach to simulate alterations in knee mechanics that may arise due to injury or disease-related changes in soft tissue properties.

Acknowledgements

This project was supported in part by the Clinical and Translational Science Award program, through the NIH National Center for Advancing Translational Sciences, grant UL1TR000427. Additional funding was provided by NIH F30AR065838, NIH EB015410, NIH AR062733, the National Science Foundation (0966535), and the UW Medical Scientist Training Program (T32GM008692). The authors also thank Anne Schmitz, PhD, and Kwang Won Choi, PhD, for their contributions to the modeling work.

References

1. Amiri, S., and D. R. Wilson. A computational modeling approach for investigating soft tissue balancing in bicruciate retaining knee arthroplasty. Comput. Math. Methods Med. 2012:652865, 2012.
2. Anderson, C. J., B. D. Westerhaus, S. D. Pietrini, C. G. Ziegler, C. A. Wijdicks, S. Johansen, L. Engebretsen, and R. F. LaPrade. Kinematic impact of anteromedial and posterolateral bundle graft fixation angles on double-bundle anterior cruciate ligament reconstructions. Am. J. Sports Med. 38:1575-1583, 2010.
3. Anderst, W., R. Zauel, J. Bishop, E. Demps, and S. Tashman. Validation of three-dimensional model-based tibio-femoral tracking during running. Med. Eng. Phys. 31:10-16, 2009.

4. Arnold, E. M., S. R. Ward, R. L. Lieber, and S. L. Delp. A model of the lower limb for analysis of human movement. Ann. Biomed. Eng. 38:269-279, 2010.

5. Askew, M., and V. Mow. The biomechanical function of the collagen fibril ultrastructure of articular cartilage. J. Biomech. Eng. 100:105-115, 1978.

6. Atkinson, P., T. Atkinson, C. Huang, and R. Doane. A comparison of the mechanical and dimensional properties of the human medial and lateral patellofemoral ligaments. *Proceedings of the 46th Annual Meeting of the Orthopaedic Research Society, Orlando, FL*. 2000.

7. Baldwin, M. A., P. J. Laz, J. Q. Stowe, and P. J. Rullkoetter. Efficient probabilistic representation of tibiofemoral soft tissue constraint. Comput. Methods Biomech. Biomed. Engin. 12:651-659, 2009.

8. Bei, Y., and B. J. Fregly. Multibody dynamic simulation of knee contact mechanics. Med. Eng. Phys. 26:777-789, 2004.

9. Benoit, D. L., D. K. Ramsey, M. Lamontagne, L. Xu, P. Wretenberg, and P. Renstrom. In vivo knee kinematics during gait reveals new rotation profiles and smaller translations. Clinical orthopaedics and related research. 454:81-88, 2007.

10. Blankevoort, L., and R. Huiskes. Ligament-bone interaction in a three-dimensional model of the knee. J. Biomech. Eng. 113:263-269, 1991.

11. Bloemker, K. H., T. M. Guess, L. Maletsky, and K. Dodd. Computational knee ligament modeling using experimentally determined zero-load lengths. Open Biomed. Eng. J. 6:33, 2012.

12. Caruntu, D. I., and M. S. Hefzy. 3-D anatomically based dynamic modeling of the human knee to include tibio-femoral and patello-femoral joints. J. Biomech. Eng. 126:44-53, 2004.

13. Chandrashekar, N., H. Mansouri, J. Slauterbeck, and J. Hashemi. Sex-based differences in the tensile properties of the human anterior cruciate ligament. J. Biomech. 39:2943-2950, 2006.

14. Chaudhari, A. M., P. L. Briant, S. L. Bevill, S. Koo, and T. P. Andriacchi. Knee kinematics, cartilage morphology, and osteoarthritis after ACL injury. Medicine and science in sports and exercise. 40:215-222, 2008.

15. Delp, S. L., and J. P. Loan. A computational framework for simulating and analyzing human and animal movement. Comput. Sci. Eng. 2:46-55, 2000.

16. Delp, S. L., J. P. Loan, M. G. Hoy, F. E. Zajac, E. L. Topp, and J. M. Rosen. An interactive graphics-based model of the lower extremity to study orthopaedic surgical procedures. IEEE Trans. Biomed. Eng. 37:757-767, 1990.

17. Dhaher, Y. Y., T. H. Kwon, and M. Barry. The effect of connective tissue material uncertainties on knee joint mechanics under isolated loading conditions. J. Biomech. 43:3118-3125, 2010.

18. Dyrby, C. O., and T. P. Andriacchi. Secondary motions of the knee during weight bearing and non-weight bearing activities. J. Orthop. Res. 22:794-800, 2004.

19. Gerdes, C. M., R. Kijowski, and S. B. Reeder. IDEAL imaging of the musculoskeletal system: robust water–fat separation for uniform fat suppression, marrow evaluation, and cartilage imaging. AJR. Am. J. Roentgenol. 189:W284-W291, 2007.

20. Gollehon, D. L., P. A. Torzilli, and R. F. Warren. The role of the posterolateral and cruciate ligaments in the stability of the human knee. A biomechanical study. J. Bone Joint Surg. Am. 69:233-242, 1987.

21. Griffith, C. J., R. F. LaPrade, S. Johansen, B. Armitage, C. Wijdicks, and L. Engebretsen. Medial Knee Injury Part 1, Static Function of the Individual Components of the Main Medial Knee Structures. Am. J. Sports Med. 37:1762-1770, 2009.

22. Grood, E., and W. Suntay. A joint coordinate system for the clinical description of three-dimensional motions: application to the knee. Journal of biomechanical engineering. 105:9, 1983.

23. Guess, T. M., G. Thiagarajan, M. Kia, and M. Mishra. A subject specific multibody model of the knee with menisci. Med. Eng. Phys. 32:505-515, 2010.

24. Halloran, J. P., M. Ackermann, A. Erdemir, and A. J. Van den Bogert. Concurrent musculoskeletal dynamics and finite element analysis predicts altered gait patterns to reduce foot tissue loading. J. Biomech. 43:2810-2815, 2010.

25. Halloran, J. P., S. K. Easley, A. J. Petrella, and P. J. Rullkoetter. Comparison of deformable and elastic foundation finite element simulations for predicting knee replacement mechanics. J. Biomech. Eng. 127:813-818, 2005.

26. Hirokawa, S., M. Solomonow, Y. Lu, Z. P. Lou, and R. D'Ambrosia. Anterior-posterior and rotational displacement of the tibia elicited by quadriceps contraction. Am J Sports Med. 20:299-306, 1992.

27. Ishigooka, H., T. Sugihara, K. Shimizu, H. Aoki, and K. Hirata. Anatomical study of the popliteofibular ligament and surrounding structures. J. Orthop. Sci. 9:51-58, 2004.

28. Kaiser, J., R. Bradford, K. Johnson, O. Wieben, and D. G. Thelen. Measurement of tibiofemoral kinematics using highly accelerated 3D radial sampling. Magn. Reson. Med. 69:1310-1316, 2013.

29. Koo, S., G. E. Gold, and T. P. Andriacchi. Considerations in measuring cartilage thickness using MRI: factors influencing reproducibility and accuracy. Osteoarthritis Cartilage. 13:782-789, 2005.

30. Lafortune, M., P. Cavanagh, H. Sommer, and A. Kalenak. Three-dimensional kinematics of the human knee during walking. Journal of biomechanics. 25:11, 1992.

31. Leardini, A., A. Cappozzo, F. Catani, S. Toksvig-Larsen, A. Petitto, V. Sforza, G. Cassanelli, and S. Giannini. Validation of a functional method for the estimation of hip joint centre location. J. Biomech. 32:99-103, 1999.

32. Levy, I. M., P. A. Torzilli, and R. F. Warren. The effect of medial meniscectomy on anterior-posterior motion of the knee. J. Bone Joint Surg. 64-A:883-888, 1982.

33. Li, G., T. Rudy, M. Sakane, A. Kanamori, C. Ma, and S. L. Y. Woo. The importance of quadriceps and hamstring muscle loading on knee kinematics and in-situ forces in the ACL. Journal of biomechanics. 32:395-400, 1999.

34. Lu, T. W., and J. J. O'connor. Bone position estimation from skin marker co-ordinates using global optimisation with joint constraints. J. Biomech. 32:129-134, 1999.

35. Markolf, K. L., W. L. Bargar, S. C. Shoemaker, and H. C. Amstutz. The role of joint load in knee stability. J. Bone Joint Surg. Am. 63:570-585, 1981.

36. Maynard, M. J., X. Deng, T. L. Wickiewicz, and R. F. Warren. The popliteofibular ligament. Rediscovery of a key element in posterolateral stability. Am. J. Sports Med. 24:311-316, 1996.

37. Miranda, D. L., M. J. Rainbow, E. L. Leventhal, J. J. Crisco, and B. C. Fleming. Automatic determination of anatomical coordinate systems for three-dimensional bone models of the isolated human knee. J. Biomech. 43:1623-1626, 2010.

38. Neptune, R. R., I. C. Wright, and A. J. van den Bogert. The influence of orthotic devices and vastus medialis strength and timing on patellofemoral loads during running. Clin. Biomech. 15:611-618, 2000.

39. Nomura, E., M. Inoue, and N. Osada. Anatomical analysis of the medial patellofemoral ligament of the knee, especially the femoral attachment. Knee Surg. Sports Traumatol. Arthrosc. 13:510-515, 2005.

40. Powell, M. J. An efficient method for finding the minimum of a function of several variables without calculating derivatives. The Computer Journal. 7:155-162, 1964.

41. Rainbow, M. J., D. L. Miranda, R. T. Cheung, J. B. Schwartz, J. J. Crisco, I. S. Davis, and B. C. Fleming. Automatic determination of an anatomical coordinate system for a three-dimensional model of the human patella. J. Biomech. 46:2093-2096, 2013.

42. Segal, N. A., D. D. Anderson, K. S. Iyer, J. Baker, J. C. Torner, J. A. Lynch, D. T. Felson, C. E. Lewis, and T. D. Brown. Baseline articular contact stress levels predict incident symptomatic knee osteoarthritis development in the MOST cohort. J. Orthop. Res. 27:1562-1568, 2009.

43. Shelburne, K. B., M. G. Pandy, F. C. Anderson, and M. R. Torry. Pattern of anterior cruciate ligament force in normal walking. J. Biomech. 37:797-805, 2004.

44. Shelburne, K. B., M. R. Torry, and M. G. Pandy. Contributions of muscles, ligaments, and the ground-reaction force to tibiofemoral joint loading during normal gait. J. Orthop. Res. 24:1983-1990, 2006.

45. Shin, C. S., A. M. Chaudhari, and T. P. Andriacchi. The influence of deceleration forces on ACL strain during single-leg landing: a simulation study. J. Biomech. 40:1145-1152, 2007.

46. Silder, A., C. J. Westphal, and D. G. Thelen. A magnetic resonance-compatible loading device for dynamically imaging shortening and lengthening muscle contraction mechanics. J. Med. Device. 3:034504, 2009.

47. Sritharan, P., Y. C. Lin, and M. G. Pandy. Muscles that do not cross the knee contribute to the knee adduction moment and tibiofemoral compartment loading during gait. J. Orthop. Res. 30:1586-1595, 2012.

48. Thelen, D. G., K. W. Choi, and A. M. Schmitz. Co-Simulation of Neuromuscular Dynamics and Knee Mechanics During Human Walking. J. Biomech. Eng. 136:021033, 2014.

49. van Eijden, T. M., W. de Boer, and W. A. Weijs. The orientation of the distal part of the quadriceps femoris muscle as a function of the knee flexion-extension angle. J. Biomech. 18:803-809, 1985.

50. Walker, P. S., J. S. Rovick, and D. D. Robertson. The effects of knee brace hinge design and placement on joint mechanics. J. Biomech. 21:965-974, 1988.

51. Westphal, C. J., A. Schmitz, S. B. Reeder, and D. G. Thelen. Load-dependent variations in knee kinematics measured with dynamic MRI. J. Biomech. 46:2045-2052, 2013.

52. Wilson, D. R., J. D. Feikes, and J. J. O'connor. Ligaments and articular contact guide passive knee flexion. J. Biomech. 31:1127-1136, 1998.

53. Wilson, D. R., J. D. Feikes, A. B. Zavatsky, and J. J. O'connor. The components of passive knee movement are coupled to flexion angle. J. Biomech. 33:465-473, 2000.

Chapter 2

Influence of patellar position on the knee extensor mechanism in normal and crouched walking

Rachel L. Lenhart, Colin R. Smith, Tom F. Novacheck, Michael H. Schwartz, Darryl G. Thelen

Abstract

Patella alta is common in cerebral palsy, especially those with crouch gait. Correction of patella alta has been advocated in the treatment of crouch, however the appropriate degree of correction and the implications for knee extensor function remain unclear. Therefore, the goal of this study was to assess the impact of patellar position on quadriceps and patellar tendon forces during normal and crouch gait. To this end, a lower extremity musculoskeletal model with a novel 12 degree of freedom knee joint was used to predict muscle forces during normal gait in a healthy adult, as well as mild (22 deg min knee flexion in stance), moderate (29 deg), and severe (65 deg) crouch gait in three children with cerebral palsy. The results showed that quadriceps and patellar tendon forces vary with both walking posture and patellar position. The degree of crouch had the larger effect, with peak quadriceps and patellar tendon forces reaching 8.1 and 4.9 times body weight in severe crouch at the normal patellar position, compared to 1.1 and 1.0 times body weight in normal walking. However, the increase in force caused by crouch can be somewhat moderated by choice of patellar position. Patella alta actually reduced quadriceps and patellar tendon loads in crouch gait, due to an enhancement of their knee extensor moment arms in flexed knee postures. In contrast, patella baja may compromise the quadriceps effective moment arm, particularly in flexed knee postures. These results are important to consider when using surgical approaches for treating patella alta in children who exhibit crouch gait patterns.

Introduction

Patella alta, or a superiorly displaced patella, is a common abnormality in cerebral palsy, especially in children who walk with a crouched gait pattern (1-3). Patella alta has long been thought to

contribute to knee extensor lag (lack of active knee extension that can be obtained passively) (3-5), through a reduced patellar tendon moment arm (3). Despite this, some groups have argued that those with patella alta display increases the knee extensor capacity (6-7). The reasons behind these discrepancies could arise in part from the strong dependence of the knee extensor moment arms on knee flexion angle, such that the effects of alta on the knee extensor mechanism may be posture dependent. Postural dependencies are very relevant in treating pathological gait, e.g. crouch, where the knee extensor mechanism undergoes loading in postures remarkably distinct from normal gait.

Patellar tendon advancement (PTA) is a procedure used to help correct quadriceps insufficiency in those with crouch gait (4). The procedure distalizes the patellar tendon insertion, moving the patellar position inferiorly (4). It is often combined with a procedure to compensate for knee flexion contractures, such as the distal femoral extension osteotomy (DFEO) (4). When included, patellar tendon advancement has shown to improve gait outcomes more than performing DFEO in isolation (8). However, questions remain. Children tend to have patella baja, or an inferior patellar position, after surgery (8). It also appears that, while gait is improved, there may be losses in other knee functional ability (in activities like stepping over an object or kicking an object) after the combined DFEO and PTA (8). Therefore, the effects of this corrective surgery and the trade-offs that may be occurring with the alteration in patellar position are not completely understood.

The purpose of this study was to investigate how patellar position (normal, alta, and baja) influence patellar tendon and quadriceps forces during walking in different postures. To do this, we used a novel musculoskeletal model in which we could simulate 6 degree of freedom (DOF) tibiofemoral and patellofemoral mechanics. We simulated varying degrees of patella alta and baja while walking in normal, mild, moderate and severe crouch. We hypothesized that the influence of patella position on the knee extensor mechanism would be posture dependent, with alta enhancing the knee extensor moment arms in flexed postures and thus reducing the quadriceps loads needed to walking in crouch.

Materials and Methods

Experimental Methods:

For the normal gait simulation, data was collected at University of Wisconsin-Madison with approval from the Health sciences Institutional Review Board. The participant (age = 28 yrs, mass = 60.4 kg, height = 1.68 m, gait speed = 1.36 m/s) had no history of chronic knee pain, injury, or surgery. A passive 8-camera motion capture system (Motion Analysis, Santa Rosa, CA) was used to track 44 reflective markers during normal walking over an overground force plate (forceplate model BP400600, AMTI, Watertown, MA).

For the crouch simulations, retrospective gait analysis data was extracted from the database at Gillette Children's Specialty Healthcare. Use of this data for research has been approved by the University of Minnesota Institutional Review Board. Marker and force plate data during overground walking at a self-selected speed were chosen for 3 children with cerebral palsy who had received clinical gait analysis as part of standard of care (9). The children with cerebral palsy were chosen based on their display of crouch gait and their ability to complete gait testing without the use of walking aids. One child each displayed mild crouch (minimum knee flexion angle during stance = 22 degrees, age = 9.4 yrs, mass = 28.2 kg, height = 1.31 m, gait speed = 0.48 m/s), another moderate crouch (minimum = 29 degrees, age = 11.0 yrs, mass = 28.7 kg, height = 1.43 m, gait speed = 1.12 m/s), and one severe crouch (minimum = 65 degrees, age = 13.2 yrs, mass = 35.9 kg, height = 1.44 m, gait speed = 0.82 m/s).

Computational Modeling:

To be able to assess soft tissue loading throughout the gait cycle, we employed a knee model developed by our group that has been previously described and validated in the literature (10). Briefly, knee skeletal, cartilage, and ligament geometries were extracted from MRI of a healthy adult female (23 yrs, 61 kg, 1.65 m). From the images, a three-body model of the knee was created with 12 DOF (6 tibiofemoral and 6 tibiofemoral) (Fig. 1). Fourteen ligament bundles, made up of sets of non-linear spring

elements (11) from the anatomical origins to insertions, connected the segments. Contact pressures during simulation were determined by penetration of the high-resolution meshes created from the cartilage geometries and an elastic foundation model (12) (Elastic Modulus = 5MPa (11, 13), Poisson's ratio = 0.45 (11, 13-15), combined cartilage thickness of 6 mm (i.e. 3 mm on each surface)) (16). For this application, the femoral cartilage geometry was extended to include the anterior femoral shaft for simulation of patella alta.

The knee model was incorporated into a lower extremity model from the literature (17), which included 44 muscle-tendon units acting about the hip, knee, and ankle (Fig. 1). The pelvis was used as the base segment with 6 DOF. The hip was modeled as a ball-in-socket joint with 3 DOF, while the ankle was one DOF allowing for dorsi/plantarflexion. The model was implemented in SIMM (18) with multibody dynamics and equations of motion determined by Dynamics Pipeline (Musculographics Inc., Santa Rosa, CA) and SD/Fast (Parametric Technology Corp. Needham MA).

The model was first scaled to each subject using segment lengths during a static trial. Inverse kinematic analysis solved for joint angles over the gait cycle using a global optimization routine that minimized the discrepancy between the measured and simulated marker positions (19). At this stage, the secondary knee motions were defined as functions of knee flexion determined by the model's behavior during a passive flexion-extension simulation (10).

To determine 12 DOF knee motion and musculotendon forces over the gait cycle, we used a novel enhanced static optimization routine which determined secondary knee kinematics based on minimizing the weighted sum of squared muscle activations and the net contact elastic energy (20). Explicitly, the cost function was

$$J = \sum_{i=1}^{m} V_i a_i^2 + W \cdot U_{contact}$$

where m is the number of muscles, V is a muscle's volume (expressed in units of mm^3), a is a muscle's activation level (between 0 and 1), U is the contact elastic energy at the tibiofemoral and patellofemoral joints (expressed in Joules), and W is the weighting factor on the contact energy (W = 500). In this formulation, muscles were assumed to have force equal to their activation level (a_i) times their maximum isometric force (F_{0i}), $F_i = a_i F_{0i}$. The solution constrained the resultant joint angles (**q**) such that the accelerations in the primary degrees of freedom (hip flexion, adduction, and internal rotation, knee flexion, and ankle dorsiflexion) had to match experimental values ($\ddot{\mathbf{q}}_j^{\text{exp}}$),

$$\ddot{\mathbf{q}}_j^{\text{exp}} = \sum_{i=1}^{m} a_i F_{0i} \hat{\ddot{\mathbf{q}}}_{ji}^{\text{muscle}}(\mathbf{q}) + \ddot{\mathbf{q}}_j^{\text{other}}(\dot{\mathbf{q}}, \mathbf{q})$$

while the accelerations in the secondary degrees of freedom were required to be zero.

$$\mathbf{0} = \sum_{i=1}^{m} a_i F_{0i} \hat{\ddot{\mathbf{q}}}_{si}^{\text{muscle}}(\mathbf{q}) + \ddot{\mathbf{q}}_s^{\text{other}}(\dot{\mathbf{q}}, \mathbf{q})$$

In these equations, accelerations (**$\ddot{q}$**) were generated by the muscles, in the primary ($\hat{\ddot{\mathbf{q}}}_{ji}^{\text{muscle}}$) and secondary ($\hat{\ddot{\mathbf{q}}}_{si}^{\text{muscle}}$) degrees of freedom, as well as by other forces ($\ddot{\mathbf{q}}^{\text{other}}$), which included external ground reactions, contact, ligament, gravitational, centripetal, and Coriolis forces. The $\ddot{\mathbf{q}}^{\text{other}}$ term also included accelerations due to the addition of a passive joint torque (M_{PJT}), which helped to modulate the changes in the secondary degrees of freedom from frame to frame.

$$M_{i_s} = -\dot{q}_i \eta_i$$

Here, $\dot{q}_i$ is the generalized speed of a secondary coordinate and η_i is a damping parameter set uniquely for each degree of freedom. See Appendix B for the values used in these simulations. It should be explicitly noted that tibiofemoral flexion was the only degree of freedom at the knee that was prescribed; the five other tibiofemoral and all patellofemoral degrees of freedom were allowed to evolve naturally in response

to the muscle, ligament, contact, external, and inertial forces acting on the limb. At this stage, kinematic data was low-pass filtered at 6 Hz, and ground reaction force data was filtered at 50 Hz. Ground reaction forces were applied directly to the feet.

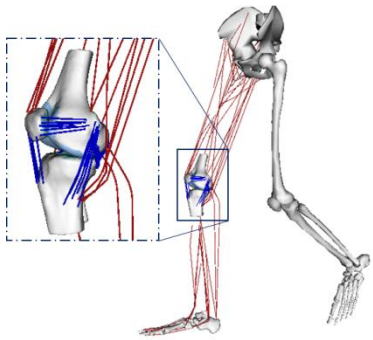

Figure 1: Lower extremity musculoskeletal model with novel knee joint with 6 degrees of freedom at both the tibiofemoral and patellofemoral joints. Ligament, cartilage, and bony geometries were taken from MR images, and the behavior was validated against dynamic MRI (10).

The process of scaling, inverse kinematics, and enhanced static optimization were repeated for all three walking postures, as well as different patellar positions. Patellar position was varied by introducing a new starting configuration for the nominal model, with the patella a set distance more superior or inferior than that noted in the nominal model. Variations from 2 cm of patella baja (2 cm inferior to the nominal position) to 4 cm of alta (4 cm superior) were considered (Fig. 2). For this paper, positive displacement will indicate patella alta, while negative displacement will indicate baja. Also note that the patellar position was changed before the model was scaled, such that the relative position would be similar across the different sized subjects. Passive forward simulation was used before the frame of the walking simulations to determine the resting position of the patella in each of the configurations.

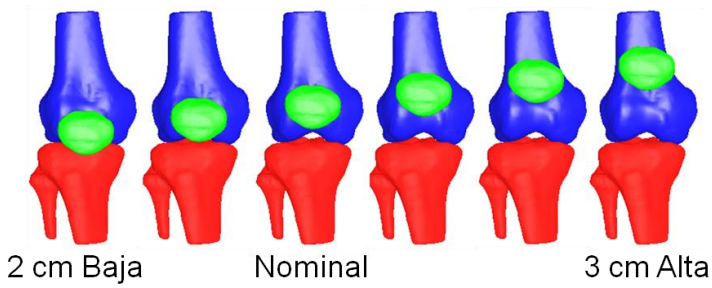

Figure 2: Demonstration of the range of patellar positions used during simulation.

From the simulations, quadriceps (sum of vastus medius, vastus intermedius, vastus lateralis, and rectus femoris) and patellar tendon forces (sum of individual patellar tendon strands) were extracted over the gait cycle. The 3D patellar tendon moment arms were calculated about the medio-lateral axis passing through the femoral condyles during the stance phase of walking. The quadriceps effective moment arm (M_{Qeff}) were calculated using the equation $M_{Qeff} = (F_{PT} * M_{PT}) / (F_Q)$, where F_Q is the force in the quadriceps, F_{PT} is the force in the patellar tendon, and M_{PT} is the patellar tendon moment arm (21). (For a complete representation of the 12 DOF knee kinematics, muscle forces, and ligament forces predicted for these simulations in the nominal patellar position, see Appendix C).

Results

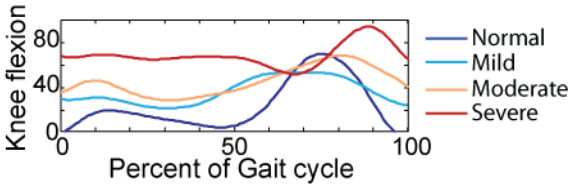

Figure 3: Knee flexion angle over the gait cycle for each of the subjects used in this analysis.

Increasing crouch severity led to greater knee flexion angles during the gait cycle (Fig. 3). Quadriceps forces varied with different walking postures and patellar positions (Fig. 4). With increasing crouch gait

severity, the quadriceps forces increased. For the normal patellar position, walking with normal gait required only 1.1 times body weight of quadriceps force, while walking with moderate crouch required just over 3 times body weight. Walking in severe crouch increased forces further, to just over 8 times body weight. Varying patellar position had a different effect depending on the walking posture. For normal walking, having 1 cm of patella alta reduced the quadriceps forces needed to 0.9 times body weight. With increasing crouch severity, more patella alta reduced quadriceps forces needed during gait. For example, 2 cm of alta minimized quadriceps forces (1.3 times body weight) during mild gait, while 3 cm of alta minimized quadriceps forces during moderate (1.9 times body weight), and 4 cm of alta (4.4 times body weight) during severe.

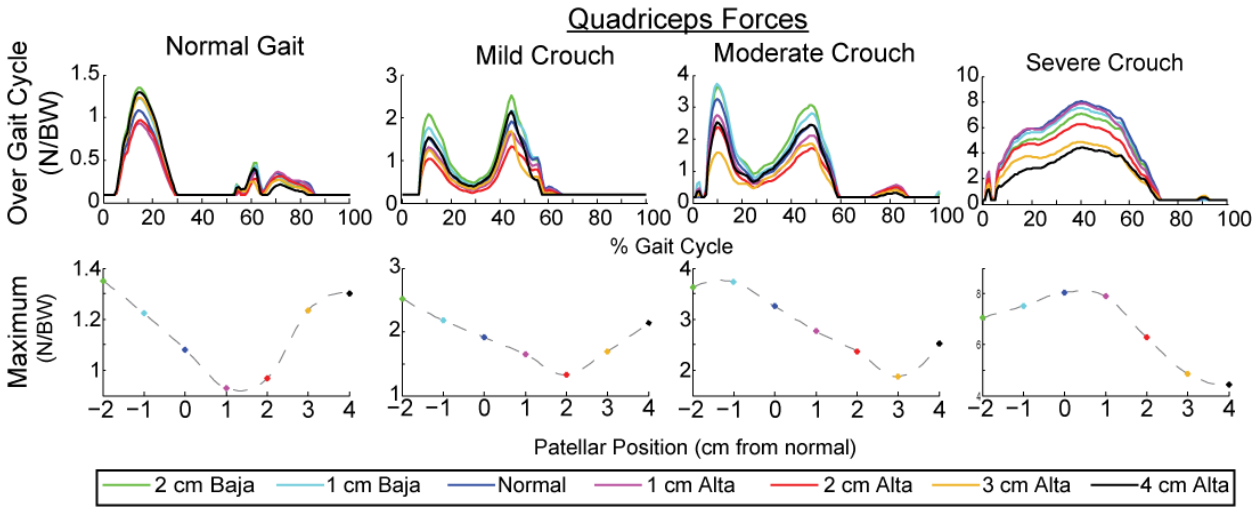

Figure 4: (Top) Quadriceps forces normalized to body weight (BW) over the gait cycle. Different colored lines indicate the different patellar positions simulated. (Bottom) Maximum quadriceps forces normalized by body weight for each patellar position.

Patellar tendon forces also varied between walking postures and patellar positions (Fig. 5), but the patterns were a bit different than the quadriceps forces. Walking with crouch again increased patellar tendon forces compared with normal. Patellar position that minimized patellar tendon forces during

normal walking was 1 cm of baja (1.0 times body weight), while 1cm alta minimized the patellar pressures for severe crouch (4.7 times body weight). Quadriceps and patellar tendon forces became more similar as the two became more in line with each other, as occurs in extreme alta for normal walking (1.30 quadriceps forces vs. 1.35 patellar tendon force, per body weight).

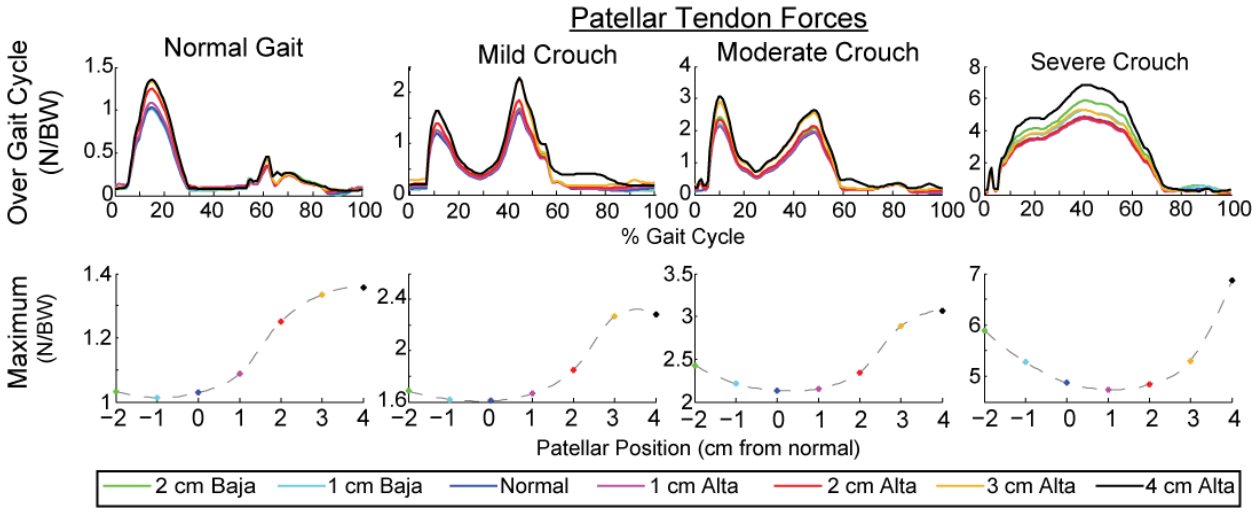

Figure 5: (Top) Patellar tendon forces normalized to body weight (BW) over the gait cycle. Different colored lines indicate the different patellar positions simulated. (Bottom) Maximum patellar tendon forces normalized by body weight versus each patellar position.

Patellar tendon and quadriceps moment arm values mirrored the changes in the forces (Fig. 6). Specifically, with increasing crouch gait severity, more superior patellar positions led to larger patellar tendon and quadriceps effective moment arms. For normal gait, the largest moment arms for the patellar tendon occurred at 1 cm of baja. However, for moderate crouch, the patellar tendon moment arm peaked at the normal patellar position. For normal walking, 3 cm of alta had 86% of the quadriceps effective moment arm compared to the normal patellar position, while 2 cm of baja had 80%. For moderate crouch, 3 cm of alta had the highest quadriceps effective moment arms at 150% of the normal position.

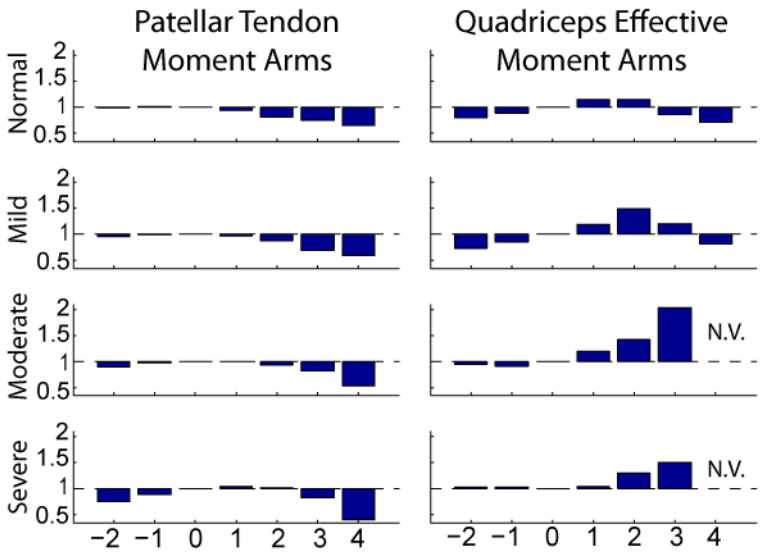

Figure 6: Patellar tendon and quadriceps moment arms for each walking posture (normal walking and mild, moderate, and severe crouch gait) at the maximum stance phase knee flexion angle. (N.V. = Not valid; calculation of the quadriceps moment arm is not valid for these cases due to extreme patellar tendon wrapping around the femoral condyles and therefore has not been shown.)

Discussion

The purpose of this study was to determine the biomechanical implications of patellar position on knee mechanics when walking in different postures. Our work indicates that patellar position has substantial consequences for extensor function. More specifically, alta increased quadriceps force requirements in normal gait, but diminished the quadriceps loads needed to walk in crouch postures. In contrast, patella baja can compromise the effective quadriceps moment arms in both normal and crouch gait, with the effect being more dramatic with knee flexion.

Patella alta has long been acknowledged in those with crouch gait and thought to contribute to knee extensor lag (the difference between passive and active knee extension capabilities) (2, 4-5, 22). Some have even theorized that alta contributes to crouch recurrence through a reduced moment arm in extended

postures (3). However, several studies imaging studies have questioned these assumptions. Sheehan and others used dynamic imaging and showed that moment arms are not necessarily reduced in those with patella alta, and in fact most of their subjects had increased moment arms (7). However, they had small subject numbers and only were able to analyze a relatively small range of knee flexion. Ward and others also studied those with patella alta, and found that while they had reduced patellar tendon moment arms, their quadriceps effective moment arms were increased (6). However, these were in healthy subjects with only a mild to moderate amount of patella alta and only a 2 dimensional technique was used to determine moment arms during a static, supine, low-load task. Unlike these studies, our work indicates a more nuanced description of how patellar position affects moment arms. We have found that both knee flexion angle and patellar position are needed to describe patellar tendon and quadriceps moment arms and forces, with the variations arising from the postural sensitivity of the patellofemoral contact force (Fig. 7)

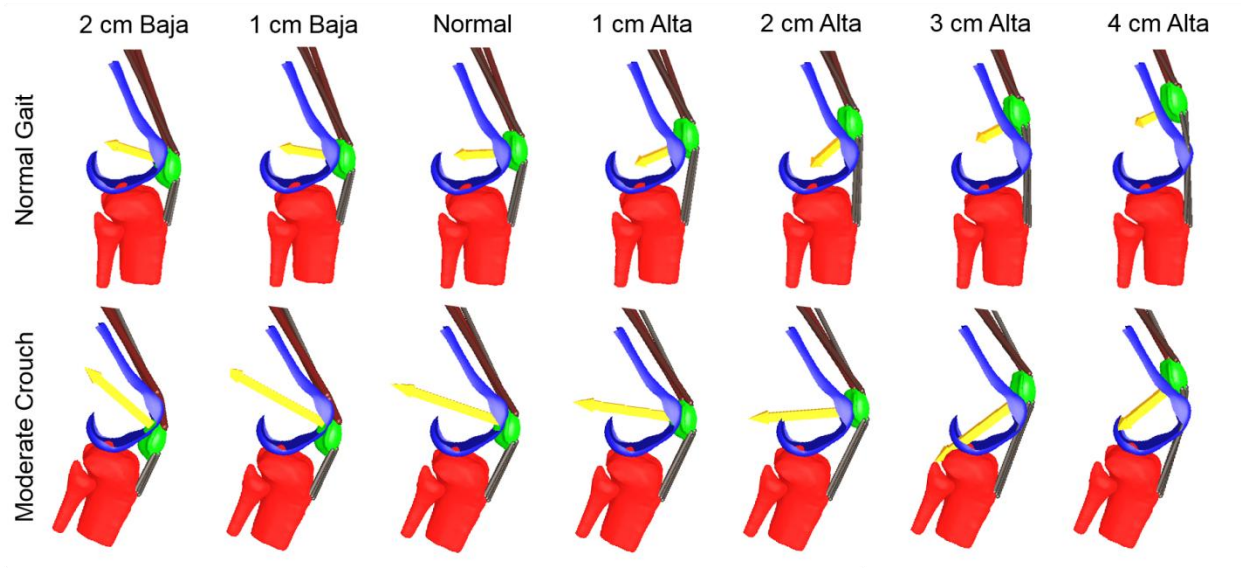

Figure 7: Demonstration of the interaction between patellar position and knee flexion angle on the determination of patellar tendon and quadriceps moment arms. Yellow arrow indicates the magnitude and direction of the patellar contact force on the femur.

Our quadriceps load estimates are generally consistent with Steele et al. (23-24) who evaluated strength requirements to walk in crouch. The strength implications were substantial, with approximately 3

times more quadriceps force need to walk in moderate crouch as compared to normal gait, with mild crouch only requiring slightly more strength than normal walking (24). Quadriceps loads during moderate crouch gait were reported to be approximately 2.5 times body weight (23). These are slightly lower than our findings (in the normal patellar position), though this could be due to model differences, as the previous study did not include the effects of ligamentous restraint or distributed cartilage contact.

These results have implications for the treatment of quadriceps insufficiency and patella alta with PTA in those with crouch gait. First it is noted that correcting crouch should be the first priority. Quadriceps forces increase with increasing crouch severity, regardless of patellar position. However, when crouch is corrected, our results indicate that placing children in baja with PTA will increase the demands on the quadriceps muscles during walking. Baja decreases the moment arm of the quadriceps about the knee, making torque generation difficult. However, the implications of this work extend beyond walking. According to our data, placing the patella in a baja position may in fact further hinder other activities that require strength in flexed postures. Given that we saw a dramatic increase in quadriceps forces with baja in crouch gait, it seems reasonable to expect that activities, such as getting out of a chair or climbing stairs, would also have these increased demands. Further, the results highlight the deleterious outcomes that could arise when correcting alta but not crouch, with more inferior positions leading to high strength requirements and more superiorly oriented patellafemoral contact loads. Further experimental work should be done to assess children exhibiting baja do report challenge or pain with flexed-knee tasks or when regressing back to a crouch gait.

We should of course mention the limitations of this work. First is the fact that we used a model based on healthy adult geometries. It is known that children with cerebral palsy tend to have other abnormalities, such as femoral anteversion and abnormal tibial slopes, that may affect the results and these should be explored in the future. We also used a simple muscle model, without accounting for spasticity, contractures, or other muscular abnormalities seen in CP. The small subject numbers also

limited this analysis, but it is expected that adding additional subjects would simply continue the trends seen here.

In conclusion, our work suggests that patellar position has implications for quadriceps forces generated during walking. Patella alta is in fact biomechanically favorable while when walking in crouch, enhancing extensor moment arms and reducing the loads on the quadriceps. In contrast, patella baja, such as after patellar tendon advancement, is beneficial in more extended postures but may raise quadriceps strength requirements in flexed postures that could arise with residual crouch, or in chair-rise and stair climbing activities. Hence, surgeons must carefully consider biomechanical consequences when determining altering patella position in procedures used to try to correct crouch gait.

Acknowledgements:

This work was supported in part by the Clinical and Translational Science Award Program, through the NIH National Center for Advancing Translational Sciences, grant UL1TR000427. The authors would also like to thank the NIH (F30AR065838) and the Medical Scientist Training Program (T32GM008692).

References:

1. Topoleski TA, Kurtz CA, Grogan DP. Radiographic abnormalities and clinical symptoms associated with patella alta in ambulatory children with cerebral palsy. Journal of Pediatric Orthopaedics. 2000;20(5):636.

2. Gage J, Schwartz M, Koop S, Novacheck T. The Identification and Treatment of Gait Problems in Cerebral Palsy. 2 ed: John Wiley and Sons; 2009.

3. Lotman DB. Knee flexion deformity and patella alta in spastic cerebral palsy. Developmental Medicine & Child Neurology. 1976;18(3):315-9.

4. Novacheck TF, Stout JL, Gage JR, Schwartz MH. Distal Femoral Extension Osteotomy and Patellar Tendon Advancement to Treat Persistent Crouch Gait in Cerebral Palsy: Surgical Technique. The Journal of Bone and Joint Surgery (American). 2009;91-A(Supplement 2):271-86.

5. Flynn JM, Weisel SW. Operative Techniques in Pediatric Orthopaedics: LWW; 2010.

6. Ward SR, Terk MR, Powers CM. Influence of patella alta on knee extensor mechanics. Journal of Biomechanics. 2005;38(12):2415-22.

7. Sheehan FT, Seisler AR, Alter KE. Three-dimensional in vivo quantification of knee kinematics in cerebral palsy. Clinical Orthopaedics and Related Research. 2008;466(2):450-8.

8. Stout JL, Gage JR, Schwartz MH, Novacheck TF. Distal femoral extension osteotomy and patellar tendon advancement to treat persistent crouch gait in cerebral palsy. The Journal of Bone and Joint Surgery (American). 2008;90(11):2470-84.

9. Davis RB, Ounpuu S, Tyburski D, Gage JR. A gait analysis data collection and reduction technique. Human Movement Science. 1991;10(5):575-87.

10. Lenhart RL, Kaiser J, Smith CR. Prediction and validation of load-dependent behavior of the tibiofemoral and patellofemoral joints during movement. Annals of Biomedical Engineering. 2015;In press.

11. Blankevoort L, Huiskes R. Ligament-bone interaction in a three-dimensional model of the knee. Journal of biomechanical engineering. 1991;113(3):263-9.

12. Bei Y, Fregly BJ. Multibody dynamic simulation of knee contact mechanics. Medical engineering & physics. 2004;26(9):777-89.

13. Caruntu DI, Hefzy MS. 3-D anatomically based dynamic modeling of the human knee to include tibio-femoral and patello-femoral joints. Journal of biomechanical engineering. 2004;126(1):44-53.

14. Askew M, Mow V. The biomechanical function of the collagen fibril ultrastructure of articular cartilage. Journal of biomechanical engineering. 1978;100(3):105-15.

15. Shin CS, Chaudhari AM, Andriacchi TP. The influence of deceleration forces on ACL strain during single-leg landing: a simulation study. Journal of biomechanics. 2007;40(5):1145-52.

16. Segal NA, Anderson DD, Iyer KS, Baker J, Torner JC, Lynch JA, et al. Baseline articular contact stress levels predict incident symptomatic knee osteoarthritis development in the MOST cohort. Journal of orthopaedic research. 2009;27(12):1562-8.

17. Arnold EM, Ward SR, Lieber RL, Delp SL. A model of the lower limb for analysis of human movement. Annals of Biomedical Engineering. 2010;38(2):269-79.

18. Delp SL, Loan JP. A computational framework for simulating and analyzing human and animal movement. Computing in Science & Engineering. 2000;2(5):46-55.

19. Lu T-W, O'connor J. Bone position estimation from skin marker co-ordinates using global optimisation with joint constraints. Journal of biomechanics. 1999;32(2):129-34.

20. Lenhart RL, Smith CR, Vignos MF, Kaiser J, Heiderscheit BC, Thelen DG. Influence of Step Rate and Quadriceps Load Distribution on Patellofemoral Cartilage Contact Pressures during Running. Journal of Biomechanics 2015;In press.

21. Yamaguchi GT, Zajac FE. A planar model of the knee joint to characterize the knee extensor mechanism. J Biomech. 1989;22(1):1-10.

22. Miller F. Cerebral Palsy. 1 ed. New York: Springer-Verlag; 2005.

23. Steele KM, DeMers MS, Schwartz MH, Delp SL. Compressive tibiofemoral force during crouch gait. Gait & Posture. 2012;35(4):556-60.

24. Steele KM, van der Krogt MM, Schwartz MH, Delp SL. How much muscle strength is required to walk in a crouch gait? Journal of Biomechanics. 2012;45(15):2564-9.

Chapter 3

The effect of crouch and patella alta on tibiofemoral and patellofemoral pressures during walking

Rachel L. Lenhart, Colin R. Smith, Tom F. Novacheck, Michael H. Scwhartz, Darryl G. Thelen

Abstract:

In children with cerebral palsy, crouch gait, and patella alta, there is concern that increased tibiofemoral and patellofemoral pressures may contribute to pain, abnormal bony growth, and long term cartilage degeneration. Surgical procedures are often used to correct crouch and alta, but there is little quantitative understanding of how the magnitude of correction affects cartilage pressures. Therefore, we employed a novel musculoskeletal model with six degrees of freedom at both the tibiofemoral and patellofemoral joints to predict cartilage contact pressures across a range of walking postures (normal, mild, moderate, and severe crouch) and patellar positions (1 cm increments from 2 cm baja to 3 cm alta). Knee motion was predicted in the context of muscle, ligament, and contact forces with an enhanced static optimization technique. Cartilage contact pressures were calculated using penetration of the cartilage meshes and an elastic foundation model. The results showed that increasing crouch severity increased both tibiofemoral and patellofemoral pressures. Severe crouch had approximately 2 and 3 times greater mean tibial and patellar pressures during stance phase respectively than in mild crouch. Patellar position also affected patellar pressures, with alta reducing pressures in crouched postures. Walking in crouch also led to posterior migration of tibiofemoral contact location. This work highlights the importance of correcting crouch for the reduction in tibiofemoral and patellofemoral contact pressures, as well as the careful consideration of the final patellar position during correction of patella alta.

Introduction:

Crouch gait is a common abnormality in cerebral palsy, characterized by excessive knee flexion during gait. This form of walking is physically demanding, and is often associated with patellofemoral

pain (1-4). While it is generally thought that this pain is due to the large mechanical demands placed on the patellofemoral joint in crouch (2), we are not aware of prior investigations of the patellofemoral contact pressures that could arise during crouched walking. Further, patella alta (a superiorly displaced patella) is nearly universal in those with crouch (4-5), and an imaging study has suggested a relationship between the degree of patella alta and patellofemoral pain (6). Hence, the relationship between alta, crouch, and patellofemoral pressures seems important to explore. Prior studies have examined tibiofemoral loading in flexed postures (7-8) and crouch gait (9), with the latter study suggesting that tibiofemoral loadings are as much as ~2.2 times higher in severe crouch than normal walking (9). It is believed that crouch may also preferentially load the posterior tibia, given that many children with crouch gait often exhibit an abnormally posterior slope to their tibial plateau (10). However, traditional gait models lack the anatomical detail needed to predict knee pressure magnitude or location.

Knee cartilage pressures are also relevant to consider in the surgical treatment of crouch gait and patella alta. Patellar tendon advancement has recently been shown to improve gait in children with pre-operative crouch (11). However, final placement of the patella tends to be in baja, or inferior to the normal patellar position (11). It is unclear how this position affects patellar pressure magnitude or location. Further treatment of crouch with patellar tendon advancement has been shown to lead to a lessening of posterior tibal slope, especially in younger children (10). Questions still remain on whether or not this could be due to alterations in tibial loading patterns.

To address these questions using musculoskeletal modeling, we have developed a model with 6 degrees of freedom at both the tibiofemoral and patellofemoral joints (12) to allow prediction of cartilage pressures in children with patella alta and crouch gait. A benefit of this model is it includes the influence of muscle forces, ligamentous restraints, and cartilage contact, allowing us to predict how knee mechanics evolve during dynamic movements such as gait. We have previously validated this model against dynamic MRI (12) and have used it to predict patellofemoral pressures during running (13).

Hence, the objective of this study was to use our modeling framework to estimate the effect of walking posture and patellar position on tibiofemoral and patellofemoral pressures. To do this, we used retrospective gait analysis data to simulate the gait of a healthy adult with normal gait and 3 children with varying degrees of crouch. Our first goal was to determine the impact of patella alta and crouch on patellofemoral pressures during walking, with an intention of understanding the impact of patellar tendon advancement procedures. Second, we aimed to evaluate the hypothesis that tibiomfemoral pressures are concentrated more posteriorly during crouch gait, and thus could possibly contribute to an increased posterior slope.

Methods:

Gait from one healthy adult with no history of knee injury, surgery, or chronic pain (age 28 yrs, 60.4 kg mass, 1.68 m height) was obtained at the University of Wisconsin-Madison under a protocol approved by the Health Sciences Institutional Review Board. Appropriate written and informed consent was obtained before testing. The participant walked overground at self-selected pace (1.36 m/s), while an 8-camera passive motion capture system (Motion Ananlysis Corp, Santa Rosa, CA) tracked trajectories of 44 retroreflective markers placed on the body. In-ground force plates (AMTI, Watertown, MA) obtained ground reaction forces.

For children with crouch gait, retrospective gait analysis data was used from the database at Gillette Children's Specialty Healthcare. This data was collected as part of standard of care (14), and the use of it for research has been approved by the University of Minnesota Institutional Review Board. All children walked at their self-selected speeds and without assistive aids. Of the children with crouch gait, one was characterized as mild (minimum knee flexion during stance = 22 degrees, age 9.4 yrs, mass = 28.2 kg, height = 1.31 m, gait speed = 0.48 m/s), one as moderate (minimum = 29 degrees, age 11.0 yrs, mass = 28.7 kg, height = 1.43 m, gait speed = 1.12 m/s), and one as severe (minimum = 65 degrees, age 13.2 yrs, mass = 35.9 kg, height = 1.44 m, 0.82 m/s) (15). A 12-camera motion capture system (Vicon

Motion Systems, Lake Forest, CA) and four overground forceplates (AMTI) recorded maker trajectories and ground reaction forces.

A lower extremity musculoskeletal model, as described in Lenhart et al., was used for simulating knee mechanics in gait (12) (Fig. 1). The model includes 44 muscle-tendon actuators acting about the hip, knee and ankle, with the musculoskeletal geometry adapted from Arnold et al. (16)). A three-body knee model included 14 multi-stranded ligament bundles and cartilage contact between articulating surfaces in the tibiofemoral and patellofemoral joints. Ligament attachments and cartilage surfaces were reconstructed from MRI images of a healthy adult female (23 yrs, 61 kg, 1.65 m). Contact pressure was determined by cartilage mesh penetration and an elastic foundation model (17) (elastic modulus = 5 MPa (18-19), Poisson's ratio = 0.45 (18-21), combined cartilage surface thickness = 6 mm (i.e. 3 mm each) (22)). For this application, femoral cartilage geometry was extended to include the anterior femur, such that cases of alta could be simulated appropriately.

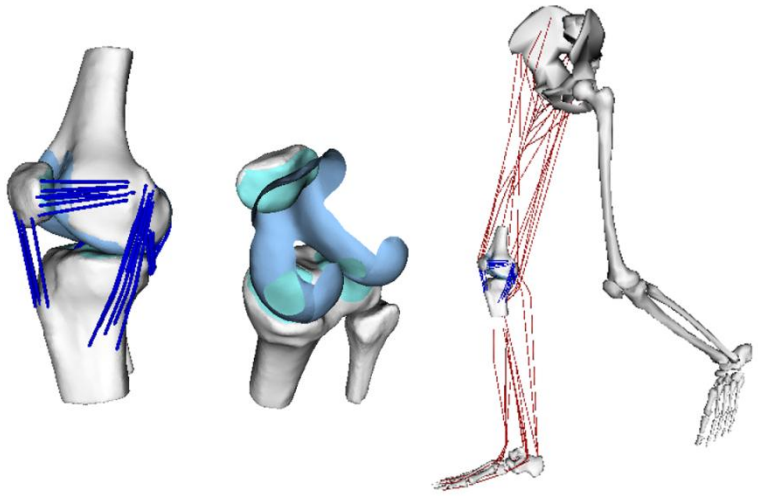

Figure 1: (Left) Close up of the three-body knee model that included descriptions of bony and cartilage geometries as well as ligament paths. (Middle) Penetration of the cartilage meshes determined contact forces and pressures at each frame of simulation. (Left) The knee was incorporated into the lower extremity musculoskeletal model of Arnold et al. (16).

For all subjects, the model was scaled based on segment lengths in a standing posture. The pelvis was the base segment with 6 degrees of freedom (dofs). The hip was modeled as a ball-in-socket joint with 3 dofs. The knee had 6 dofs at the tibiofemoral and patellofemoral joints. The ankle allowed plantar- and dorsiflexion with 1 degree of freedom. Inverse kinematics determined the joint ankles over the gait cycle using global optimization which minimized the discrepancy between the measured and predicted marker locations (23). During this routine, secondary tibiofemoral and all patellofemoral kinematics were estimated based on passive behavior of the model (12).

We used an enhanced static optimization (ESO) technique (13) to simultaneously solve for soft tissue, muscle, and contact forces at every frame of the gait cycles simulated. ESO estimates muscle activations and secondary knee kinematics (non-sagittal tibiofemoral angles, tibiofemoral translations, and all patellofemoral dofs) that minimized a cost function defined, *J*, as the weighted sum of squared muscle activations (a) and the net cartilage contact elastic energy ($U_{contact}$):

$$J = \sum_{i=1}^{m} V_i a_i^2 + W \cdot U_{contact} \qquad (1)$$

while satisfying dynamic equations of motion. Note that varying the secondary knee kinematics in ESO inherently alters both ligament loads and contact pressure patterns. In eq. (1), V is volume of muscle *i* (in units of mm^3), m is the number of muscles and W (=500) is the relative weight placed on the cost function. For each muscle, we assumed the force scaled linearly with activation and its assumed maximum isometric force capacity (i.e. $F_i = a_i F_{0i}$). The dynamic constraints required that the muscle forces together with the internal knee loads exactly produced the measured hip flexion, hip adduction, hip internal rotation, knee flexion, and ankle dorsiflexion accelerations while generating zero accelerations in the secondary tibiofemoral and all patellofemoral degrees of freedom. Pelvis position and accelerations were prescribed to experimental values, such that whole body dynamics were implicitly accounted for.

For each gait cycle, a passive forward simulation was used to determine the initial guess of locations for the first frame of the optimization, which was selected to be a frame of swing before heel strike. Our ESO solution technique was to linearize the above optimization problem such that the constraints are linear in both muscle activations and secondary degrees of freedom. After solving, we adjusted the muscle activations and secondary kinematics of the knee, and then resolved the linearization optimization problem iteratively until we converged on a solution that satisfied the full nonlinear constraints described above. In practice, the ESO solves fairly quickly such that a full cycle of gait is analyzed in ~5 minutes on a standard desktop computer.

Simulations were re-run with patellar positions ranging from 2 cm of patella baja to 3 cm of patella alta (Fig 2). For each simulation, patellofemoral and tibiofemoral contact location and magnitude information were extracted across each of the walking cycles.

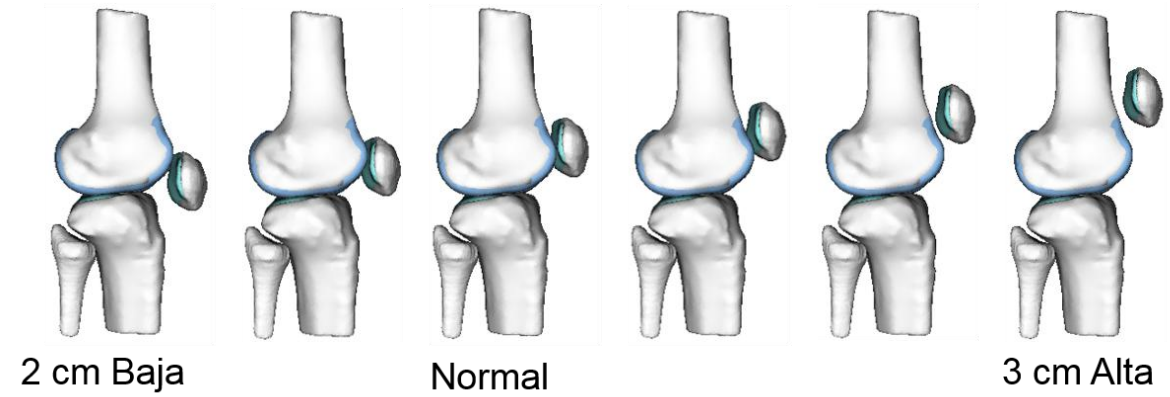

Figure 2: Demonstration of different patellar positions tested. Note that before running the enhanced static optimization, a passive simulate ion determined the configuration of the knee in the initial frame in order to ensure appropriate contact between the patella and distal femur.

Results:

Quadriceps, tibiofemoral, and patellofemoral forces all increased with crouch severity, but by differing amounts (Fig. 3). Quadriceps (sum of vastii and rectus femoris) forces increased over seven-fold in severe crouch as compared to normal walking, reaching magnitudes of 8.1 times body weight (BW) during stance (vs. 1.1 BW in normal). Similarly, patellofemoral force increased dramatically with crouch, with peak loads of 0.7, 1.4, 2.9 and 6.3 times body weight in normal, mild, moderate and severe crouch, respectively. While peak tibiofemoral forces in normal (3.2 BW) and mild (2.8 BW) crouch were of similar magnitude, the changes to the moderate (4.3 BW) and severe (6.1 BW) conditions were more substantial.

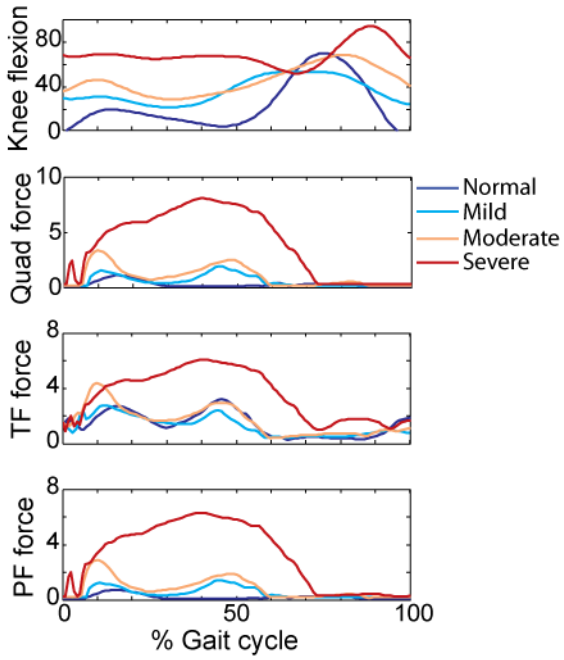

Figure 3: Knee flexion angle and quadriceps (Quad, sum of vastii and rectus femoris forces), tibiofemoral (TF) and patellofemoral (PF) forces across the gait cycle for different walking postures at the normal patellar position. All forces are all expressed as Newtons per body weight.

Similar to the PF loading, patellar contact pressure increased with crouch gait severity (Fig. 5). However, the patellar position that minimized patellofemoral pressure was posture-dependent. For normal walking, slight patella baja (1 cm) induced the lowest mean patellar pressures over the gait cycle (0.86 MPa) and at the first peak of the ground reaction force (1.7 MPa) (Fig 5). In moderate crouch, minimum mean patellar pressures occurred at the normal patellar position (1.6 MPa), or at 1 cm of alta at the first peak of the ground reaction force (2.4 MPa). In severe crouch, mean pressures in stance (3.9 MPa) and at the first peak (4.6 MPa) PF pressures were minimal with 2 cm of alta.

Both crouch and patellar position influenced the location of patellofemoral contact pressures (Fig. 4). In a normal patellar position, moderate and severe crouch induced 3.2 and 8.0 mm of superior migration in the patellar center of pressure averaged over stance as compared to the normal and mild conditions. However the location of patellar pressure in crouch was normalized by introducing 1 cm of alta in moderate crouch, and ~2 cm of alta in severe crouch.

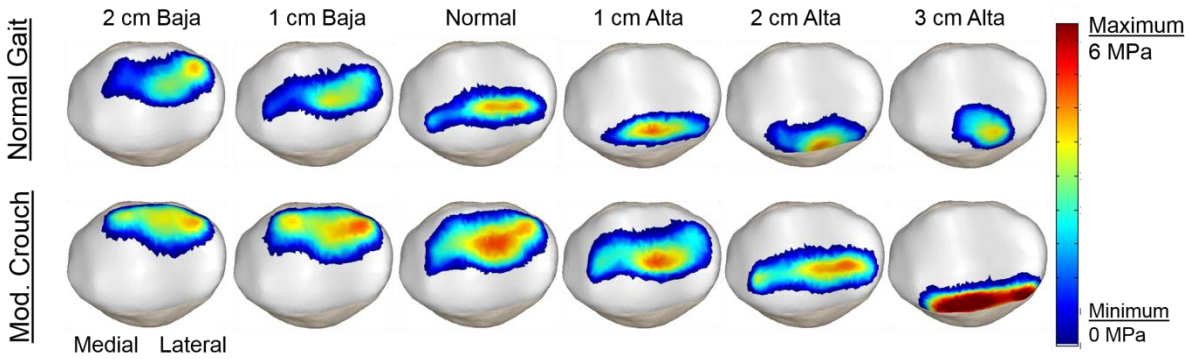

Figure 4: Patellofemoral pressures during normal and moderate crouch gait with a variety of patellar positions at the first peak in the ground reaction force. In the moderate crouch, 1 cm of patella induced minimum pressures at this time point, while 1 cm of baja led to lowest pressures during normal walking.

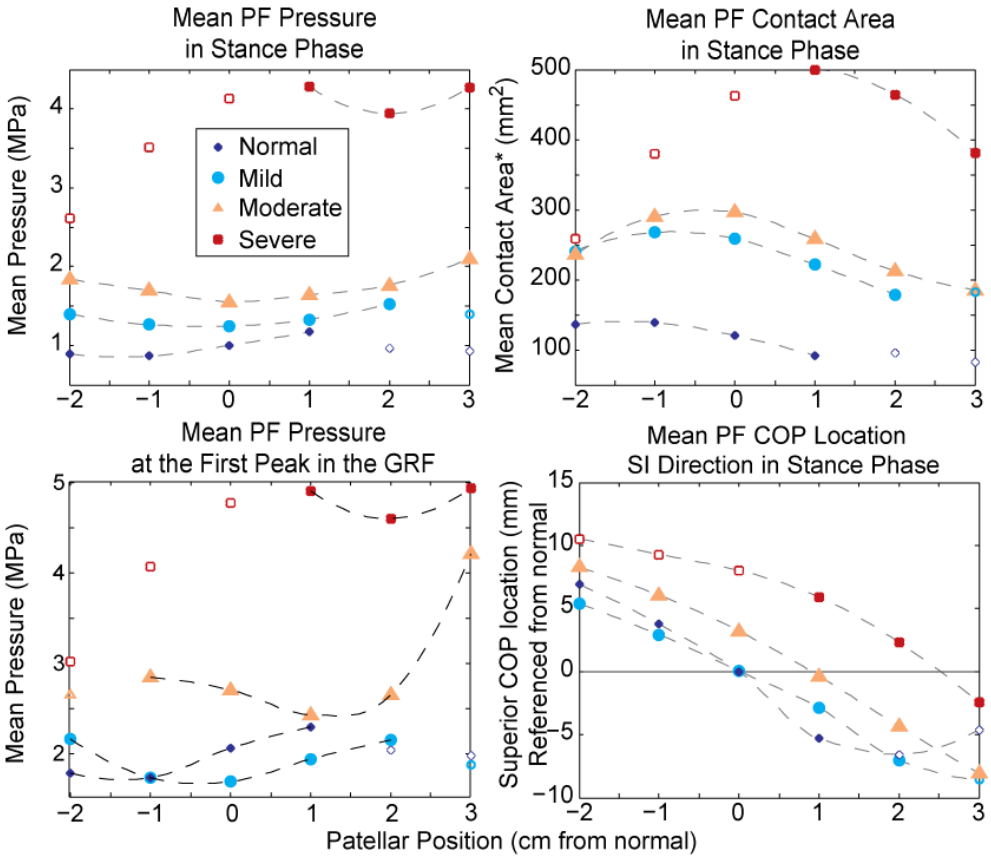

Figure 5: Patellofemoral (PF) contact metrics calculated for different walking postures and patellar positions. Patellar position is referenced from normal, such that -2 is equal to 2 cm of baja and +2 is 2 cm of alta. Mean PF pressures are given both averaged over stance phase (top left) and at the first peak in the ground reaction force (GRF) (bottom left). The contact area (top right) for crouch conditions is *multiplied by the ratio of total cartilage area in the normal adult to that of the particular child walking with crouch to account for size differences. The contact center of pressure (COP) location (bottom right) in the superior-inferior (SI) direction is given referenced to the location determined for the normal walking posture and normal patellar position (0 cm). Open symbols represent simulations in which there was wrapping of the quadriceps tendon over the distal femur (extreme baja positions), or wrapping of the patellar tendon over the distal femur and/or distal patellar penetration into femoral mesh (extreme alta positions). Data points with wrapping or abnormal penetration are omitted from the curve fits shown.

Tibiofemoral (TF) pressures increased with crouch severity, though the results varied over the gait cycle (Fig. 6). At the normal patellar position, mean pressures averaged over the stance phase of normal gait were 2.5 MPa (Fig. 7). Comparing the crouch gait conditions, mean TF pressures increased markedly from mild (2.0 MPa) and moderate (2.4 MPa) to severe (4.0 MPa) crouch gait. Alterations in patellar position had a much smaller influence on tibiofemoral pressures across the walking cycle as compared to walking posture, with all crouch conditions changing mean pressure by 0.2 MPa or less across the range of patellar positions considered. Increasing crouch severity led to a posterior migration of the tibiofemoral center of pressure location. When considering the case of normal patellar position, the tibiofemoral contact location in severe crouch gait tended to be 5.7 mm posterior to the location in the mild crouch gait condition. Patellar position had a larger impact on the center of pressure locations in the more severe crouch cases.

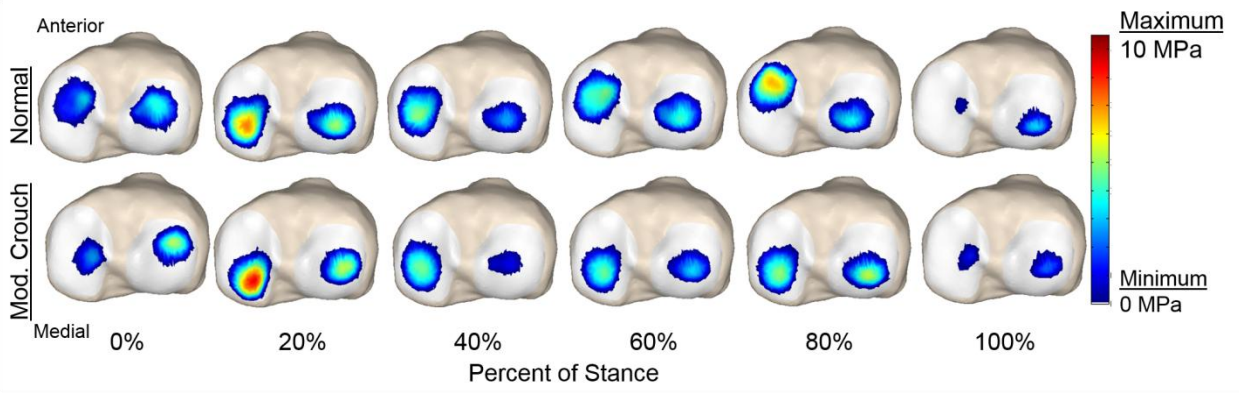

Figure 6: Tibiofemoral pressures over stance phase for normal and moderate crouch gait. Both representative gait cycles exhibited a peak on the medial plateau in the first half of stance, but the moderate crouch case exhibited more even pressure distribution in the second half of stance.

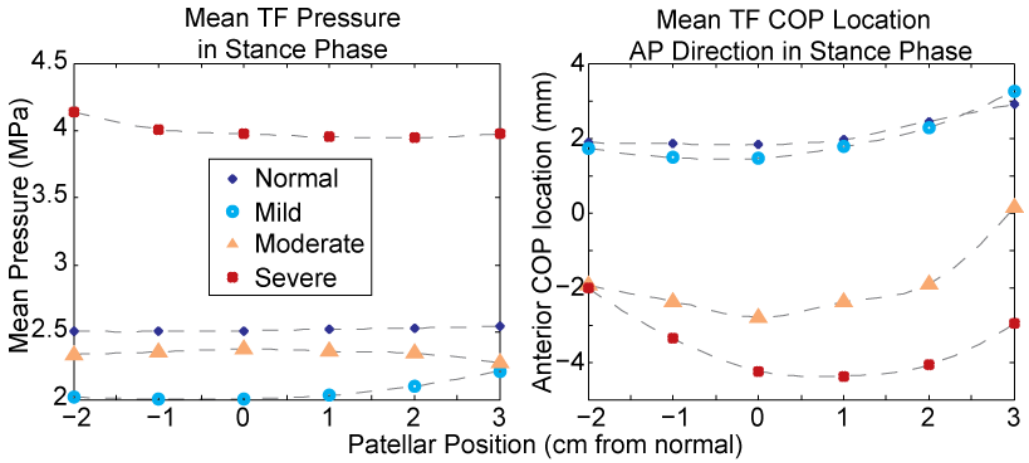

Figure 7: Tibiofemoral (TF) mean pressures and center of pressure (COP) location in the anterior direction over the stance phase of gait for a variety of patellar positions and walking postures. Patellar positions are given in cm from normal patellar position in the nominal unscaled model, such that -2 is equal to 2 cm of patella baja, while +2 is equal to 2 cm of patella alta.

Discussion:

The goal of this project was to determine the effect of patellar position and a crouched walking posture on patellofemoral and tibiofemoral pressures during walking. We found that both patellofemoral and tibiofemoral pressures increase with crouch severity, but patellofemoral pressures exhibit larger changes. Patellar position also altered the magnitude and location of patellofemoral contact. Interestingly, the models suggest that alta may actually be mechanically beneficial in crouch since it acts to slightly reduce pressure magnitudes and normalize contact location. Tibiofemoral pressures also migrated posteriorly with increasing crouch severity, a factor which could affect skeletal growth and give rise to posteriorly sloped tibial plateaus. Hence, changes in these pressures should be considered when surgically treating a child with crouch gait.

Our estimates of net knee loads are generally consistent with prior studies. Steele and others found that increasing crouch severity increased tibiofemoral contact forces during walking, with values very similar to the ones we found (Steele et al. findings: Normal gait = 3.0, mild = 3.2, moderate = 4.2, severe = 6.5 times body weight) (9). The patellofemoral force during normal walking has been estimated between 0.5 and 1 N times BW (24-25), and during stair climbing between 3.3 and 3.5 times BW (24-25), similar to our normal and moderate crouch findings. Some in vivo work has tried to assess the effect of crouch gait on contact forces. Kinney and others sought to determine how crouch gait changed contact forces in an older adult wearing an instrumented total knee replacement (26). They found that mild and moderate crouch increased contact forces in the medial compartment by 4 and 13% over the gait cycle, while reducing contact forces in the lateral compartment by 12 and 9%.

It is recognized that joint contact pressures may directly contribute to patellofemoral pain and abnormal skeletal growth in children who exhibit crouch. However despite this clinical relevance, we are not aware of prior investigations of knee cartilage pressures in crouch gait. In normal walking, tibiofemoral and patellofemoral pressures during normal walking have been estimated to be between 1.7-3.1 MPa (27) and 2.4 MPa (28-29), respectively, which are comparable to estimates in this study. While both tibiofemoral and patellofemoral pressure magnitudes increase in crouch, our models suggest the effect on patellofemoral joint is more dramatic with patellofemoral forces growing more than five-fold from normal to severe crouch. The differential effect on the patellofemoral joint is attributable to the more flexed knee posture creating a more acute angle between the quadriceps and patellar tendons, which directly increases the contact load at the patellofemoral joint (30-31). Similar effects are present in stair climbing, where the patellofemoral pressure estimates (4-5 MPa) (32) are comparable to that seen in our severe crouch condition. While crouch-induced increases in TF pressure were more modest, there was a marked posterior migration of the contact location on the tibial plateaus in moderate and severe crouch ((Fig. 7). This result lends credence to the belief that abnormal mechanical loading of tibiofemoral joint may contribute to the posterior tibial slope (10).

This work has implications for the surgical treatment of crouch gait. First, our analysis of patellar position effects would suggest that patella alta may actually be mechanically beneficial when walking in crouch. Specifically, our models suggest that patella alta both reduces patellar pressure magnitudes and normalizes patellar contact location. The former effect seems to be attributable to the enhanced patellar tendon and quadriceps moment arms that arise with patella alta in flexed knee postures (See Chapter 2). Current crouch gait treatments often include a patellar tendon advancement (PTA) surgery to correct an extension deficit and/or to tighten the quadriceps when performed in conjunction with a distal femoral osteotomy. The procedure concurrently corrects patella alta by relocating the patella inferiorly. Our models show that a normal patellar position can enhance moment arms and reduce contact pressures in normal gait, suggesting the final patellar position should be carefully chosen. Current PTA procedures often leave children in patella baja. While baja might lead to reasonable pressures during walking, this position can result in abnormally large and superior patellar pressures if the child exhibits residual crouch (Fig. 5 and 6). Baja may also be problematic when a child attempts activities requiring strength in flexed postures, such as getting out of a chair or climbing stairs, as these activities will likely also generate these high pressures. There are also salient effects of crouch gait treatment on tibiofemoral loading to consider. In particular, changes in tibial plateau loading has implications for long-term cartilage health (33) and skeletal growth in developing children (10). Indeed, a prior study found that children who were treated with a distal femoral extension osteotomy for crouch exhibited a reduction in the posterior tibial slope, (10), which our models would suggest could arise from the contact pressure moving anteriorly on the tibial plateau as a more upright gait is achieved (Fig. 6).

This work has several limitations which should be acknowledged. First, we used a generic model with geometries based on a single healthy adult. It is known that those with cerebral palsy have abnormalities, such as femoral anteversion and an abnormal tibial slope, which may affect results. We only used 4 subjects for this analysis, and some variation in joint load estimates likely exists due to the particular walking pattern that a subject adopts. Hence while our results provide fundamental insight into

the overall effects of differing gait severity, there is a need to consider more subjects to assess how robust the pressure patterns are across subjects. Another limitation is comparing normal adult gait to children with cerebral palsy. Scaling our model to the size of a child likely has unintended effects that makes comparison of our adult to the children difficult, especially at the tibiofemoral joint. Here we have tried to emphasize our comparisons among the crouch gait conditions, but future work will compare the crouched gait with normal gait from age- and sized-matched typically developing children. Also, the pressure predictions are limited by the assumption of uniform cartilage properties. In the future, we will add in variable cartilage thickness based on our MR images, as well as variable mechanical properties, to account for cartilage-on-bone contact that is occurring with extreme alta. Finally, our modeling efforts necessarily rely on optimization techniques (Eq. 1) to resolve muscle redundancy when estimating internal soft tissue loads. Given that muscle forces aren't directly measurable, it is not possible to directly validate this aspect of our analysis. For this reason, our analysis is designed to primarily looking at sensitivities of tissue loading to variations in patellar position while maintaining the same assumed muscle redundancy. We utilized different optimization routines to resolve muscle redundancy and found that while it changed the absolute load estimates, the general effects of crouch and patellar position were not dependent on the redundancy assumptions.

In conclusion, we have shown that walking posture substantially effects on knee joint loadings during walking, with crouch postures dramatically increasing patellofermoal contact pressures and inducing a posterior migration of the tibiofemoral contact. While patella alta seems to diminish patellofemoral contact pressures in crouch, both alta and baja positions can give rise to high and abnormally located pressure patterns in more upright gait. These findings have important implications for the surgical treatment of crouch gait.

Acknowledgements:

This work was supported in part by the Clinical and Translational Science Award Program, through the NIH National Center for Advancing Translational Sciences, grant UL1TR000427. The authors would also like to thank the NIH (F30AR065838) and the Medical Scientist Training Program (T32GM008692).

References:

1. Gage J, Schwartz M, Koop S, Novacheck T. The Identification and Treatment of Gait Problems in Cerebral Palsy. 2 ed: John Wiley and Sons; 2009.

2. Senaran H, Holden C, Dabney KW, Miller F. Anterior knee pain in children with cerebral palsy. Journal of Pediatric Orthopaedics. 2007;27(1):12-6.

3. Miller F. Cerebral Palsy. 1 ed. New York: Springer-Verlag; 2005.

4. Topoleski TA, Kurtz CA, Grogan DP. Radiographic abnormalities and clinical symptoms associated with patella alta in ambulatory children with cerebral palsy. Journal of Pediatric Orthopaedics. 2000;20(5):636.

5. Lotman DB. Knee flexion deformity and patella alta in spastic cerebral palsy. Developmental Medicine & Child Neurology. 1976;18(3):315-9.

6. Sheehan FT, Babushkina A, Alter KE. Kinematic Determinants Of Anterior Knee Pain In Cerebral Palsy, A Case-Control Study. Archives of Physical Medicine and Rehabilitation. 2012;93(8):1431-40.

7. Perry J, Antonelli D, Ford W. Analysis of knee-joint forces during flexed-knee stance. The Journal of Bone & Joint Surgery. 1975;57(7):961-7.

8. Thambyah A, Goh JC, De SD. Contact stresses in the knee joint in deep flexion. Medical engineering & physics. 2005;27(4):329-35.

9. Steele KM, DeMers MS, Schwartz MH, Delp SL. Compressive tibiofemoral force during crouch gait. Gait & Posture. 2011.

10. Patthanacharoenphon C, Maples D, Saad C, Forness M, Halanski M. The Effects of Patellar Tendon Advancement on the Proximal Tibia. Journal of Children's Orthopaedics. 2013;7(2):139-46.

11. Stout JL, Gage JR, Schwartz MH, Novacheck TF. Distal femoral extension osteotomy and patellar tendon advancement to treat persistent crouch gait in cerebral palsy. The Journal of Bone and Joint Surgery (American). 2008;90(11):2470-84.

12. Lenhart RL, Kaiser J, Smith CR. Prediction and validation of load-dependent behavior of the tibiofemoral and patellofemoral joints during movement. Annals of Biomedical Engineering. 2015;In press.

13. Lenhart RL, Smith CR, Vignos MF, Kaiser J, Heiderscheit BC, Thelen DG. Influence of Step Rate and Quadriceps Load Distribution on Patellofemoral Cartilage Contact Pressures during Running. Journal of Biomechanics 2015;In press.

14. Davis RB, Ounpuu S, Tyburski D, Gage JR. A gait analysis data collection and reduction technique. Human Movement Science. 1991;10(5):575-87.

15. Steele KM, Seth A, Hicks JL, Schwartz MH, Delp SL. Muscle contributions to vertical and fore-aft accelerations are altered in subjects with crouch gait. Gait & Posture. 2013;38(1):86-91.

16. Arnold EM, Ward SR, Lieber RL, Delp SL. A model of the lower limb for analysis of human movement. Annals of Biomedical Engineering. 2010;38(2):269-79.

17. Bei Y, Fregly BJ. Multibody dynamic simulation of knee contact mechanics. Medical engineering & physics. 2004;26(9):777-89.

18. Blankevoort L, Huiskes R. Ligament-bone interaction in a three-dimensional model of the knee. Journal of biomechanical engineering. 1991;113(3):263-9.

19. Caruntu DI, Hefzy MS. 3-D anatomically based dynamic modeling of the human knee to include tibio-femoral and patello-femoral joints. Journal of biomechanical engineering. 2004;126(1):44-53.

20. Shin CS, Chaudhari AM, Andriacchi TP. The influence of deceleration forces on ACL strain during single-leg landing: a simulation study. Journal of biomechanics. 2007;40(5):1145-52.

21. Askew M, Mow V. The biomechanical function of the collagen fibril ultrastructure of articular cartilage. Journal of biomechanical engineering. 1978;100(3):105-15.

22. Segal NA, Anderson DD, Iyer KS, Baker J, Torner JC, Lynch JA, et al. Baseline articular contact stress levels predict incident symptomatic knee osteoarthritis development in the MOST cohort. Journal of orthopaedic research. 2009;27(12):1562-8.

23. Lu T-W, O'connor J. Bone position estimation from skin marker co-ordinates using global optimisation with joint constraints. Journal of biomechanics. 1999;32(2):129-34.

24. Chen Y-J, Scher I, Powers CM. Quantification of patellofemoral joint reaction forces during functional activities using a subject-specific three-dimensional model. J Appl Biomech. 2010;26(4):415-23.

25. Reilly DT, Martens M. Experimental analysis of the quadriceps muscle force and patello-femoral joint reaction force for various activities. Acta Orthopaedica. 1972;43(2):126-37.

26. Kinney AL, Besier TF, Silder A, Delp SL, D'Lima DD, Fregly BJ. Changes in in vivo knee contact forces through gait modification. Journal of orthopaedic research. 2013;31(3):434-40.

27. Mamat N, Nor M, Osman NAA, Oshkour A, editors. Numerical measurement of contact pressure in the tibiofemoral joint during gait. Biomedical Engineering (ICoBE), 2012 International Conference on; 2012: IEEE.

28. Powers CM, Ward SR, Chen Y-j, Terk MR. The effect of bracing on patellofemoral joint stress during free and fast walking. The American journal of sports medicine. 2004;32(1):224-31.

29. Ward SR, Powers CM. The influence of patella alta on patellofemoral joint stress during normal and fast walking. Clinical Biomechanics. 2004;19(10):1040-7.

30. Hefzy M, Yang H. A three-dimensional anatomical model of the human patello-femoral joint, for the determination of patello-femoral motions and contact characteristics. Journal of biomedical engineering. 1993;15(4):289-302.

31. Hirokawa S. Three-dimensional mathematical model analysis of the patellofemoral joint. Journal of biomechanics. 1991;24(8):659-71.

32. Powers CM, Ward SR, Chen Y-J, Terk MR. Effect of bracing on patellofemoral joint stress while ascending and descending stairs. Clinical Journal of Sport Medicine. 2004;14(4):206-14.

33. Andriacchi TP, Mündermann A, Smith RL, Alexander EJ, Dyrby CO, Koo S. A framework for the in vivo pathomechanics of osteoarthritis at the knee. Annals of Biomedical Engineering. 2004;32(3):447-57.

Chapter 4

The Effect of Distal Femoral Extension Osteotomy on Muscle Lengths after Surgery

Rachel L. Lenhart, Michael H. Schwartz, Tom F. Novacheck, Darryl G. Thelen

Abstract:

The distal femoral extension osteotomy (DFEO) is a surgical procedure often used in the treatment of crouch gait. The procedure removes a wedge of bone and creates an extension deformity of the distal femur, thereby compensating for static knee flexion contractures that often exist in children who exhibit crouch. However, the effects of DFEO on skeletal and muscle lengths are incompletely understood, but are important determinants of post-surgical function. Therefore, the purpose of this study was to investigate the changes in femur, quadriceps, and hamstring lengths with DFEO, and to determine the sensitivity to surgical factors such as DFEO wedge apex location and magnitude. The analysis suggests that DFEO shortens the femur, quadriceps, and hamstrings relative to lengths seen in an extended posture. However relative to a contracted posture, DFEO tends to lengthen the hamstrings. Muscle lengths were more sensitive to anterior wedge apex location than superior location. These results are consistent with the clinically observed need for simultaneous patellar tendon advancement (PTA) to re-tighten the quadriceps following DFEO. Hence, these findings highlight the importance of considering surgical parameters and concurrent surgeries when planning treatments for crouch gait.

Introduction:

Crouch gait is a common gait abnormality in cerebral palsy, especially as children reach adolescence (1). Historically, crouch has been challenging to treat, and recurrence is common (2-3). The distal femoral extension osteotomy and patellar tendon advancement are surgical procedures recently advocated to be performed simultaneously in the treatment of crouch gait (4). The procedures have been shown to improve gait kinematics, especially at the knee joint (5).

Despite these benefits, many questions regarding the specifics of the procedure remain. Several of those questions revolve around location and magnitude of the DFEO wedge and its effects on muscle lengths (6). Cuneiform wedges are suggested in the case of larger contractures to help avoid neurovascular compromise in the posterior compartment (4). However, the amount of stretch and the ideal amount of femoral shortening has not been quantified.

Musculoskeletal modeling can be used to simulate deformities and the surgical procedures used to treat pediatric gait disorders. For example, prior studies have investigated the influence of crouch postures and bony deformities on muscle lengths and moment arms (7-8). Further, musculoskeletal models can be coupled with computational dynamics to simulate the functional implications both gait disorders and treatments (9). However, most models to date do not include sufficient anatomical complexity and degrees of freedom at the knee to fully capture the effects of an extension osteotomy. We have recently introduced a novel musculoskeletal model that includes 6 degrees of freedom (dof) at the tibiofemoral and patellofemoral joints (10). This model incorporates the effects of contact and ligamentous constraints and has been validated against in vivo measures of tibiofemoral and patellofemoral motion during unloaded and loaded activities.

The objective of this study was to use this model to determine the effects of a knee flexion contracture and DFEO procedure on femur, quadriceps, and hamstrings lengths. To do this, we first tightened the posterior capsule ligaments to simulate a contracture. Then the DFEO was virtually performed and the post-surgical mechanical behavior of the knee was determined. A sensitivity study was performed to assess outcomes with different DFEO wedge locations and magnitudes. We hypothesized that the DFEO would both shorten the quadriceps and hamstrings compared to the upright position, however hamstrings length would increase from the contracted position.

Methods:

The surgical procedure has been detailed by Novacheck, et al. (4), but will be described briefly here. First an anterior wedge of bone is removed from the distal femur with the same magnitude as the knee flexion contracture (Fig. 1). The distal cut for the wedge is placed parallel to the tibia (which is flexed relative to the femur due to the contracture), and the proximal cut is placed perpendicular to the femoral shaft. The wedge apex location can be varied, such that either a triangular wedge is created if the apex is at the posterior surface of the femur or a cuneiform wedge is created if the apex is more posterior. Just prior to creation of the distal cut, a chisel is placed 5-10 mm more distal and parallel to the intended cut plane. This chisel location will later become the location of the fixation plate (blue structure in Fig. 1). A rotation about the wedge apex and a translation along the proximal cut plane are completed such that the fixation plate lines up with the femoral shaft. The goal is to maintain the knee flexion-extension axis in the nominal anterior-posterior location.

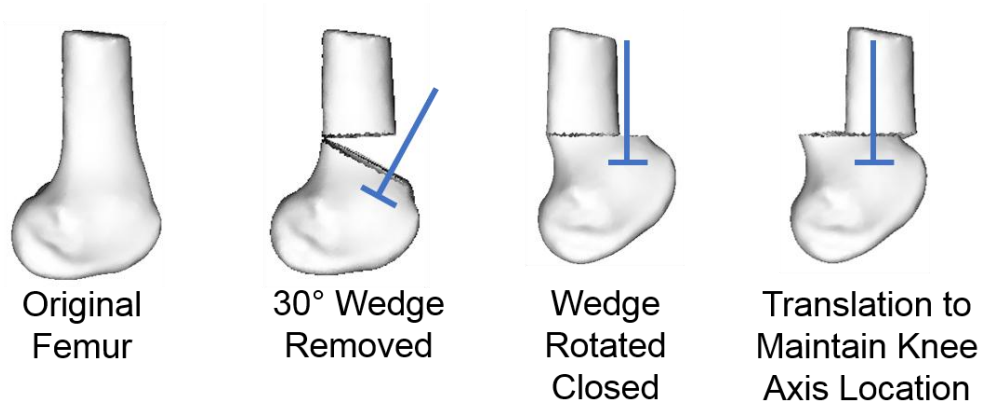

Figure 1: Demonstration of a 30 degree DFEO procedure. A 30 degree wedge is removed from the femur. Then based on the placement of the chisel/fixation plate location (represented by the blue structure), the wedge is rotated and translated to achieve a similar knee flexion extension axis.

The creation of the lower extremity model with 6 dof tibiofemoral and patellofemoral joints has been described elsewhere (10). In brief, we used bone and cartilage geometries and ligament path descriptions from MR images of a healthy adult female (mass 61 kg, height 1.65 m) to create a 3 body knee model (Fig. 2). Sets of non-linear spring elements (11) forming the 14 ligament bundles connected ligament origins and insertions. Cartilage contact pressures were determined by the penetration of the cartilage meshes and an elastic foundation model (12). The cartilage properties were assumed based on literature values (elastic modulus = 5 MPa (11, 13), Poisson's ratio = 0.45 (11, 13-15), combined cartilage surface thickness = 6 mm (i.e. 3 mm each) (16)). This knee model was then inserted this model into a lower extremity model from the literature that included 44 musculotendon units acting about the hip, knee, and ankle (17). We should note that this formulation allowed for knee mechanics to evolve naturally, as functions of the muscle, ligament, contact, inertial, and external forces.

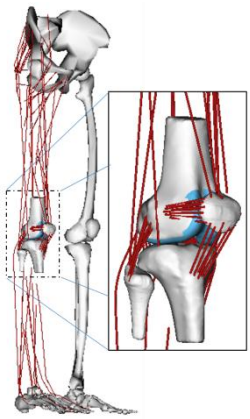

Figure 2: Model of the lower extremity used in this work.

To better replicate the functional state of a child with crouch gait, the model was altered to include a knee flexion contracture. The reference strain of the posterior capsule bundles were increased such that the knee remained flexed to 30 degrees even when a 5 Nm torque was applied during a passive forward simulation.

To model the DFEO, we virtually translated and rotated the distal femoral segment relative to the proximal femur (Fig. 3). To do this, an anterior wedge of bone was removed and the distal fragment was rotated about the wedge apex to close the wedge, and then the distal fragment was translated such that the knee axis remained at the same anterior-posterior location, as described above. The articular cartilage surfaces and ligament origins and insertions were retained as they were in the pre-surgical state. For each procedure, a passive forward simulation was run in which muscles were assumed to be minimally active (1% activation level). Simulations were continued until both the tibiofemoral and patellofemoral joints settled into new equilibrium configurations. The new lengths of the quadriceps and hamstrings were determined and compared to the lengths of these muscles in the nominal model as well as to their length in the case of knee flexion contracture.

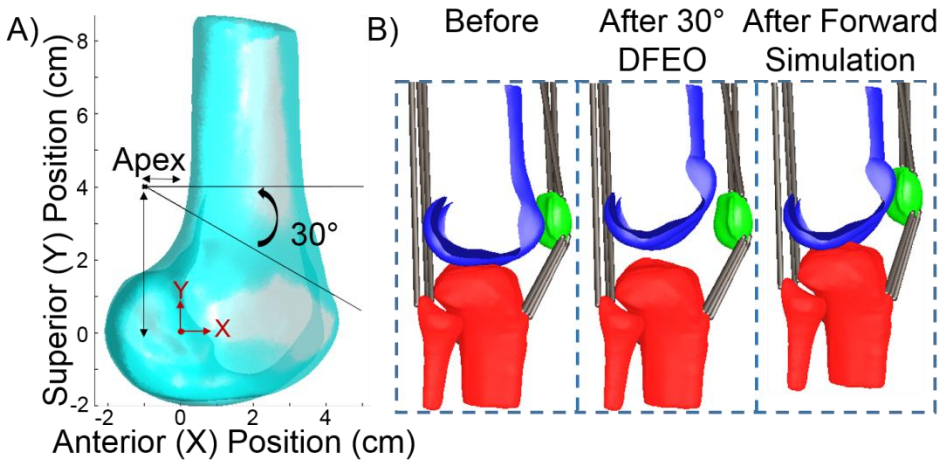

Figure 3: A) Creation of the DFEO wedge. Sensitivity analyses were conducted by moving the wedge apex in the anterior-posterior and superior-inferior directions as well as by changing the size of the wedge. B) The femur is shown before being virtually cut. Then, the altered orientations of the distal femur shows results after removal of 30 degree anterior wedge from A, and after forward simulation to close the resultant gap between bones.

To determine the sensitivity to wedge apex location, the superior and anterior locations of the wedge apex were modified and the simulations re-run. To determine the sensitivity to wedge magnitude, the wedge angle was modified between 10 and 30 degrees in 10 degree increments.

Results:

Varying the anterior location of the apex of the DFEO wedge had a larger effect on femur and muscle lengths than varying the superior position (Fig. 4). The osteotomy tended to increase semimembranosus (SM) lengths compared to their state in a contracted posture, though they were shorter than lengths that would occur in a fully extended knee. Vastus medialis (VM) lengths were substantially reduced compared to that seen in both extended and contracted postures pre-surgically.

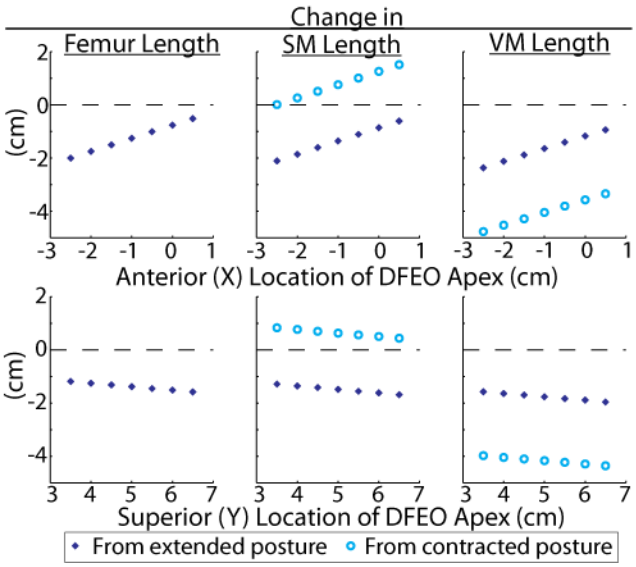

Figure 4: Change in femur, semimembranosus (SM), and vastus medialis (VM) lengths between the original model and model with DFEO performed. Muscle lengths are referenced to the model both in an extended posture and to the model with a 30 degree knee flexion contracture. Nominal Y location for the DFEO wedge was 4.0 cm, and X location was -1.0 cm.

The same trends held if the wedge angle was less than 30 degrees, though the magnitude of change was altered (Fig. 5). Shifting the superior location of the wedge had only a very minor effect on muscle lengths when the wedge angle was 10 degrees, with lengths changing less than 0.02 cm for every centimeter of change in location.

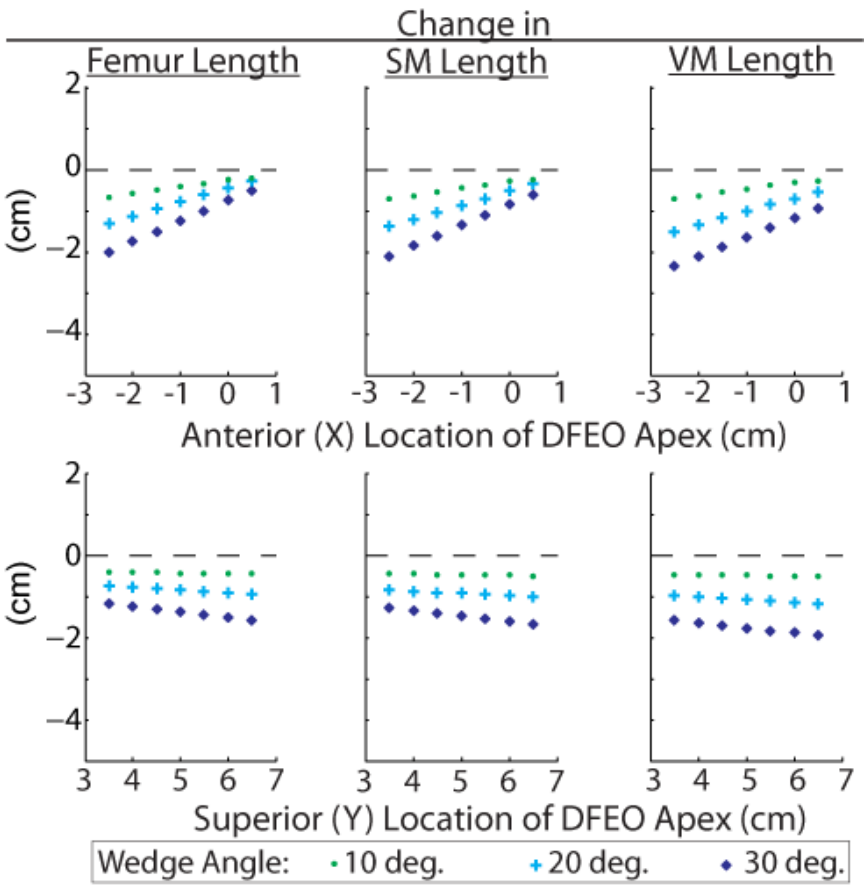

Figure 5: Change in femur, semimembranosus (SM), and vastus medialis (VM) lengths with changes in wedge apex location and magnitude. Changes are from an extended posture. Nominal apex location is Y = 4.0 cm, X = -1.0 cm.

Simply closing the wedge by rotating the distal fragment around the cut apex translates the knee axis anteriorly, so posterior translation is needed maintain the knee axis position. The superior-inferior

location of the wedge apex location had a larger effect on the distance needed to translate the distal segment to keep the knee axis at the same anterior-posterior location (Fig. 6). A 1.0 cm change in the superior location of the apex changes the translation distance (or chisel location) by 0.5 cm. In contrast, a 1.0 cm change in the anterior location of the apex needed a 0.1 cm change in translation.

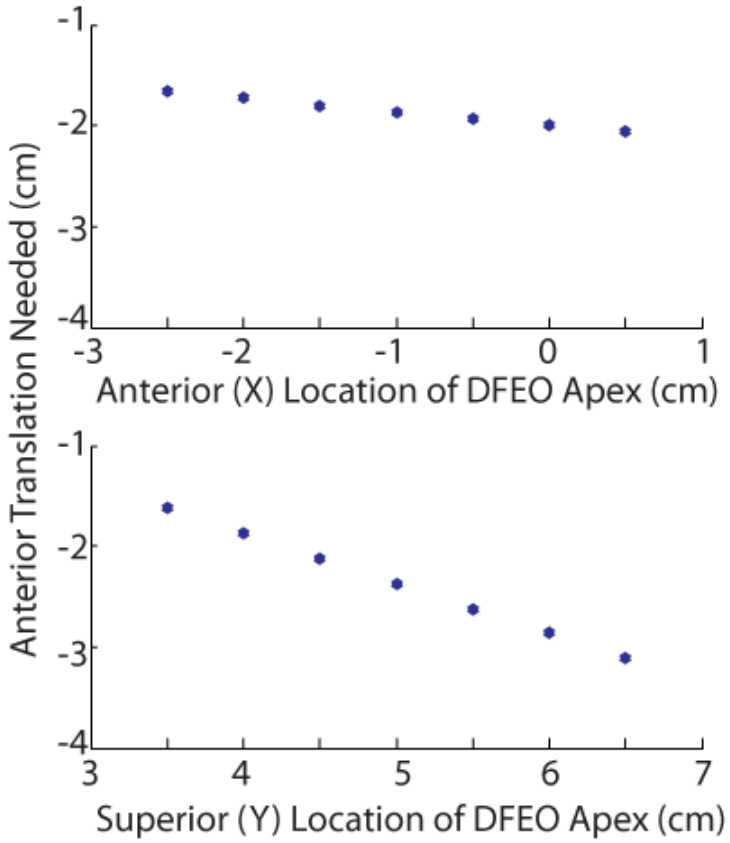

Figure 6: Posterior translation of the distal fragment after rotation for different wedge apex locations. Nominal Y location for the DFEO wedge was 4.0 cm, and X location was -1.0 cm. The magnitude of these changes also represents how far anterior the knee axis would be if the wedge was simply closed with no translation.

For the nominal wedge condition, changing the amount of posterior translation after rotation of the distal fragment around the wedge apex had a small affect on muscle lengths. No translation led to

more lengthening of the hamstrings from the contracted position, but less quadriceps shortening. The translation had a larger effect on quadriceps lengths than hamstrings lengths (Fig. 7). A posterior translation of 2.5 cm changed the hamstrings lengths by 0.2 cm compared to no posterior translation, while the quadriceps lengths changed by 0.4 cm from no translation. The effects were non-linear.

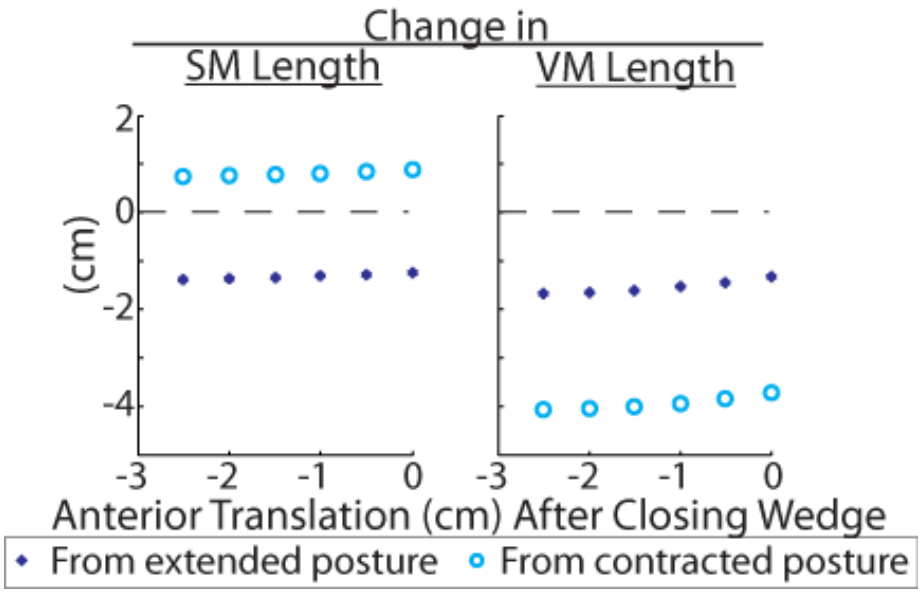

Figure 7: Changes in semimembranosus (SM) and vastus medialis (VM) lengths with differences in the posterior translation of the distal fragment. These changes are for a wedge of X=-1.0 cm, Y= 4.0 cm, and angle 30 degrees.

Discussion:

The aim of this project was to examine the effect of wedge location and magnitude on femur and muscle lengths after DFEO surgery. The results show that changing the anterior-posterior location of the wedge had a much larger effect on muscle and femur lengths than changing the superior-inferior location. However, changing the super-inferior position had a much larger effect on the knee axis location, with higher positions requiring more translation after rotation. Similar trends held for changes in muscle

lengths held when the wedge angles were changed, but with a lesser magnitude. Posterior translation also had a small effect on muscle lengths. These relationships are important for surgeons to understand when completing a DFEO as part of the treatment of crouch gait.

Several other studies have been done looking at the sensitivities of muscle lengths with surgery. However, these models have been limited in their ability to make predictions of muscles surrounding the knee joint due to the limited degrees of freedom present in these models. With the creation of our model with 6 degrees of freedom at the tibiofemoral and patellofemoral joints that also includes the effects of cartilage contact, we are able to make robust predictions about changes in both bony and muscle lengths that occur with this shortening procedure. Another benefit of using this model is that it has the ability to make predictions in both static and dynamic conditions. In future work, we intend to determine how the DFEO parameters affect the resulting knee mechanics after surgery. Of particular interest is the change in contact location, as has been theorized to contribute to changes in tibial slope after surgery (18).

No matter what the location of the osteotomy, changes in muscle lengths occurred. Compared to the contracted position, the hamstrings were lengthened after surgery. More posterior locations, which led to a cuneiform wedge of bone being removed, led to less lengthening of the hamstrings than when a triangular wedge of bone was removed with an anterior wedge apex (X = 0.5 cm). Lengthening of the hamstrings is of clinical concern, as lengthening of the hamstrings may introduce tension in the posterior compartment structures. However, this data does lend support to the idea that surgical hamstring lengthening may not be needed at the time of DFEO + PTA (6). The change in quadriceps lengths are also of interest clinically. Patellar tendon advancement is often done in conjunction with the DFEO to tighten the quadriceps mechanism. This work shows that distal translation of the patellar insertion on the order of 2 cm is needed to achieve normal quadriceps lengths (when comparing to the upright configuration). Interestingly, this is approximately the amount of translation recommended in the surgery currently (4).

In the current operative technique as described by Novacheck et al. (4), the surgeon aims to keep the flexion-extension axis of the knee in the anterior-posterior location. This requires translation of the distal fragment, which is achieved by correct placement of the chisel along the cut plane. A superior location the osteotomy apex requires a more anterior chisel location (or larger translation of the distal segment), as rotation about this high apex moves the knee axis anterior. If the osteotomy is high enough, the translation is likely not clinically achievable, as it results in severely displaced distal and proximal segments (Fig. 7). This is important to consider surgically, as high osteotomies will be expected to alter the location of the knee axis of the patient. This alteration in the femoral axis likely has important implications for muscle moment arms and torque generation, and possibly tibiofemoral contact location. These changes will be the subject of future work.

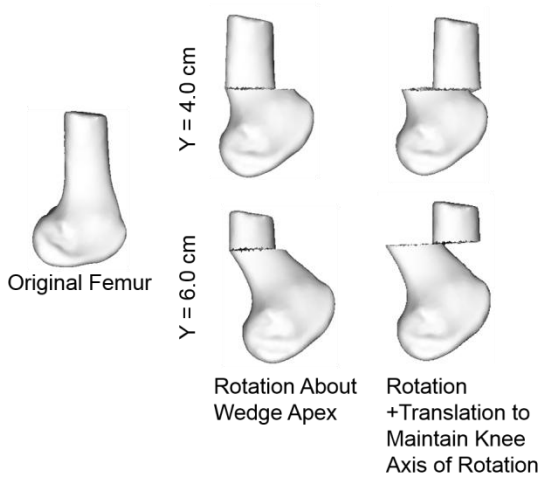

Figure 7: A look at the change in the knee axis locations with two wedge apex locations. All wedges removed are of 30 degree magnitude. (Top) A wedge location of X = 0.0 cm, Y = 4.0 cm shows only a small anterior translation of the femoral axis (left), which can be corrected with posterior translation (right). (Bottom) A wedge location of X = 0.0 cm, Y = 6.0 cm shows a greater translation of the femoral axis with rotation of the distal segment (left). Translation of the distal fragment to have the knee axis in the original position shows discontinuity between the two segments. This is not clinically feasible, and likely represents a case in which the knee axis will change with surgery.

The results did show that the magnitude of posterior translation of the distal fragment had a small effect on muscle lengths. Changing the amount of translation had a non-linear effect on muscle lengths, due to the three dimensional change in the muscle path. It is important to note that all sensitivities were determined for only one wedge location. It is possible that larger magnitude changes may occur for more superior osteotomy locations, as this would change the knee axis, and hence muscle paths, more. However, we do expect the same trends to arise.

There are a few limitations to this study which should be mentioned. First is our use of an otherwise normal lower extremity model. Many children with crouch gait receiving this surgery have other bony (e.g. femoral anteversion) or positional (e.g. increased pelvic tilt) abnormalities that may affect our results. In future work, we will determine the sensitivity of our results to these common abnormalities seen in CP. All of our procedures assumed a cut made perpendicular to the sagittal plane, and did not include any effects of out-of-plane cuts or femoral derotations that are often performed concurrently.

In conclusion, the location and magnitude of the DFEO can have substantial effect on the muscle and femur lengths seen after surgery. These should be carefully considered when using the surgery to offset knee flexion contractures underlying crouch gait.

Acknowledgements: This work was supported in part by the Clinical and Translational Science Award Program, through the NIH National Center for Advancing Translation Sciences, grant UL1TR000427. The authors would also like to NIH (F30AR065838) and the UW Medical Sciences Training Program (T32GM008692).

References:

1. Wren TAL, Rethlefsen S, Kay RM. Prevalence of specific gait abnormalities in children with cerebral palsy: influence of cerebral palsy subtype, age, and previous surgery. Journal of Pediatric Orthopaedics. 2005;25(1):79.

2. Rethlefsen SA, Yasmeh S, Wren TA, Kay RM. Repeat hamstring lengthening for crouch gait in children with cerebral palsy. Journal of Pediatric Orthopaedics. 2013;33(5):501-4.

3. Dhawlikar S, Root L, Mann R. Distal lengthening of the hamstrings in patients who have cerebral palsy. Long-term retrospective analysis. The Journal of Bone and Joint Surgery (American). 1992;74(9):1385-91.

4. Novacheck TF, Stout JL, Gage JR, Schwartz MH. Distal Femoral Extension Osteotomy and Patellar Tendon Advancement to Treat Persistent Crouch Gait in Cerebral Palsy: Surgical Technique. The Journal of Bone and Joint Surgery (American). 2009;91-A(Supplement 2):271-86.

5. Stout JL, Gage JR, Schwartz MH, Novacheck TF. Distal femoral extension osteotomy and patellar tendon advancement to treat persistent crouch gait in cerebral palsy. The Journal of Bone and Joint Surgery (American). 2008;90(11):2470-84.

6. Healy M, Schwartz M, Stout J, Gage J, Novacheck T. Is simultaneous hamstring lengthening necessary when performing distal femoral extension osteotomy and patellar tendon advancement? Gait and Posture. 2011;33(1):1-5.

7. Arnold AS, Blemker SS, Delp SL. Evaluation of a deformable musculoskeletal model for estimating muscle–tendon lengths during crouch gait. Annals of Biomedical Engineering. 2001;29(3):263-74.

8. Arnold AS, Delp SL. Rotational moment arms of the medial hamstrings and adductors vary with femoral geometry and limb position: implications for the treatment of internally rotated gait. Journal of biomechanics. 2001;34(4):437-47.

9. Delp SL, Anderson FC, Arnold AS, Loan P, Habib A, John CT, et al. OpenSim: open-source software to create and analyze dynamic simulations of movement. IEEE Trans Biomed Eng. 2007;54(11):1940-50.

10. Lenhart RL, Kaiser J, Smith CR. Prediction and validation of load-dependent behavior of the tibiofemoral and patellofemoral joints during movement. Annals of Biomedical Engineering. 2015;In press.

11. Blankevoort L, Huiskes R. Ligament-bone interaction in a three-dimensional model of the knee. Journal of biomechanical engineering. 1991;113(3):263-9.

12. Bei Y, Fregly BJ. Multibody dynamic simulation of knee contact mechanics. Medical engineering & physics. 2004;26(9):777-89.

13. Caruntu DI, Hefzy MS. 3-D anatomically based dynamic modeling of the human knee to include tibio-femoral and patello-femoral joints. Journal of biomechanical engineering. 2004;126(1):44-53.

14. Shin CS, Chaudhari AM, Andriacchi TP. The influence of deceleration forces on ACL strain during single-leg landing: a simulation study. Journal of biomechanics. 2007;40(5):1145-52.

15. Askew M, Mow V. The biomechanical function of the collagen fibril ultrastructure of articular cartilage. Journal of biomechanical engineering. 1978;100(3):105-15.

16. Segal NA, Anderson DD, Iyer KS, Baker J, Torner JC, Lynch JA, et al. Baseline articular contact stress levels predict incident symptomatic knee osteoarthritis development in the MOST cohort. Journal of orthopaedic research. 2009;27(12):1562-8.

17. Arnold EM, Ward SR, Lieber RL, Delp SL. A model of the lower limb for analysis of human movement. Annals of Biomedical Engineering. 2010;38(2):269-79.

18. Patthanacharoenphon C, Maples D, Saad C, Forness M, Halanski M. The Effects of Patellar Tendon Advancement on the Proximal Tibia. Journal of Children's Orthopaedics. 2013;7(2):139-46.

Chapter 5

Real-time imaging of dynamic patellar tendon moment arms in cerebral palsy: a preliminary report

Rachel L. Lenhart, Tom F. Novacheck, Michael H. Schwartz, Darryl G. Thelen

Abstract:

Patella alta is found in nearly all children with cerebral palsy and crouch gait, and has traditionally been thought to hinder knee extension ability. However, recent imaging studies have this assumption. The surgical relocation of the patella using patellar tendon advancement seems to improve walking ability in these children, but the final patellar position is abnormally inferior. Understanding the direct impact of this surgical choice on muscle moment arms is important to maximize functional abilities in those with crouch. Therefore, we aimed to examine patellar tendon moment arms in those with cerebral palsy and crouch gait as compared to those in typically developing children. In this preliminary study, a real-time MR imaging technique was used to capture motion during knee flexion-extension in four typically developing children and one child with cerebral palsy. Patellar tendon moment arms at each frame were measured using a manual technique. Despite major limitations, early results suggest reduced moment arms in the child with cerebral palsy over the range of motion measured. Future work will expand subject numbers and compare the moment arms in children before and after patellar tendon advancement.

Introduction:

Patella alta, or a superiorly displaced patella, is a common problem in children with cerebral palsy, especially those with crouch gait (1). Historically, surgeons have considered this alta to contribute to reduced knee extension (2-3). However, more recent imaging work has questioned this assumption, finding that those with alta may not have reduced extensor force generating capacity (4-5). Due to recent

modeling results, our group has developed a more nuanced hypothesis, specifically that patellar tendon moment arm varies with both patellar position and knee flexion angle. We posit that while those with patella alta may have reduced moment arms in extended postures, they may actually see increased moment arms when in more flexed positions. While this theory grew out of modeling results, it has yet to be tested experimentally.

Patellar tendon advancement is a surgical procedure used to treat children with cerebral palsy who exhibit patella alta and extensor lag (the difference between passive and active knee extension capability) (6). This procedure repositions the patella more distally and is thought to tighten the quadriceps mechanism and correct knee extensor insufficiency. This procedure seems to have good functional outcomes, but children tend to have an abnormally inferior patella, or patella baja, after the surgery (7). Our initial modeling results indicate that while this position might increase moment arms in extended postures, it might instead compromise moment arms in extended postures.

The goal of this project was to verify our model predictions that both knee angle and patellar position influence patellar tendon moment arms. We used MR imaging to calculate patellar tendon moment arms over a range of knee angles. A real-time sequence was used in order to obtain these measurements during active motion and not require repeatable cycles (8). In order to evaluate the impact of patellar position, we tested both typically developing children and a child with cerebral palsy with patella alta. Our hypothesis was that patellar tendon moment arms would peak at approximately 20-30 degrees for normal patellar position, while those with patella alta would have maximum patellar tendon moment arms at more flexed postures.

Methods:

Four typically developing children and one child with cerebral palsy were recruited to complete MRI testing at Gillette Children's Specialty Healthcare (Table 1). All volunteers were preliminarily screened and excluded if they had any contraindications for MRI testing or any physical and neurological

limitations that might preclude completion of the experimental protocol. The typically developing children were required to be currently free of knee pain and to have never had lower extremity surgery. The child with cerebral palsy was scheduled to undergo patellar tendon advancement to treat knee extensor lag. The protocol was approved by the University of Minnesota's Institutional Review Board.

Table 1: Subject Demographics

	M/F	Age	Femur Length (mm)	Weight	Leg Tested	Epicondylar Width (mm)	Koshino Index (@ knee flexion)	Approximate Koshino Index Z-score	CP Subtype	GMFCS Level
Typically Developing										
C1	F	12.2	422	47.6	R	75.4	1.34 (0)	0.36		
C2	F	12.2	427	47.6	R	74.5	1.37 (0)	0.67		
C4	F	9.1	402	35.2	R	68.1	1.26 (0)	-0.45		
C5	M	11.4	398	38.6	R	80.3	1.21 (5)	-1.00		
Mean (SD)		11.2 (1.5)	412 (14)	42.3 (6.3)		74.6 (5.0)		-0.10 (0.76)		
Cerebral Palsy										
CP1	F	12.3	426	47.6	R	76.6	1.37 (25)	2.32	Hemiplegic	1

Subjects were asked to lie supine on the MRI table with their leg bent over a custom built wedge device to allow flexion and extension of the knee within the bore. A Siemens Body Matrix Coil (Siemens Corporation, Washington D.C.) was placed over the knee and secured in such a way as the coil would not be disturbed during testing. Each subject was placed in a 1.5-T Siemens Avanto scanner (Siemens Corporation, Washington D.C.) and asked to flex and extend his/her knee to the beat of a metronome, completing one flexion-extension cycle in six seconds. While this rate was suggested, it was not rigidly enforced as the exact rate was not important due to the real-time nature of the scan.

Scanning parameters were adapted from Fiorentino et al. (8). A sagittal imaging plane was defined that bisected the ACL and ran through the shaft of the tibia. A real-time spoiled gradient-recalled echo imaging sequence was used while the subject actively flexed and extended his/her knee for 30 seconds. The imaging parameters used were as follows: TR = 576.3 ms, TE = 2.16, flip angle = 8 deg, field-of-view = 210 x 300 mm^2, imaging matrix = 180 x 256, slice thickness = 7 mm, time per frame = 300 ms. The result was a set of images across the knee flexion extension cycle in the mid-sagittal plane (Fig 1).

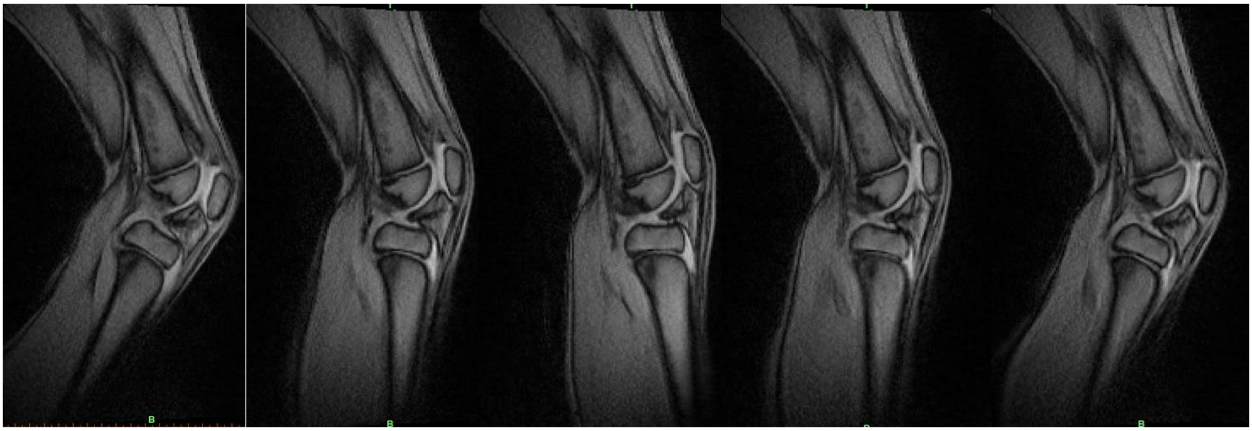

Figure 1: Example images during knee flexion extension taken during real-time imaging.

Patellar tendon moment arm was determined in an individual frame using the technique shown in Figure 2. First the knee flexion angle was determined by determining the angle between the femoral and tibial shafts. The intersection of these lines was estimated as the axis of rotation. The patellar tendon was bisected with a separate line. Then a perpendicular line was then drawn from the axis of rotation to the patellar tendon line of action. The length of this line was determined to be the patellar tendon moment arm. This process was repeated for all frames for all subjects.

Figure 2: Determination of patellar tendon moment arm. The purple line indicates the knee flexion angle. The orange line indicates the bisection of the patellar tendon. The green line is the patellar tendon moment arm, the perpendicular distance from the axis of rotation to the line of action of the patellar tendon.

Patellar tendon moment arms for each subject were normalized by the average epicondylar width for the control subjects, as has been done by others (4). Epicondylar widths were taken from high resolution static knee scans (Space, TR=1000 ms, TE = 30 ms, slice thickness 0.8, Imaging Matrix 256x256, Field of View 200 x 200 mm^2). Moment arms were plotted versus knee flexion angle. The data for the control subjects was fit using a quadratic best fit curve. To determine the influence of patellar position, the Koshino Index (9) was also obtained for each subject using these static images.

Results:

All control subjects had a patellar position that was within one standard deviation of normal, as indicated by the Koshino Index z-score (Table 1). The child with cerebral palsy had a patella that was very superiorly displaced, as indicated by the Koshino Index z-score of 2.3.

All control subjects' patellar tendon moment arm versus knee flexion angle data was well fit by a quadratic best fit curve, as demonstrated in Figure 3, with an R^2 value of 0.24 and $p<0.01$. The variance in

the data is less explained using a linear regression (not shown), with $R^2 = 0.18$ ($p<0.01$). The data from one cerebral palsy subject indicated reduced patellar tendon moment arms over the range of motion obtained.

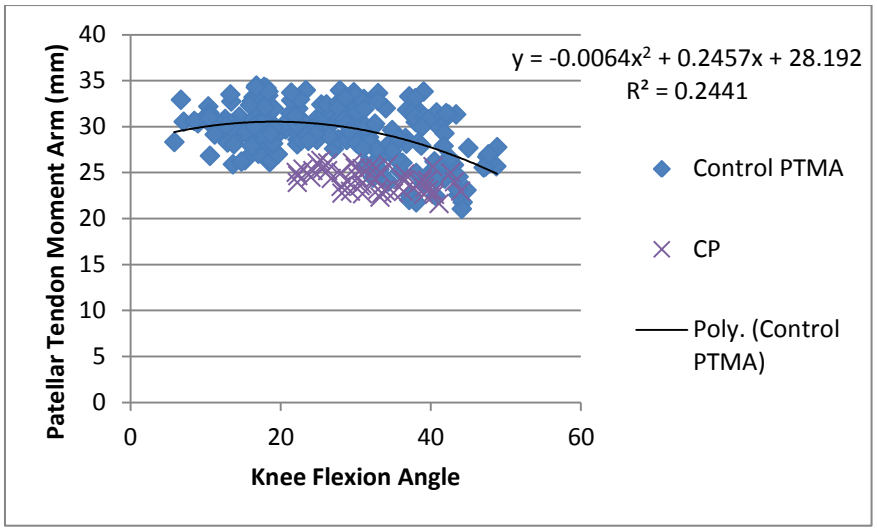

Figure 3: Patellar tendon moment arm vs. knee flexion angle as determined with dynamic MRI. Blue triangles represent control subject data points, while purple crosses represent data from a subject with cerebral palsy. Data from the control subjects is also fit with a best-fit curve.

Discussion:

The goal of this study was to verify model predictions regarding the effect of patellar position on patellar tendon moment arms. Though the results are extremely preliminary, the results indicate that patellar tendon moment arms do vary with moment arm. Typically developing children tend to have moment arms that are well fit with a quadratic curve, and tend to peak around 20 degrees. Our one child with cerebral palsy and patella alta exhibited reduced moment arms over the range of motion obtained.

This study represents very preliminary data and the methods and analysis techniques are still being improved. The method used thus far to analyze the patellar tendon moment arms is subject to a fair amount of user error and makes some simplistic assumptions about knee function. Since the differences of

moment arms we hope to see are on the order of millimeters, it is important that our technique is as repeatable and reliable as possible. We are currently working on a technique using image processing to help us more accurately track the bones during the flexion extension cycle. This will also allow us to move away from the assumption that knee flexion-extension axis occurs exactly at the intersection of the shaft of the femur and tibia. We will instead be able to use the instantaneous center of rotation (ICR) method for determining the knee flexion-extension axis (10). We believe that implementing the semi-automated tracking technique along with the ICR method will help improve our repeatability and our confidence in our results.

One other limitation that may need to be further explored was the small range of motion achieved by our participant with cerebral palsy. Because this child experienced extensor lag (20 deg), she was not able to actively extend more than was achieved in the scanner. We did obtain some images while a researcher passively flexed and extended her knee, in which she was able to obtain a much more extended posture. However, when this occurred, the patellar tendon tended to go slack and have a visible kink, precluding the ability to calculate a moment arm. With more subjects, this limitation may still exist precluding our ability to make conclusions about the patellar tendon moment arm in extended postures in those with patella alta. However, our child did have reduced moment arms in the range of motion tested. It is our thought that the moment arm had not yet peaked, and perhaps even more flexion range of motion is needed to bring out the difference here.

Despite the major limitations, our data does seem to indicate that there is a trend of patellar tendon moment arms following a quadratic function of knee angle. The knee angle had a peak at approximately 20 degrees. Interestingly, this corresponds to approximately the maximum stance phase knee flexion angle during walking, suggesting that patellar position might be optimized in typically developing children for minimizing quadriceps/patellar tendon forces during walking. Our child with cerebral palsy had patella alta that was greater than 2 standard deviations from the normal, and showed patellar tendon moment arms that were much reduced through knee flexion angles between 22 and 44

degrees. It is difficult to make conclusions from just one subject, especially when the analysis method is limited. However, it does seem that this amount of patella alta shows reduced moment arms over this range.

While comparing typically developing children to those with cerebral palsy and patella alta is a good first step, we hope to extend this work in the future and help make surgical recommendations regarding treatment with patellar tendon advancement. Therefore, in future work, we intend to test children before and after patellar tendon advancement to determine more precisely the impact of the surgery on patellar tendon moment arms. We hope to tease out the impact of final patellar position on the final moment arm profile. The framework for completing this project is in place, but with follow-up times on the order of one year, it will take some time to recruit and follow-up with sufficient subject numbers.

In conclusion, our preliminary data seems to suggest that the patellar tendon moment arm is dependent on knee angle and on patellar position. However, more subject data and a more reliable/repeatable method of determining a patellar tendon moment arm are needed before firm conclusions can be made.

Acknowledgements: This work was supported in part by the Clinical and Translational Science Award Program, through the NIH National Center for Advancing Translational Sciences, grant UL1TR000427. The Burrough's Wellcome Fund, the International Society of Biomechanics, the University of Wisconsin Medical Scientist Training Program (T32GM008692), and the National Institutes of Health (F30AR065838) provided additional support. The authors would also like to thank Jarred Kaiser, Martin McLean, and Richard Kijowski, MD for their expertise in MR imaging.

References:

1. Topoleski TA, Kurtz CA, Grogan DP. Radiographic abnormalities and clinical symptoms associated with patella alta in ambulatory children with cerebral palsy. Journal of Pediatric Orthopaedics. 2000;20(5):636.

2. Gage J, Schwartz M, Koop S, Novacheck T. The Identification and Treatment of Gait Problems in Cerebral Palsy. 2 ed: John Wiley and Sons; 2009.

3. Lotman DB. Knee flexion deformity and patella alta in spastic cerebral palsy. Developmental Medicine & Child Neurology. 1976;18(3):315-9.

4. Sheehan FT, Seisler AR, Alter KE. Three-dimensional in vivo quantification of knee kinematics in cerebral palsy. Clinical Orthopaedics and Related Research. 2008;466(2):450-8.

5. Ward SR, Terk MR, Powers CM. Influence of patella alta on knee extensor mechanics. Journal of Biomechanics. 2005;38(12):2415-22.

6. Novacheck T, Stout J, Gage J, Schwartz M. Distal Femoral Extension Osteotomy and Patellar Tendon Advancement to Treat Persistent Crouch Gait in Cerebral Palsy: Surgical Technique. The Journal of Bone and Joint Surgery (American). 2009;91-A(Supplement 2):271-86.

7. Stout J, Gage J, Schwartz M, Novacheck T. Distal femoral extension osteotomy and patellar tendon advancement to treat persistent crouch gait in cerebral palsy. The Journal of Bone and Joint Surgery (American). 2008;90(11):2470-84.

8. Fiorentino NM, Lin JS, Ridder KB, Guttman MA, McVeigh ER, Blemker SS. Rectus Femoris Knee Muscle Moment Arms Measured in Vivo During Dynamic Motion With Real-Time Magnetic Resonance Imaging. Journal of Biomechanical Engineering. 2013;135:0445011-5.

9. Koshino T, Sugimoto K. New measurement of patellar height in the knees of children using the epiphyseal line midpoint. Journal of Pediatric Orthopaedics. 1989;9(2):216-8.

10. Tsaopoulos DE, Baltzopoulos V, Maganaris CN. Human patellar tendon moment arm length: measurement considerations and clinical implications for joint loading assessment. Clinical Biomechanics. 2006;21(7):657-67.

Chapter 6:

Evaluation of the Random Forest Algorithm for predicting outcomes of crouch gait surgery at multiple institutions

Rachel L. Lenhart, Darryl G. Thelen, Tom F. Novacheck, Michael H. Schwartz

Abstract:

The distal femoral extension osteotomy and patellar tendon advancement (DFEO + PTA) are surgical procedures used together in the treatment of crouch gait that is gaining widespread adoption across the world. Despite the enthusiasm surrounding the procedure regarding its positive effects on walking ability, there is no clear understanding of which patients will benefit from surgery. The purpose of this study was to determine if the random forest algorithm could predict improvement in mean stance phase knee flexion angle after DFEO + PTA based on pre-surgical variables alone. Secondarily, investigation into whether the resultant predictive model was specific to predicting results of DFEO + PTA, and if the model could predict outcomes at a multiple institutions was undertaken. Therefore, retrospective data from Gillette Children's Specialty Healthcare was obtained on 65 limbs receiving DFEO + PTA. The random forest needed only 17 variables to predict outcomes with 92% accuracy. Pre-operative mean stance phase knee flexion was the most important predictor. The results were specific to DFEO +PTA, with the accuracy dropping to 58 and 60% when predicting results of other treatments for crouch gait, single event multilevel surgery or hamstring lengthening surgery respectively. Preliminarily, the model was able to accurately classify outcomes for 26 out of 30 patients from a separate institution. Therefore, the use of the random forest algorithm can be used in the prediction of outcomes after DFEO + PTA, and early results suggest that these predictions may be generalizable to other institutions.

Introduction:

The combination of distal femoral extension osteotomy and patellar tendon advancement (DFEO + PTA) (1) is gaining popularity as a surgical treatment of crouch gait. The distal femoral extension osteotomy (DFEO) creates an extension deformity of the distal femur to compensate for knee flexion contractures while the patellar tendon advancement (PTA) corrects quadriceps insufficiency by tightening the quadriceps muscle-tendon unit (1). The combined procedures have been shown to produce more improvement in knee kinematics than either procedure alone (2). However, variation in both surgical criteria and results exist, and there is not a clear understanding of how pre-operative status (e.g. crouch gait severity, age, etc.) might affect the results of surgery.

The Random Forest algorithm is a powerful classification technique that uses numerous decision trees to determine classification of individual instances (3). This technique has been used in fields as diverse as genetic analysis and neuroimaging, and has recently been pioneered in the field of gait analysis. Outcomes of psoas surgery have been predicted with 78% accuracy (4), and surgical criteria for femoral derotational osteotomy has been extracted retrospectively (5). This technique has shown to be an extremely powerful tool and is currently in use to help surgeons make decisions regarding surgical procedures for individual patients. It seems reasonable that this technique could be used to predict outcomes of DFEO + PTA, helping to reduce the rates of poor outcomes.

Despite its increasing popularity for predicting outcomes in gait analysis, no work has been done to determine if results from a random forest created at one institution can be generalized to other institutions. Gait analysis techniques as well as surgical indications and technique can differ across institutions, making it difficult to know whether the results from one institution could be used more generally to make predictions about children being considered to undergo a particular intervention. This seems particularly relevant for the DFEO + PTA, which is a newly re-adopted surgical procedure (2), and very few institutions have enough long term data to make their own random forest model.

Therefore, the purpose of this study was to use the random forest algorithm to determine if pre-surgical variables could predict outcomes of the DFEO + PTA. Secondarily, we hoped to determine if our results were specific to DFEO + PTA, by analyzing the predictive ability of the model when it was used to forecast results of single event multilevel surgery (SEMLS) or hamstring surgery. Finally, we investigated whether the model's predictive abilities were generalizable to other institutions. To do this we used our model created from data from Gillette Children's Specialty Healthcare (St. Paul, MN) to predict outcomes at Mary Free Bed Rehabilitation Hospital (Grand Rapids, MI).

Methods:

We retrospectively reviewed the gait analysis database at Gillette Children's Specialty Healthcare for children with cerebral palsy treated with DFEO + PTA and had received both pre and post-operative gait analysis as part of routine clinical care. Children were included if they were a maximum of 21 years of age at the time of pre-operative gait analysis. Time from pre-operative gait analysis to surgery was allowed to be 0-12 months, while time from surgery to post-operative gait analysis was 9-24 months. We did not exclude patients based on prior or concurrent procedures. Both limbs were included as independent observations if both received DFEO + PTA. Gillette had 65 limbs that met our criteria.

The primary outcome considered was the improvement in mean knee flexion angle during the stance phase of walking. As defined by Hicks et al. (6), the outcome was considered positive if the change in mean knee flexion angle during stance was at least 10 degrees or if the value was less than 18 degrees post-operatively.

Variables considered for inclusion in the random forest algorithm included birth history, developmental history, surgical history, other concurrent surgical procedures, functional measures, physical exam, and kinematic gait analysis data. If 5% of the data was missing for a particular variable, it was excluded. Of the 416 variables originally extracted, this left 337, with some developmental history, physical exam, and oxygen consumption testing metrics being excluded for lack of sufficient data (See

Appendix D). These remaining variables were then used as input into the random forest algorithm as implemented in MATLAB with the Statistics Toolbox (2014a).

Based on convergence of the misclassification probability, the number of trees in the forest was chosen to be 350. A random forest was then created with all potential predictors included. To determine which variables were essential to the classification, the predictor variables were sorted in order of the magnitude of increase in prediction error when the values of that particular variable were permuted. Because the random forest often does better at predicting with a smaller number of variables, we then attempted to reduce the number of our predictors to less than or equal to 25. To do this, the algorithm was re-run with between 2 and 25 variables from the importance rankings. The final choice of 17 predictors was chosen based on first maximizing the Matthew's correlation coefficient and then area under the receiver operating characteristic curve. The final model was assessed using classification performance metrics. Significance was tested using Pearson's Chi-squared test with Yates' Continuity Correction using R (version 3.2.0, The R Foundation for Statistical Computing, Vienna, Austria). The criterion for significance was set at $p = 0.05$.

To determine if the model was specific to DFEO + PTA, we used the model to predict results after single event multi-level surgery (SEMLS: >1 orthopedic procedure exclusive of hardware removal), as well as a procedure traditionally used in the treatment of crouch, hamstring lengthening. To do this, we took limbs from the Gillette database that had not received DFEO + PTA, but had received SEMLS, and met our other inclusion criteria. We then used the model to predict which would have a positive outcome, and compared that to the actual outcome as determined by post-operative gait analysis. The same scheme for identifying "control" limbs was also applied to hamstring surgery.

To determine if the model could predict results at another institution, we retrospectively reviewed the gait analysis database at Mary Free Bed Rehabilitation Hospital for children who had received DFEO + PTA. Data were obtained on the 17 predictor variables, as well as the outcome metrics. These data were

used with our final forest model from the Gillette data to determine how well the Gillette model predicted the outcomes at Mary Free Bed. The degree of agreement was assessed again using confusion matrix statistics.

Results:

The final random forest model contained 17 variables, including physical exam, gait analysis, and developmental history data (Table 1). Most of the metrics were from gait analysis, and the majority involved knee flexion metrics. The most important variable was the pre-operative mean stance phase knee flexion angle.

Table 1: Metrics determined to be important for predicting the outcome of DFEO and PTA surgery. These are ranked in order of importance to the prediction as determined by the increase in impurity of the classification (calculated using the Gini's Diversity Index) caused by a given predictor.

Rank	Metric	Type	Importance
1	Mean Stance Phase Knee Flexion Angle	Gait Kinematics	0.4142
2	Mean Knee Flexion Angle over the Gait Cycle	Gait Kinematics	0.3795
3	Minimum Knee Flexion Angle	Gait Kinematics	0.3482
4	Minimum Stance Phase Knee Flexion Angle	Gait Kinematics	0.3006
5	Minimum Swing Phase Knee Flexion Angle	Gait Kinematics	0.2905
6	Range of Motion of Knee Flexion over the Gait Cycle	Gait Kinematics	0.2244
7	Initial Contact Knee Flexion	Gait Kinematics	0.2172
8	Type of Assistive Device Needed when walking began, Right	Developmental History	0.2152
9	Swing Phase Range of Motion for Knee Internal Rotation	Gait Kinematics	0.1890
10	Foot off Knee Flexion Angle	Gait Kinematics	0.1846

11	Type of Assistive Device Needed when walking began, Left	Developmental History	0.1764
12	Maximum Stance Phase Knee Flexion Angle	Gait Kinematics	0.1634
13	Range of Motion of Pelvic Tilt over the Gait Cycle	Gait Kinematics	0.1297
14	Timing of Maximum Knee Flexion Angle	Gait Kinematics	0.1083
15	Prior Baclofen	Medical/Surgical History	0.0899
16	Hip Flexion Range of Motion	Physical Exam	0.0868
17	Initial Contact Pelvic Tilt Angle	Gait Kinematics	0.0826

Most of the limbs (53 of 65) had an improvement in mean stance phase knee flexion angle (i.e. >10 degree improvement or post-operative <18 degrees) after DFEO + PTA. The random forest correctly predicted the outcomes of 60 of the 65 limbs for an accuracy of 92% (Table 2). The model also had 98% sensitivity, correctly predicting 52 of 53 who had a positive outcome. In contrast, the model only had 67% specificity, predicting only 8 of 12 of the limbs that had a negative outcome. The positive predictive value was 93% and the negative predictive value was 89%. The relative risk was 8.4, the Matthew's correlation coefficient was 0.73, and the area under the receiver operating curve was 0.87.

Table 2: Confusion matrix for children receiving DFEO and PTA. The outcome determination was related to the improvement in mean knee flexion angle. Results are significant to $p<0.001$.

	Predicted negative outcome	Predicted positive outcome
Actually had a negative outcome	8	4
Actually had a positive outcome	1	52

Although the random forest cannot give exact cut-offs or causal relationships between predictor variables and their outcomes, observing variable distributions as well as kinematic differences is of interest. Histograms of a few selected variables of interest in the predicted groups are shown in Figure 1. Some trends emerge, though it is clear that complexity exists in the model's predictions. The knee flexion kinematics, such as the mean stance knee flexion, minimum knee flexion, and minimum stance phase knee flexion skew to larger values in the group predicted to have a positive outcome. Range of motion skewed toward smaller values in children who had a positive outcome.

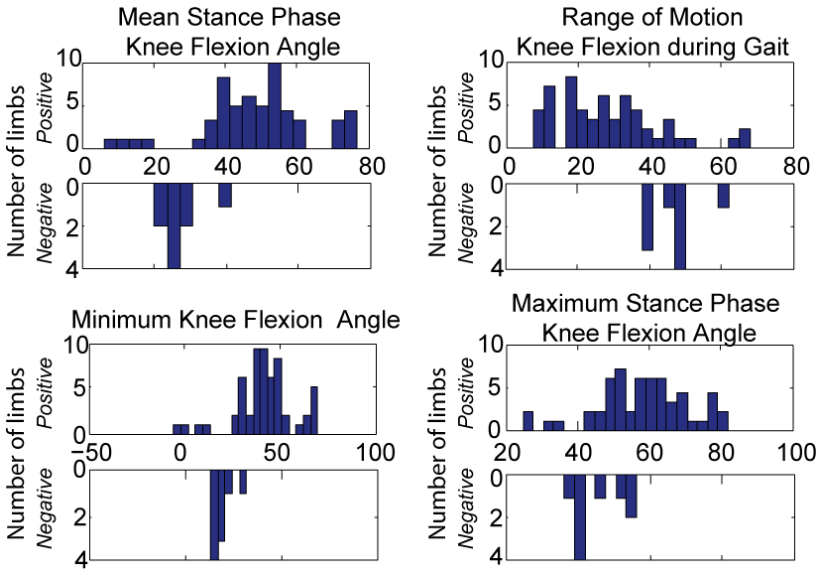

Figure 1: Histogram of variable values for children predicted to have a positive (bars going up) or negative (bars going down) outcome from DFEO + PTA.

Differences between the correctly predicted positive and negative outcomes can also clearly be seen in kinematic plots (Figs. 2 and 3). Comparing pre-operative data (Fig. 2), knee flexion profile curve of the group that saw a positive outcome is clearly further from normal than that of limbs that had a negative outcome. Some differences also emerge in other degrees of freedom including pelvic rotation, hip adduction, and foot progression angle. Looking at the pre- and post-operative curves for each of these

groups (Fig. 3), the improvement in knee flexion kinematics toward the normal values in the group with a positive outcome is clearly evident. Foot progression also improved, however there was a worsening of anterior pelvic tilt, which has also been noted clinically (2). In the group with a poor outcome, the gait kinematics change only slightly.

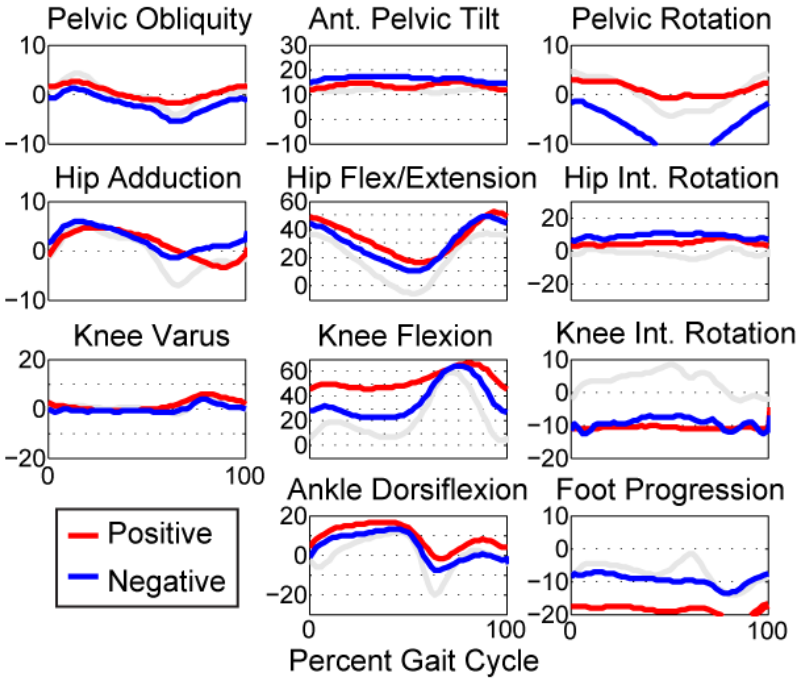

Figure 2: Pre-operative kinematic data comparing the group of children who were accurately predicted to have a positive outcome, and those that were accurately predicted to have a negative outcome. The gray band indicates the average for typically developing children.

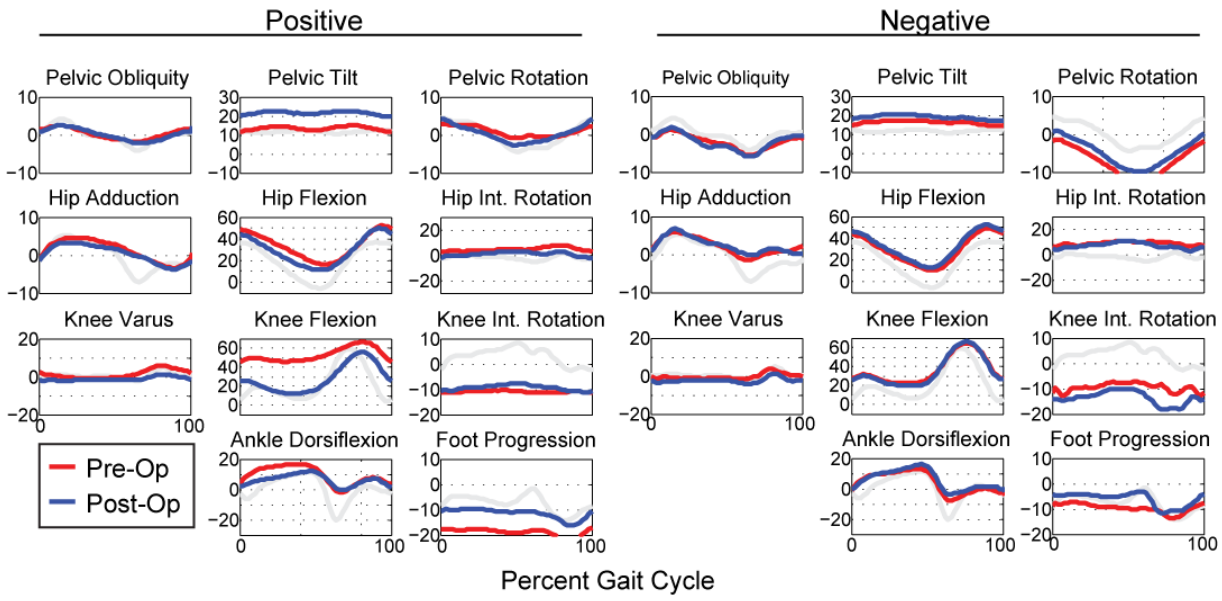

Figure 3: Kinematic data comparing pre- and post-operative kinematics in children correctly predicted to have a positive outcome (left) and correctly predicted to have a negative outcome (right).

Despite the fact that the random forest predicted results after DFEO + PTA, it was unclear whether this model was specific to predicting the results of this procedure, and perhaps similar predictors could predict improvement in knee flexion from other interventions as well. When using the model to predict the results of SEMLS, the model did not do as well. The model only accurately predicted 518 out of 896 limbs (58% accuracy). This was only slightly better (132 out of 220, accuracy = 60%) for predicting the outcomes of hamstring surgery.

Table 3: Confusion matrix created using the model from the DFEO and PTA investigation to predict results from SEMLS. The goal was to determine how specific the predictors of DFEO and PTA were to improvement in mean knee flexion angle. Chi-square test with Yates' continuity correction gives $p<0.001$.

	Predicted negative outcome	Predicted positive outcome
Actually had a negative outcome	237	232

Actually had a positive outcome	146	281

Table 4: Confusion matrix created using the model from the DFEO + PTA investigation to predict results from hamstring surgery, a traditional procedure used in the treatment of crouch. The goal was to determine how specific the predictors of DFEO and PTA were to improvement in mean knee flexion angle. Chi-square test with Yates' continuity correction gives $p = 0.004$.

	Predicted negative outcome	Predicted positive outcome
Actually had a negative outcome	60	52
Actually had a positive outcome	36	72

Compared to predicting other procedures, the model preliminarily did better when classifying the results of DFEO + PTA from another institution. When trying to predict results of DFEO+PTA regardless of underlying condition or time to follow-up gait analysis, the model correctly predicted 26 out of 29 limbs from Mary Free Bed, for an accuracy of 90% (Table 5). The model had a high sensitivity (93%), but decreased specificity (50%) compared to the predictions of the Gillette data. The positive predictive value was similar (96%), but the negative predictive value was reduced (33%). The relative risk (1.4) and Matthew's Correlation coefficient (0.35) were also decreased. The area under the receiver operating curve was similar at 0.83. When excluding the patients not meeting our inclusion criteria in creation of the model (underlying causes other than CP = 4 patients with myelomeningocele, 8 limbs; follow-up greater than 24 months = 3 patients, 6 limbs), 14 of 15 limbs were correctly predicted, though there were no negative limbs that had a negative outcome according to our definition.

Table 5: Confusion matrix created using the model from the DFEO and PTA results from Gillette and using that to predict results from Mary Free Bed regardless of underlying condition and time to follow-up.

	Predicted negative outcome	Predicted positive outcome
Actually had a negative outcome	1	1
Actually had a positive outcome	2	25

Table 6: Confusion matrix created using the model from the DFEO and PTA results from Gillette and using that to predict results from Mary Free Bed that had similar inclusion and exclusion criteria as the model created.

	Predicted negative outcome	Predicted positive outcome
Actually had a negative outcome	0	0
Actually had a positive outcome	1	14

Discussion:

The purpose of this project was to determine if the random forest algorithm could predict improvement in mean knee flexion angle. Secondarily, we hoped to show that our results were specific to predicting improvement after DFEO + PTA, and that our results were generalizable to other institutions. We found that our random forest algorithm could predict outcomes with high accuracy with only 17 predictor variables. Most of the predictor variables were related to knee flexion kinematics over the gait cycle. We also found, as expected, that our model was not as robust at predicting improvement in stance phase knee flexion angle after SEMLS or hamstring surgery. However, our preliminary results suggest that it could generally predict results from a different institution, though with slightly decreased accuracy and negative predictive value.

One interesting, and possibly expected result was that the pre-operative mean stance phase knee flexion angle was the best predictor of the improvement in mean stance phase knee flexion angle. Indeed, a post-hoc linear regression analysis with the Gillette data (Fig. 4) showed that 62% of the variance in

improvement in knee flexion could be explained by the pre-operative knee flexion angle ($p<0.05$). This seems to suggest that patients with more severe crouch will have a greater benefit from the surgery. In contrast, children with less severe crouch seem to receive much less benefit. This is an important finding, as DFEO + PTA are significant procedures with long recovery time. It seems that surgeons should carefully consider whether to do the procedure on only mildly affected children given these results.

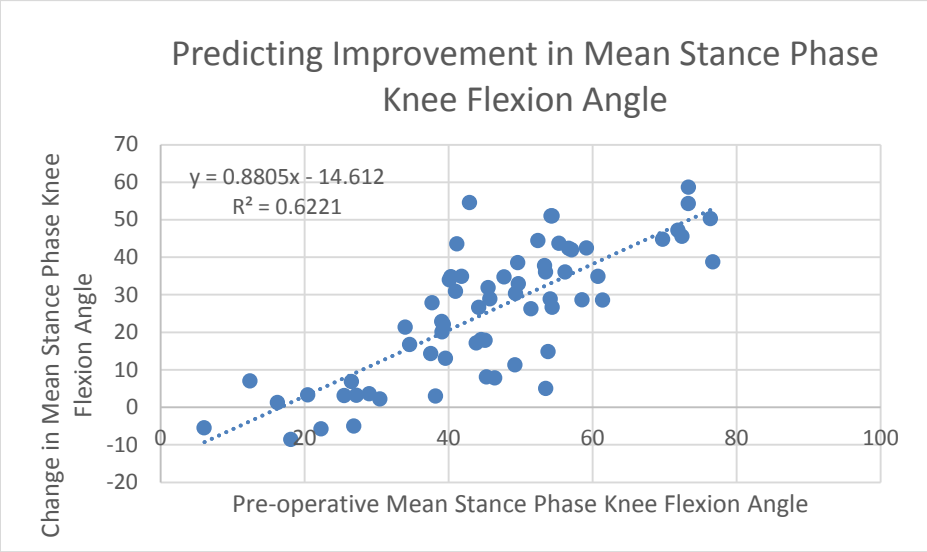

Figure 4: Scatter plot of change in stance phase mean knee flexion angle vs. pre-operative mean knee flexion angle.

Unfortunately, one limitation of the random forest is that we cannot explain exactly how certain predictors affect the result. The classification is based on a complex interaction of variables across hundreds of decision trees. It is also unclear why some variables rise to the top as important predictors. For example, why the type of assistive device at the time of walking initiation was important is not entirely clear. We speculate that it could be related to the child's motor control, but the exact cause cannot be elucidated. The inclusion of prior Baclofen is thought to be linked to underlying or management of

tone, but this cannot be confirmed. However, future studies could probe some of these potential links as they might be helpful in further understanding the outcomes of DFEO+PTA in individual children.

As with other random forest studies in gait analysis (4-5, 7), most of the predictors that emerged were taken directly from the gait kinematics, with only hip flexion range of motion taken from the physical exam. This is important to note and seems to suggest the importance of obtaining accurate, objective, 3D motion analysis data in order to better predict outcomes of surgery. Given that the primary goal is of the treatment is improvement walking status, and that passive or isometric performance are not well correlated with dynamic function in CP (8-11), it is intuitive that measurements taken during walking may be better predictors than those from the physical exam. Further, metrics from gait analysis tend to be more repeatable than physical exam metrics (11-14), likely making classification using gait data more consistent. As with other random forest studies (4-5, 7), these findings add to the evidence that gait analysis information is important for determining whether or not a child will have a good outcome after a particular procedure.

Our initial results indicate that our model is specific for results after DFEO + PTA. While the significance testing showed that the predictions were not independent of the actual outcomes, the model did not do nearly as good of a job predicting results of other procedures. Interestingly, the predictive ability was approximately the same in predicting results of SEMLS and hamstring surgery, even though hamstring surgery has traditionally been thought of as a procedure to help treat crouch gait (15-16). Though the reasoning for this is unclear, a few possible explanations exist. The results could be related to the high recurrence rate of crouch after hamstring lengthening (17-19). Indeed a high percentage of the patients had a negative outcome after hamstring lengthening, and the model was particularly poor at predicting who would have an unsuccessful surgery. Perhaps with this muscular procedure, incomplete understanding of the effects of lengthening on musculotendon properties contributes to both variable techniques and results. This variability would make predicting results, even using gait analysis data, difficult. An alternative explanation could be simply that another set of variables, decision trees, or

decision tree splits better predicts results of hamstring lengthening than those chosen for predicting improvement after DFEO + PTA.

Our initial results indicate that the random forest does a fairly good job of classifying results after DEFO + PTA at a different institution, even when the criteria for inclusion were not exactly the same as that used to create the model. This has implications for the use of this model more broadly. Gillette has one of the largest gait analysis services in the world, and is a leader in DFEO + PTA, making it an ideal setting to create this model. Given the classification of the Mary Free Bed data was good, it seems reasonable that other institutions may be able to use the model pre-operatively to determine if a particular patient would be likely to do well after DFEO + PTA. Further, it seems that one could relax the criteria for inclusion and still see a robust result. However, there are differing surgical approaches for performing DFEO + PTA, which should be considered in applying the model across institutions. In particular, Gillette surgeons tend to perform the PTA by advancing the patellar tendon insertion distally (by itself or by tibial tubercle bone block in a skeletally mature patient) (1), whereas other institutions may use other techniques, such as imbricating or shortening the patellar tendon (20). The effect of these variations on outcomes is yet to be determined, as the surgeons referring to Mary Free Bed use similar surgical approaches to those at Gillette. Finally, it is important to recognize the small number of cases of a negative outcome in the Mary Free Bed data. Data from more institutions is needed to fully test the robustness of the model, and caution should be used in its implementation before that analysis is complete.

This study has several limitations that we should note. Data was taken from a historical database and did not take into account changes that may have occurred with the procedure over time. This study also did not include any surgical variables, which, if added, may have improved our predictive capabilities. For example, the published surgical criteria state that the DFEO wedge should match the amount of knee flexion contracture. Therefore, we might expect that children whose surgical wedge angle did not match well with their knee flexion contracture might have had a bad result. In future work we

hope to add in these surgical variables to determine if they contribute to a good outcome. Another is that we characterized a good outcome based solely on mean stance phase knee flexion angle. One might argue that the surgery is more interested in correcting the minimum stance phase knee flexion angle or overall gait normalcy, in which case another metric might be preferable. We chose the mean stance phase knee flexion angle based on a similar study in the literature (6), though it would be easy enough to explore predictors of improvement in other metrics. Post-hoc analysis looking at the improvement in the Gait Deviation Index (GDI, (21)) found similar predictors as important, including many of the knee flexion kinematics. We also did not penalize for cases of recurvatum post-surgically. The data clearly showed some instances of overcorrection, however, these were still labeled as a good outcome. Finally, we also only tested our predictive abilities against one other institution. In future work, we hope to compare to more labs, including some international ones, as adoption of DFEO + PTA has been worldwide.

In conclusion, we have found that the random forest algorithm can be used to predict outcomes of DFEO + PTA. We found that pre-operative mean knee flexion angle was the best predictor, with post-hoc analysis suggesting that children with worse pre-operative condition tend to do better. Further, we found that our results seem to be generalizable to other institutions, though more work is needed to see if this holds across more diverse institutions. Overall, the random forest is a powerful predictive tool that can be used to predict outcomes of DFEO + PTA, and has the potential to be implemented to help make surgical decisions in children with crouch gait.

Acknowledgements: The authors would like to recognize the staff at the James R. Gage Center for Gait and Motion Analysis at Gillette Children's Specialty Healthcare, as well as those at Mary Free Bed (MFB) Rehabilitation Hospital. Special thanks to Amy Lenz for her help gathering the MFB data. This work was supported in part by the Clinical and Translational Science Award Program, through the NIH National Center for Advancing Translational Sciences, grant UL1TR000427. The authors would also like

to thank the Burrough's Wellcome Fund, the University of Wisconsin Medical Scientist Training Program (T32GM008692), and the National Institutes of Health (F30AR065838).

References

1. Novacheck TF, Stout JL, Gage JR, Schwartz MH. Distal Femoral Extension Osteotomy and Patellar Tendon Advancement to Treat Persistent Crouch Gait in Cerebral Palsy: Surgical Technique. The Journal of Bone and Joint Surgery (American). 2009;91-A(Supplement 2):271-86.

2. Stout JL, Gage JR, Schwartz MH, Novacheck TF. Distal femoral extension osteotomy and patellar tendon advancement to treat persistent crouch gait in cerebral palsy. The Journal of Bone and Joint Surgery (American). 2008;90(11):2470-84.

3. Breiman L. Random forests. Machine learning. 2001;45(1):5-32.

4. Schwartz MH, Rozumalski A, Truong W, Novacheck TF. Predicting the outcome of intramuscular psoas lengthening in children with cerebral palsy using preoperative gait data and the random forest algorithm. Gait & Posture. 2012.

5. Schwartz M, Rozumalski A, Novacheck T. Femoral derotational osteotomy: Surgical indications and outcomes in children with cerebral palsy. Gait & Posture. 2014;39(2):778-83.

6. Hicks JL, Delp SL, Schwartz MH. Can biomechanical variables predict improvement in crouch gait? Journal of Pediatric Orthopaedics. 2007;27(6):658-67.

7. Ries AJ, Novacheck TF, Schwartz MH. A data driven model for optimal orthosis selection in children with cerebral palsy. Gait & Posture. 2014;40(4):539-44.

8. Lee LW, Kerrigan DC, Della Croce U. Dynamic Implications of Hip Flexion Contractures1. American journal of physical medicine & rehabilitation. 1997;76(6):502-8.

9. McMulkin ML, Gulliford JJ, Williamson RV, Ferguson RL. Correlation of static to dynamic measures of lower extremity range of motion in cerebral palsy and control populations. Journal of Pediatric Orthopaedics. 2000;20(3):366-9.

10. Dallmeijer A, Baker R, Dodd K, Taylor N. Association between isometric muscle strength and gait joint kinetics in adolescents and young adults with cerebral palsy. Gait & Posture. 2011;33(3):326-32.

11. Thompson NS, Baker RJ, Cosgrove AP, Saunders JL, Taylor TC. Relevance of the popliteal angle to hamstring length in cerebral palsy crouch gait. Journal of Pediatric Orthopaedics. 2001;21(3):383-7.

12. Schwartz MH, Trost JP, Wervey RA. Measurement and management of errors in quantitative gait data. Gait & Posture. 2004;20(2):196-203.

13. McGinley JL, Baker R, Wolfe R, Morris ME. The reliability of three-dimensional kinematic gait measurements: a systematic review. Gait & Posture. 2009;29(3):360-9.

14. McDowell BC, Hewitt V, Nurse A, Weston T, Baker R. The variability of goniometric measurements in ambulatory children with spastic cerebral palsy. Gait & Posture. 2000;12(2):114-21.

15. Gage JR. Surgical treatment of knee dysfunction in cerebral palsy. Clinical orthopaedics and related research. 1990;253:45.

16. Baumann J, Ruetsch H, Schürmann K. Distal hamstring lengthening in cerebral palsy. International orthopaedics. 1980;3(4):305-9.

17. Rethlefsen SA, Yasmeh S, Wren TA, Kay RM. Repeat hamstring lengthening for crouch gait in children with cerebral palsy. Journal of Pediatric Orthopaedics. 2013;33(5):501-4.

18. Dreher T, Vegvari D, Wolf SI, Geisbüsch A, Gantz S, Wenz W, et al. Development of knee function after hamstring lengthening as a part of multilevel surgery in children with spastic diplegia. The Journal of Bone & Joint Surgery. 2012;94(2):121-30.

19. Dhawlikar S, Root L, Mann R. Distal lengthening of the hamstrings in patients who have cerebral palsy. Long-term retrospective analysis. The Journal of Bone and Joint Surgery (American). 1992;74(9):1385-91.

20. Joseph B, Reddy K, Varghese RA, Shah H, Doddabasappa SN. Management of severe crouch gait in children and adolescents with cerebral palsy. Journal of Pediatric Orthopaedics. 2010;30(8):832-9.

21. Schwartz MH, Rozumalski A. The gait deviation index: a new comprehensive index of gait pathology. Gait & Posture. 2008;28(3):351-7.

Conclusions

This thesis has explored changes in musculoskeletal mechanics in children with crouch gait and patella alta and the influence of corrective surgery on these mechanics. The results have shown that patellar position is an important determinant of knee extension capabilities during walking, helping to explain the clinical improvements seen with patellar tendon advancement (PTA). Patellar position and walking posture also play a crucial role in tibiofemoral and patellofemoral pressure magnitude and location. Correction of crouch with the distal femoral extension osteotomy (DFEO) has real effects on muscle lengths, regardless of wedge location and orientation. Finally, in terms of improvement in knee flexion kinematics, patients with more severe crouch tend to obtain more benefit from DFEO and PTA than children that are less severely affected.

Despite the strides that this work has taken to help understand crouch gait, patella alta, and their treatments, there are many more facets which need understanding and further work. The modeling arm of the research has many low hanging fruit for future directions. One perhaps obvious one would be examining the impact of knee flexion contractures on simulations of walking. While these may not have a big influence on quadriceps forces or maximum stance phase knee flexion, it seems that contractures might lead to subtle changes in kinematics and contact location at transition phases, such as at heel strike or near toe off as the knee comes close to full extension. Since subtle kinematic changes are hypothesized to contribute to degenerative cartilage changes (1), these changes seem important to consider, especially in the context of DFEO surgery. Another obvious next step is to explore the changes that occur with bony abnormalities common with cerebral palsy, such as femoral anteversion, tibial torsion, or an abnormal tibial slope. Due to attachment points on the proximal femur, femoral anteversion may affect the line of action, lengths, and 3D moment arms of muscles such as the vastus lateralis and biceps femoris short head. Tibial torsion affects the ability of several muscles to extend the hip and knee (2-3), and so could impact our predictions about quadriceps forces. Further, torsion or subsequent derotation in either the femur or tibia may increase patellofemoral pressures during walking (4). It is also expected that tibial

slope may also affect anterior translation of the tibia during stance phase. In the simulation of DFEO, I believe the next step is to better understand the implications of the DFEO for the PTA. It is now clear that there is some link between the two procedures through the changing of the quadriceps lengths through the DFEO. Does baja result just from removing the slack created from the DFEO? Another avenue will be examining how the DFEO affects muscle moment arms, especially of the quadriceps and hamstrings. Finally, I hope to soon move beyond the analysis of geometric changes and begin to simulate walking with the altered knee model. One particular direction would be to attempt to recreate the study of Healy et al. (5) with our deformed model to determine the effect of DFEO on hamstrings lengths during walking.

The imaging work is the least developed of the arms of this project and has the most potential to be expanded to gain insights. The goal of the project as it stands is to compare patients before and after DFEO + PTA and PTA only to typically developing children. The goal is primarily to help to validate our modeling predictions regarding knee motion and extension moment arms before and after surgery. However, with our rich set of images, there is much potential to expand the project. We will be able to directly compare bony and cartilage geometries to determine if surgery leads to changes in these structures. The images will also contain more accurate muscle volume measurements that we can use in the scaling of our models. With enough subject numbers, we may even begin to tease out effects of including rectus femoris transfer (6) along with the DFEO + PTA.

For the random forest, the comparisons to other institutions is still lacking in subject numbers. This summer, I will be traveling to Leuven, Belgium to begin to add subjects to this aim of the project. I also think that it would be beneficial to add surgical parameters to the list of predictors, such as pre- and post-operative Koshino indices, location and magnitude of the DFEO wedge, and perhaps even change in knee axis location. I would also like to look more into the predictors of patellar tendon advancement alone, to see if the milder crouch subjects (i.e. the ones that don't do well with DFEO + PTA) would be predicted to have a good outcome after PTA alone. Futher investigation into the predictors of improvements after hamstring lengthening, in order to determine what exactly predicts improvements

after that surgery, is also of interest. Whether similar predictors fall out with different split criteria or a different set of predictors are important will be important to determining the utility of making predictions for improvement with hamstring surgery, and may give important insights to surgeons regarding the procedure's usefulness (or not) and what changes to expect in walking ability after surgery. Given the number of patients receiving this procedure worldwide, I think the potential impact of this exploration is large.

Overall, this thesis has used several modalities to explore a gap in the understanding of crouch gait and its treatment. I am excited to use these tools in the future both to further explore these problems and the issues surrounding other gait and movement abnormalities in child with disabilities.

References

1. Andriacchi TP, Mündermann A, Smith RL, Alexander EJ, Dyrby CO, Koo S. A framework for the in vivo pathomechanics of osteoarthritis at the knee. Annals of Biomedical Engineering. 2004;32(3):447-57.

2. Hicks J, Arnold A, Anderson F, Schwartz M, Delp S. The effect of excessive tibial torsion on the capacity of muscles to extend the hip and knee during single-limb stance. Gait & Posture. 2007;26(4):546-52.

3. Schwartz M, Lakin G. The effect of tibial torsion on the dynamic function of the soleus during gait. Gait & Posture. 2003;17(2):113-8.

4. Lee TQ, Morris G, Csintalan RP. The influence of tibial and femoral rotation on patellofemoral contact area and pressure. Journal of Orthopaedic & Sports Physical Therapy. 2003;33(11):686-93.

5. Healy M, Schwartz M, Stout J, Gage J, Novacheck T. Is simultaneous hamstring lengthening necessary when performing distal femoral extension osteotomy and patellar tendon advancement? Gait and Posture. 2011;33(1):1-5.

6. Novacheck TF, Stout JL, Gage JR, Schwartz MH. Distal Femoral Extension Osteotomy and Patellar Tendon Advancement to Treat Persistent Crouch Gait in Cerebral Palsy: Surgical Technique. The Journal of Bone and Joint Surgery (American). 2009;91-A(Supplement 2):271-86.

Appendix A

Table of ligament element properties used in the knee model. (dMCL = deep medial collateral ligament; sMCL = superficial medial collateral ligament; pACL = posteriolateral anterior cruciate ligament; aACL = anteriomedial anterior cruciate ligament; aPCL = anteriolateral posterior cruciate ligament; pPCL = posteriomedial posterior cruciate ligament; LCL = lateral collateral ligament; PT = patellar tendon; LPFL = lateral patellofemoral ligament; MPFL = medial patellofemoral ligament; pmCAP = posteriomedial capsule; PFL = popliteofibular ligament; CAP = posterior capsule; ITB = iliotibial band)

Ligament Bundle	Element #	Stiffness (N)	Reference Strain (N/strain)
dMCL	1	500	0.04
dMCL	2	500	-0.04
dMCL	3	500	0
dMCL	4	500	0.04
dMCL	5	500	0.04
sMCL	1	500	0.04
sMCL	2	500	0.04
sMCL	3	500	0.05
sMCL	4	500	0.05
sMCL	5	500	0.05
sMCL	6	500	0.05
pACL	1	820	0.03
pACL	2	820	0.01
pACL	3	820	-0.05
pACL	4	820	-0.12
pACL	5	820	-0.02
pACL	6	820	-0.03
aACL	1	820	-0.14
aACL	2	820	-0.05
aACL	3	820	-0.08
aACL	4	820	-0.14
aACL	5	820	-0.14
aACL	6	820	-0.12
aPCL	1	900	0.03
aPCL	2	900	-0.1
aPCL	3	900	0.03
aPCL	4	900	-0.04
aPCL	5	900	-0.02
pPCL	1	300	-0.05
pPCL	2	300	-0.12

pPCL	3	300	-0.08
pPCL	4	300	-0.12
pPCL	5	300	-0.1
LCL	1	600	0.06
LCL	2	600	0.06
LCL	3	600	0.06
LCL	4	600	0.06
PT	1	3000	0.02
PT	2	3000	0.02
PT	3	3000	0
PT	4	3000	0.01
PT	5	3000	0
PT	6	3000	0.02
LPFL	1	150	0.01
LPFL	2	150	-0.1
LPFL	3	150	0.01
LPFL	4	150	-0.12
LPFL	5	150	0.01
LPFL	6	150	0.01
LPFL	7	150	-0.08
LPFL	8	150	-0.08
MPFL	1	150	-0.05
MPFL	2	150	0.01
MPFL	3	150	0.01
MPFL	4	150	-0.06
MPFL	5	150	-0.03
MPFL	6	150	0.01
pmCAP	1	500	0.05
pmCAP	2	500	0.05
pmCAP	3	500	0.02
pmCAP	4	500	-0.02
pmCAP	5	500	0.05
PFL	1	440	0.01
PFL	2	440	-0.12
PFL	3	440	-0.03
PFL	4	440	-0.14
PFL	5	440	-0.1
CAP	1	500	0.04
CAP	2	500	0.04
CAP	3	500	0.04
CAP	4	500	0.03
CAP	5	500	0.04
CAP	6	500	0.04
CAP	7	500	0.04
CAP	8	500	0.04

ITB	1	10000	0.02

Appendix B

Damping in Passive Joint Torque at Tibiofemoral and Patellofemoral Degrees of Freedom

Degree of Freedom:	η
Tibiofemoral Anterior Translation	100.0
Tibiofemoral Superior Translation	100.0
Tibiofemoral Lateral Translation	100.0
Tibiofemoral Flexion	0.1
Tibiofemoral Adduction	5.0
Tibiofemoral Rotation	5.0
Patellofemoral Anterior Translation	50.0
Patellofemoral Superior Translation	50.0
Patellofemoral Lateral Translation	50.0
Patellofemoral Flexion	0.2
Patellofemoral Rotation	10.0
Patellofemoral Tilt	10.0

Units are in N-s/m for the translational degrees of freedom and N-m-s/rad for the rotational degrees of freedom.

Appendix C

Knee Kinematics and Muscle and Ligament Forces Determined with Enhanced Static Optimization

(all are given for normal patellar position)

Abbreviations: TF = tibiofemoral, PF = patellofemoral, tx = anterior translation, ty = superior translation, tz = lateral translation, flex = flexion, add = adduction, rot = rotation

During Normal Walking

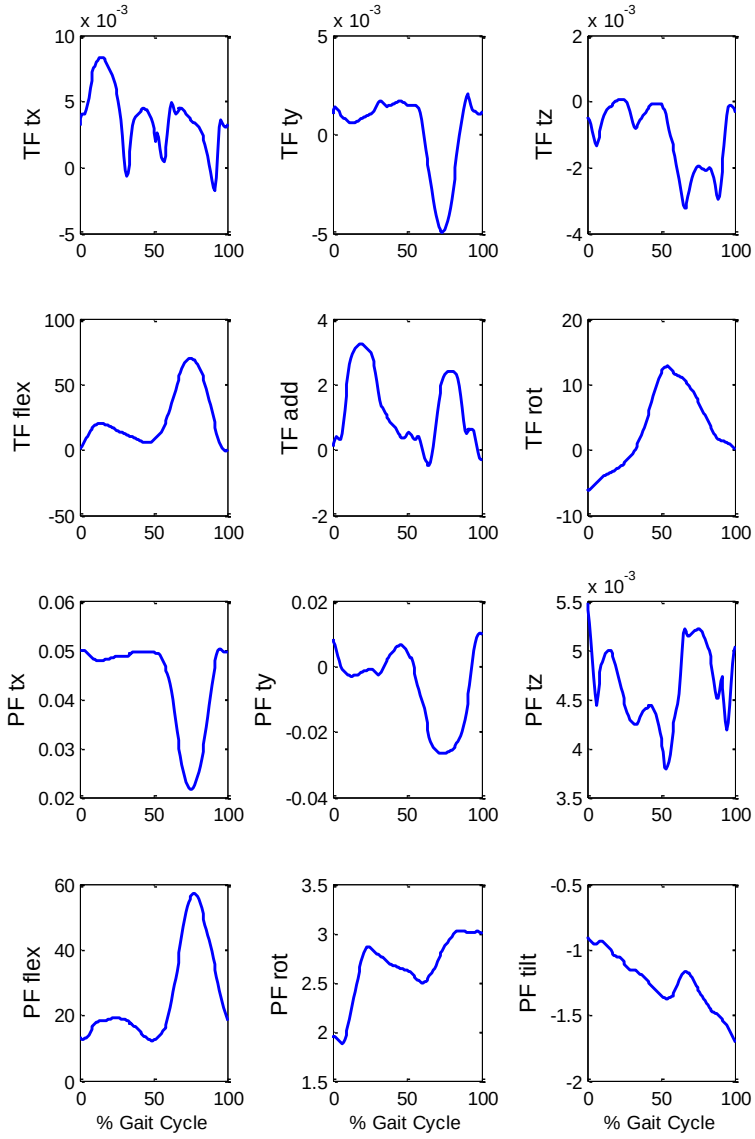

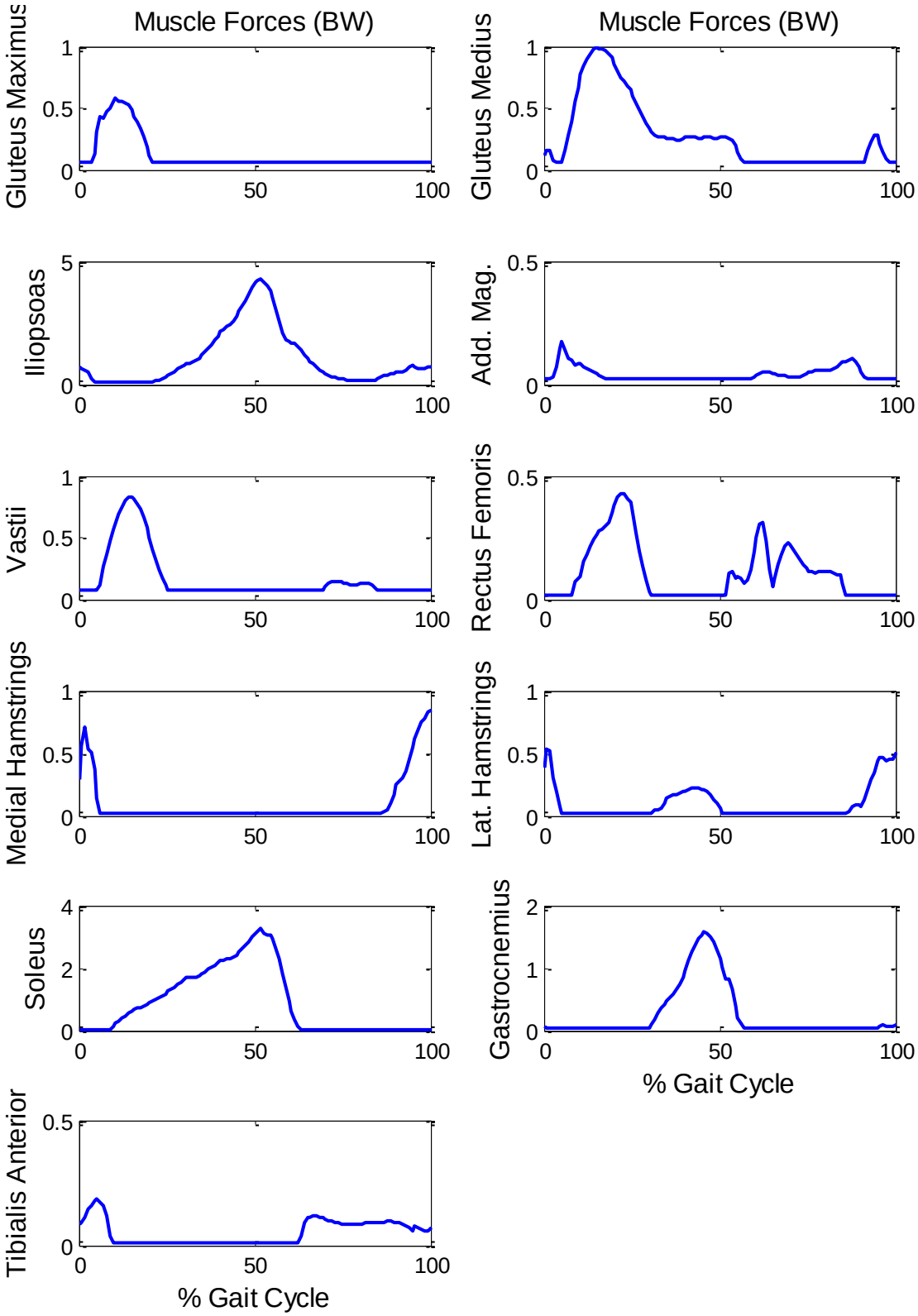
Muscle Forces (BW)
Gluteus Maximus
Muscle Forces (BW)
Gluteus Medius
Iliopsoas
Add. Mag.
Vastii
Rectus Femoris
Medial Hamstrings
Lat. Hamstrings
Soleus
Gastrocnemius
Tibialis Anterior
% Gait Cycle
% Gait Cycle

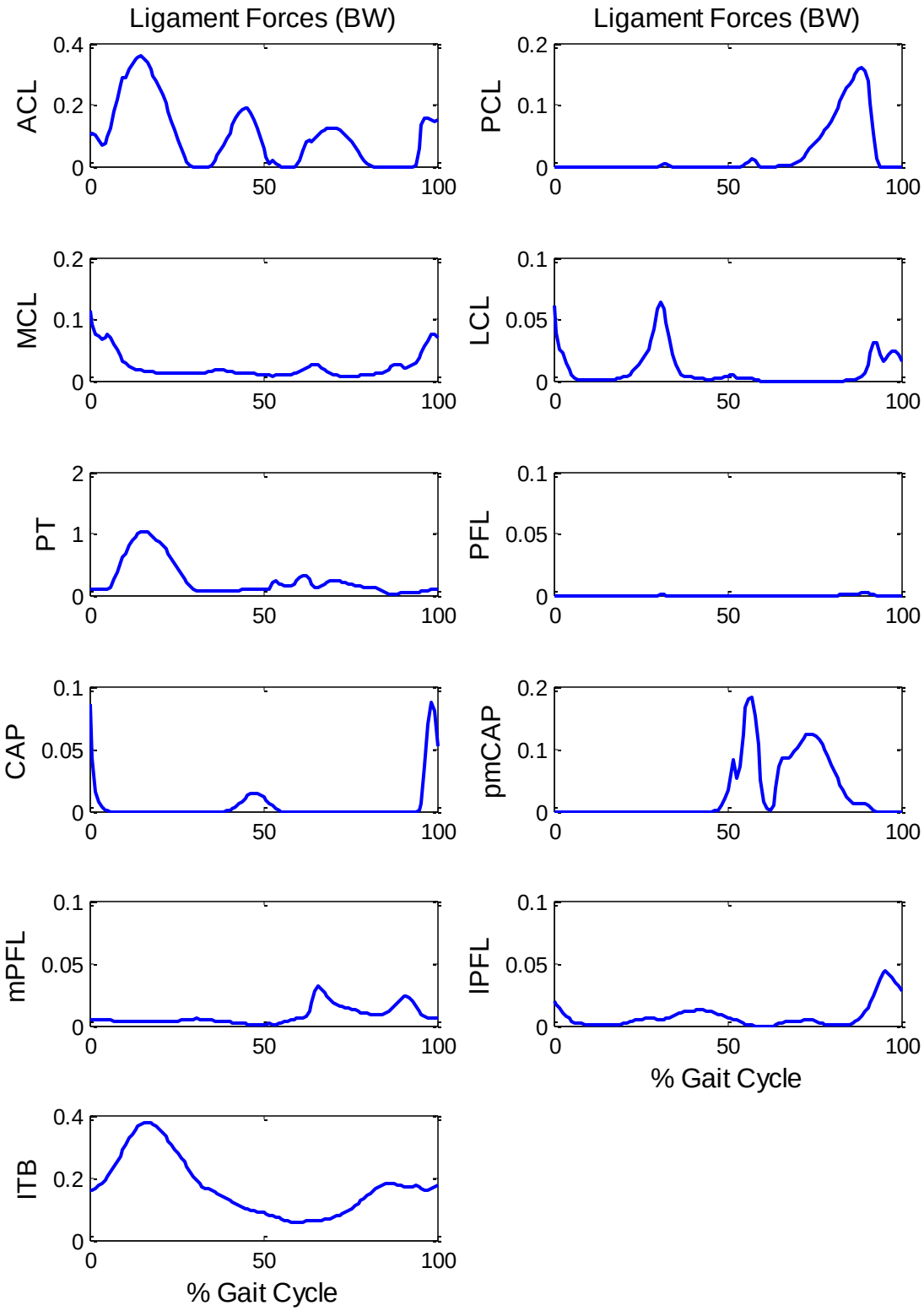
Ligament Forces (BW)
Ligament Forces (BW)
ACL
PCL
MCL
LCL
PT
PFL
CAP
pmCAP
mPFL
lPFL
ITB
% Gait Cycle
% Gait Cycle

Mild Crouch

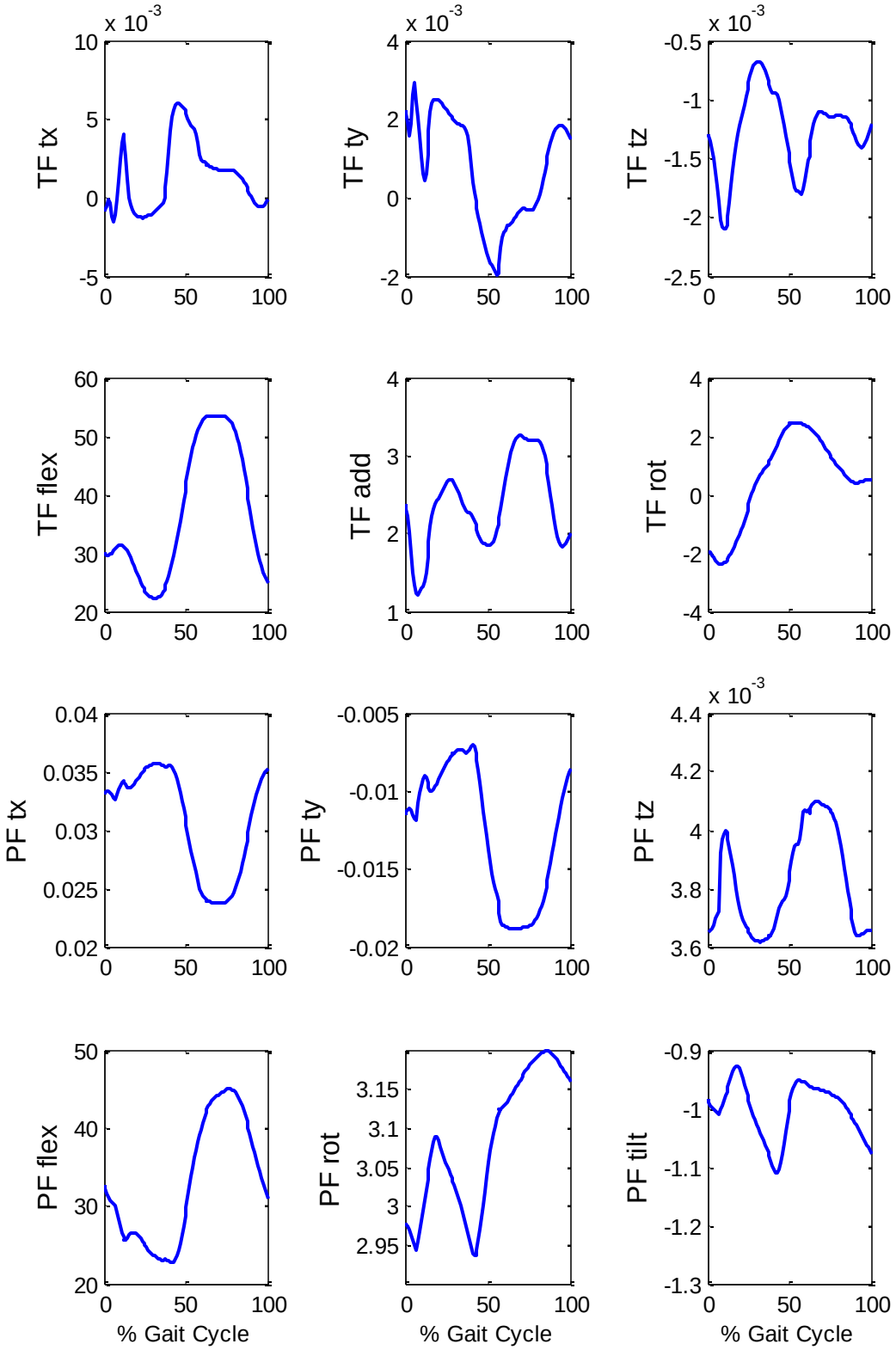
x 10^-3
TF tx
TF ty
TF tz
TF flex
TF add
TF rot
PF tx
PF ty
PF tz
PF flex
PF rot
PF tilt
% Gait Cycle

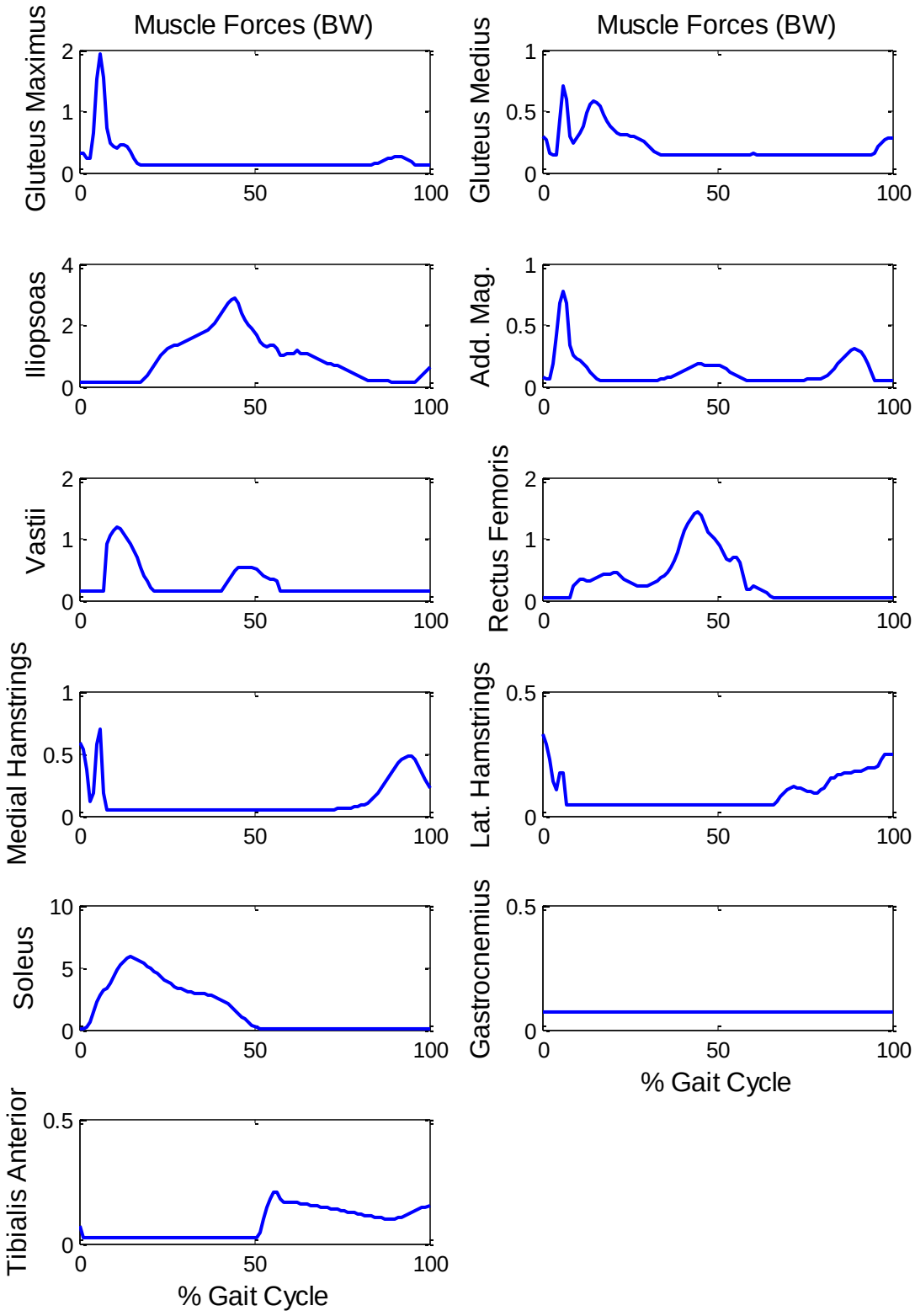
Muscle Forces (BW)
Gluteus Maximus
Gluteus Medius
Iliopsoas
Add. Mag.
Vastii
Rectus Femoris
Medial Hamstrings
Lat. Hamstrings
Soleus
Gastrocnemius
Tibialis Anterior
% Gait Cycle

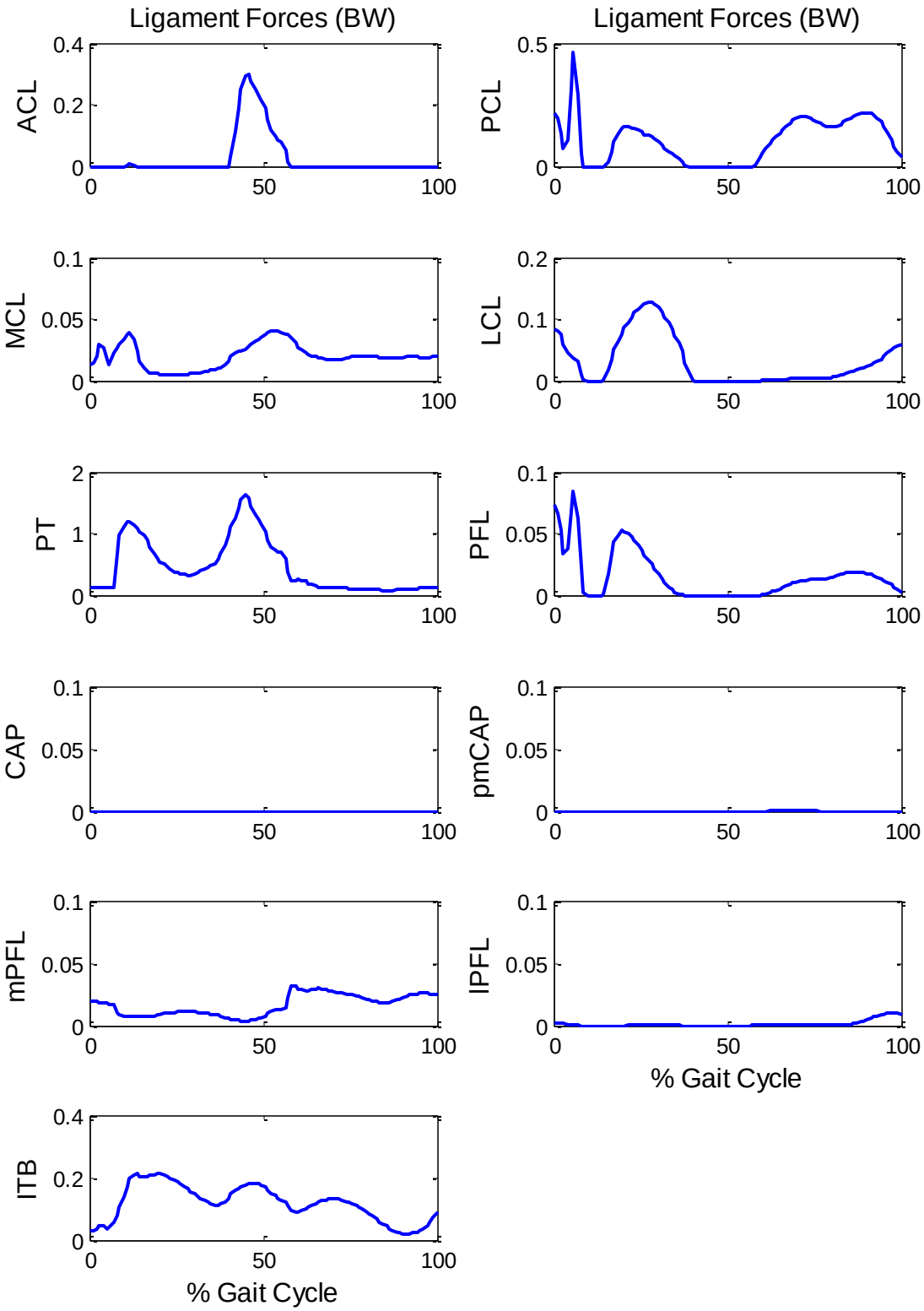
Ligament Forces (BW)
Ligament Forces (BW)
ACL
PCL
MCL
LCL
PT
PFL
CAP
pmCAP
mPFL
lPFL
ITB
% Gait Cycle
% Gait Cycle

Moderate Crouch

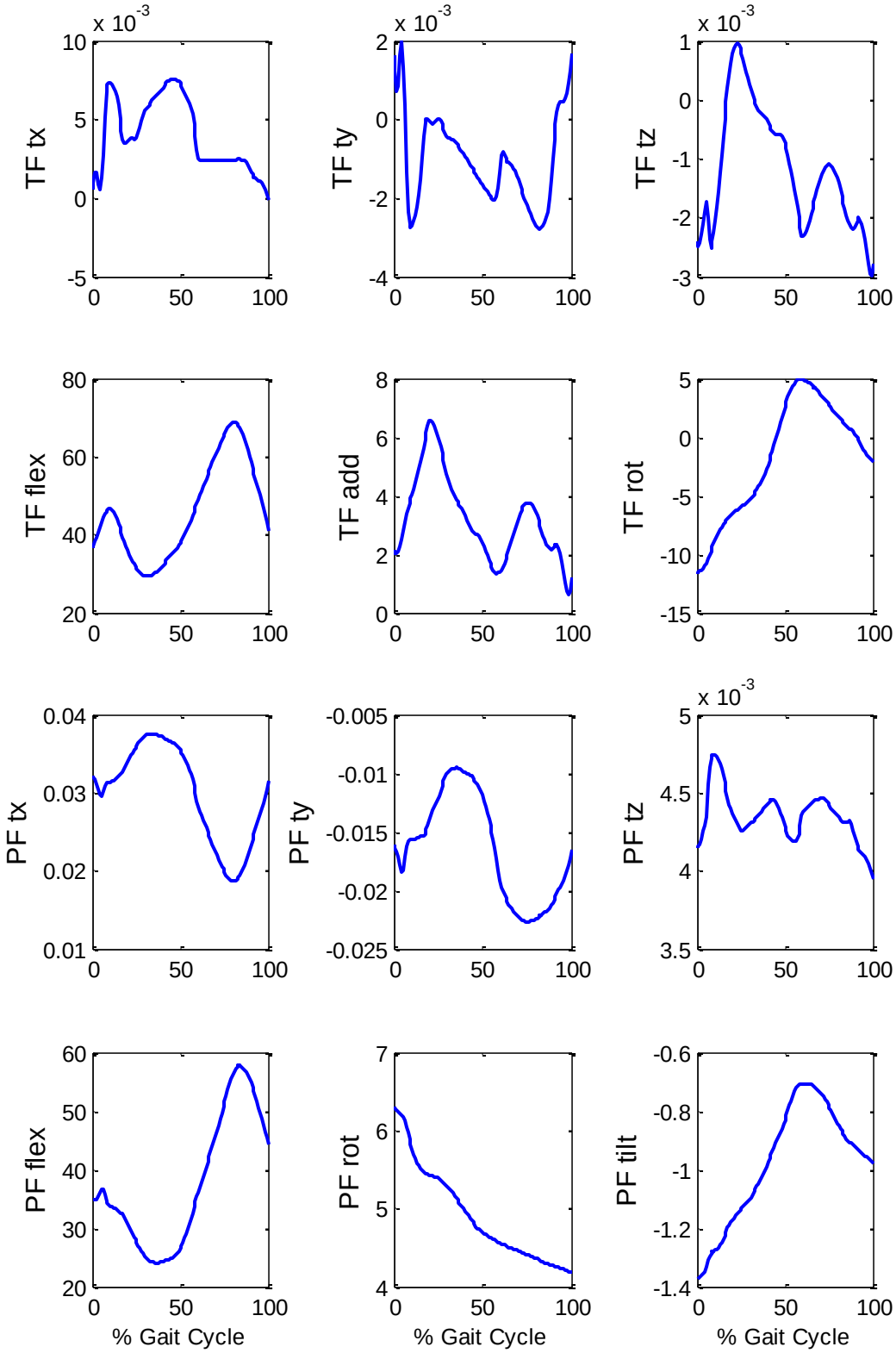

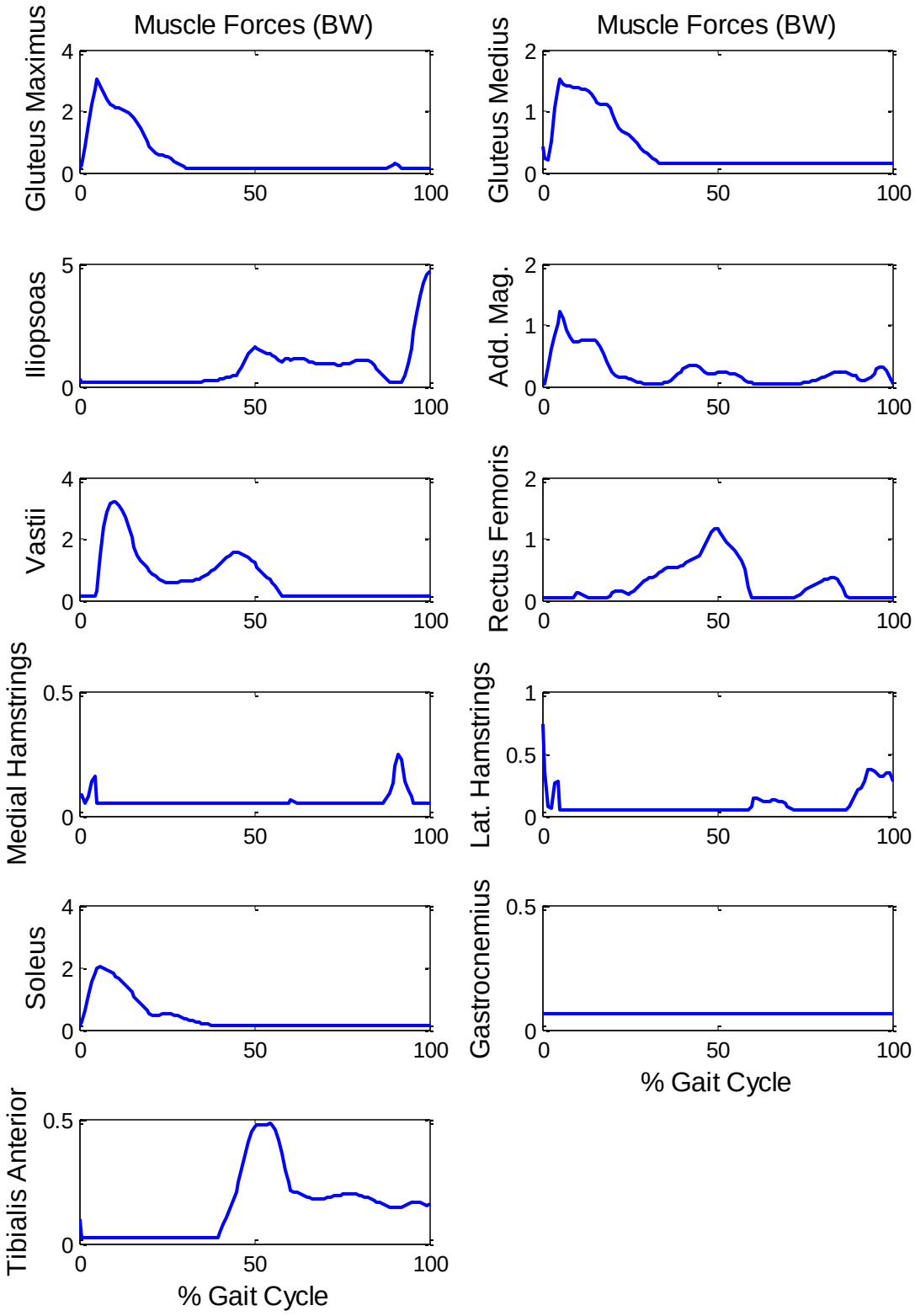
Muscle Forces (BW)
Gluteus Maximus
Muscle Forces (BW)
Gluteus Medius
Iliopsoas
Add. Mag.
Vastii
Rectus Femoris
Medial Hamstrings
Lat. Hamstrings
Soleus
Gastrocnemius
Tibialis Anterior
% Gait Cycle
% Gait Cycle

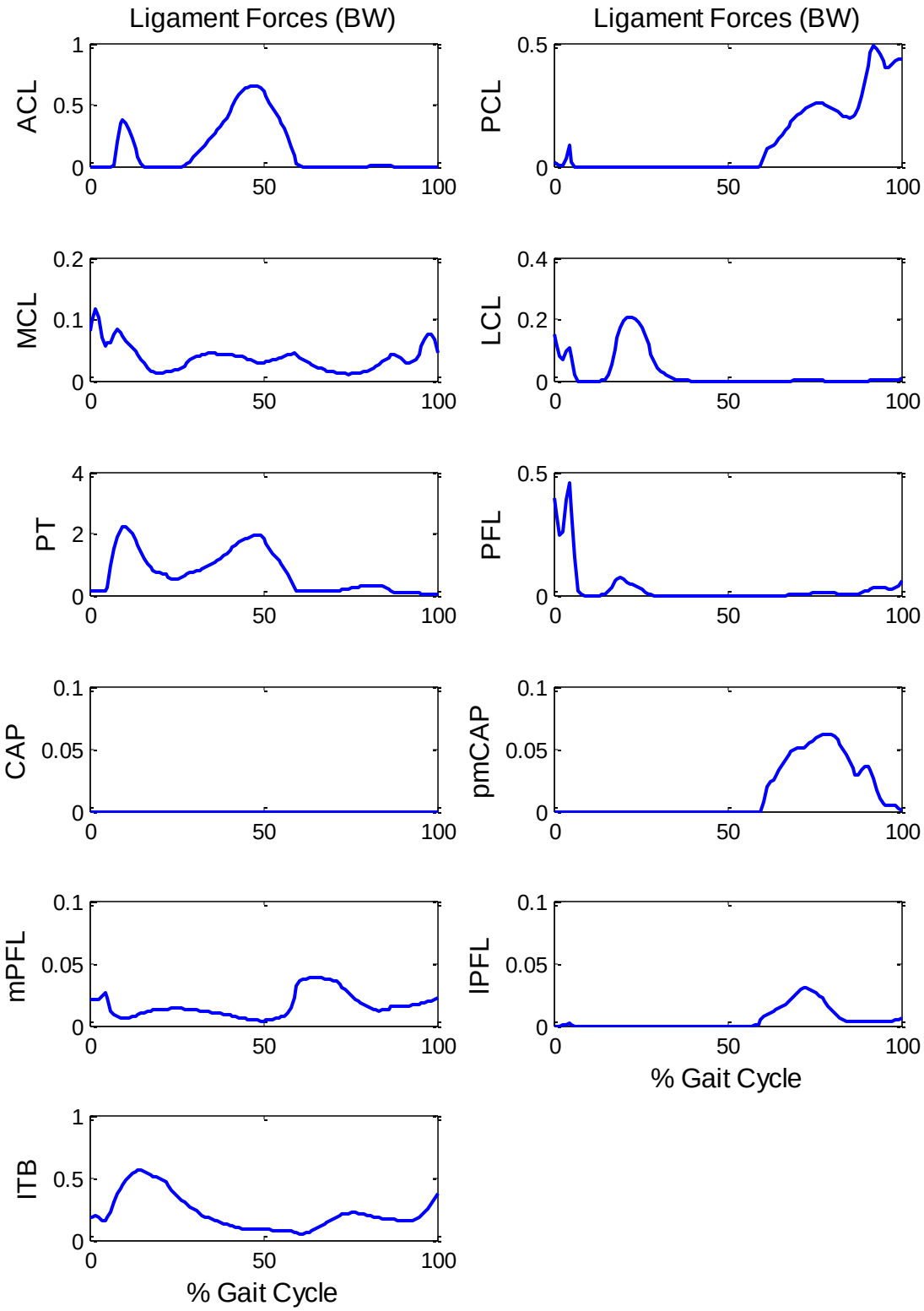
Ligament Forces (BW)
Ligament Forces (BW)
ACL
PCL
MCL
LCL
PT
PFL
CAP
pmCAP
mPFL
lPFL
ITB
% Gait Cycle
% Gait Cycle

Severe Crouch

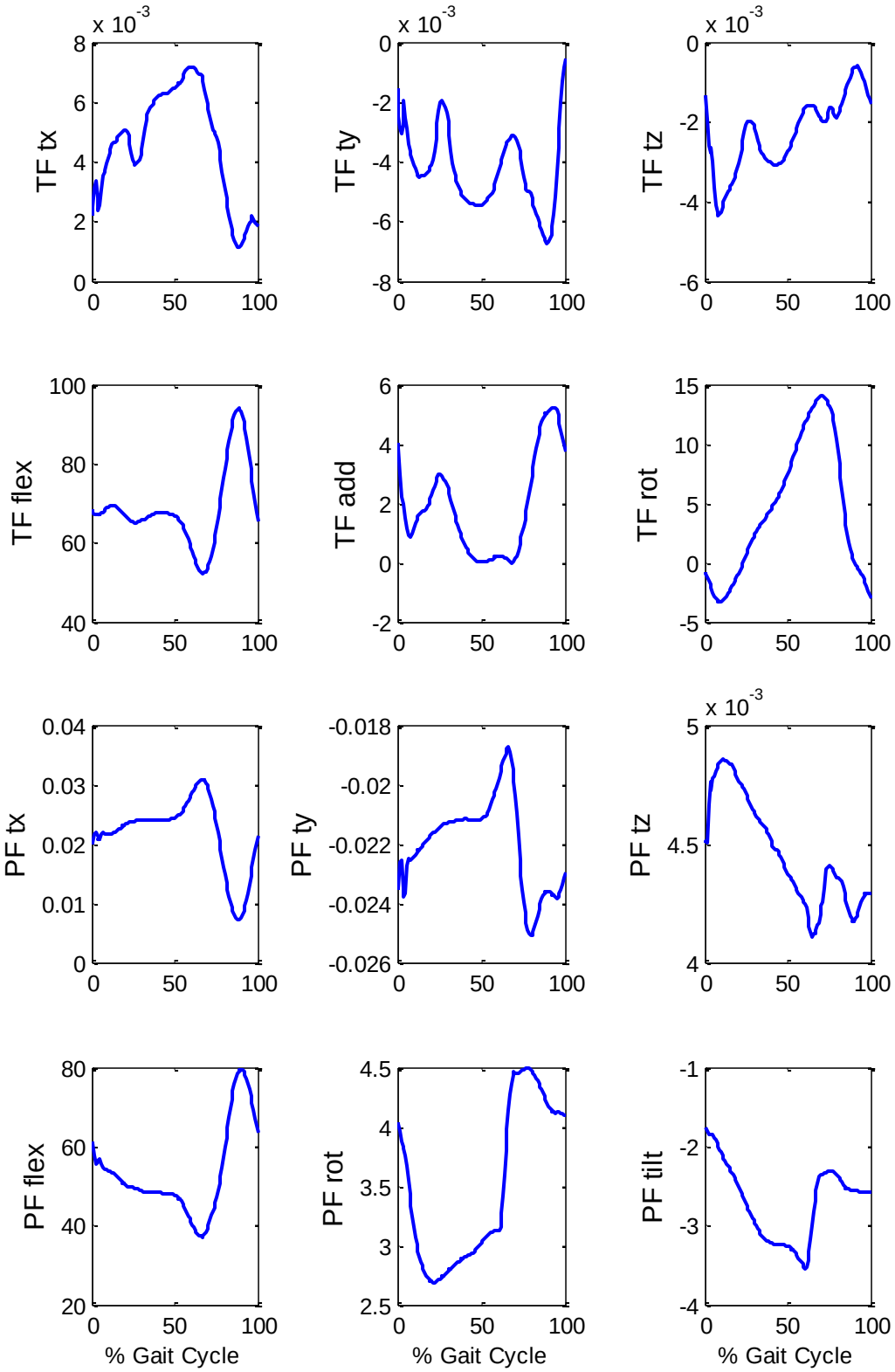

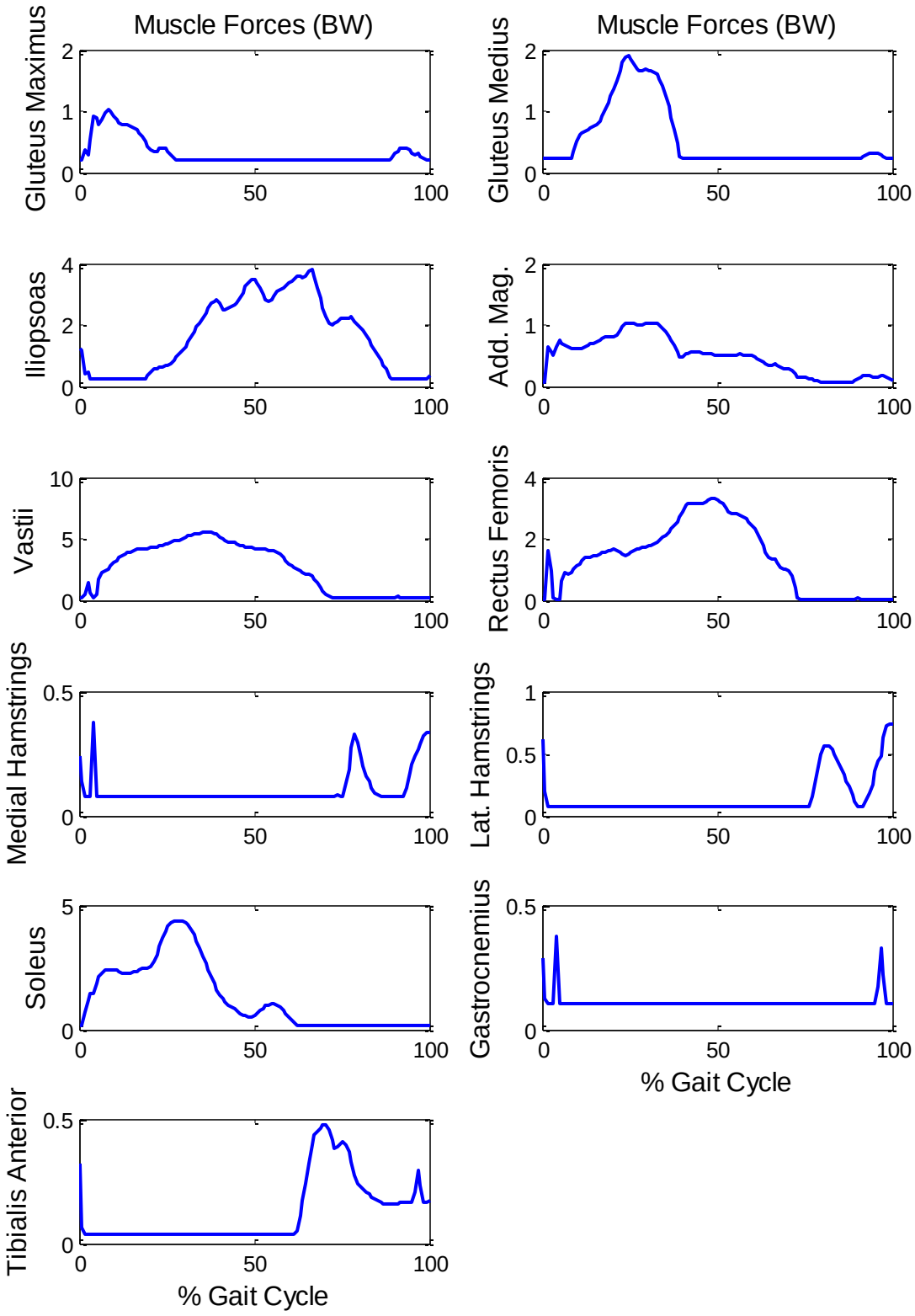
Muscle Forces (BW)
Gluteus Maximus
Gluteus Medius
Iliopsoas
Add. Mag.
Vastii
Rectus Femoris
Medial Hamstrings
Lat. Hamstrings
Soleus
Gastrocnemius
Tibialis Anterior
% Gait Cycle

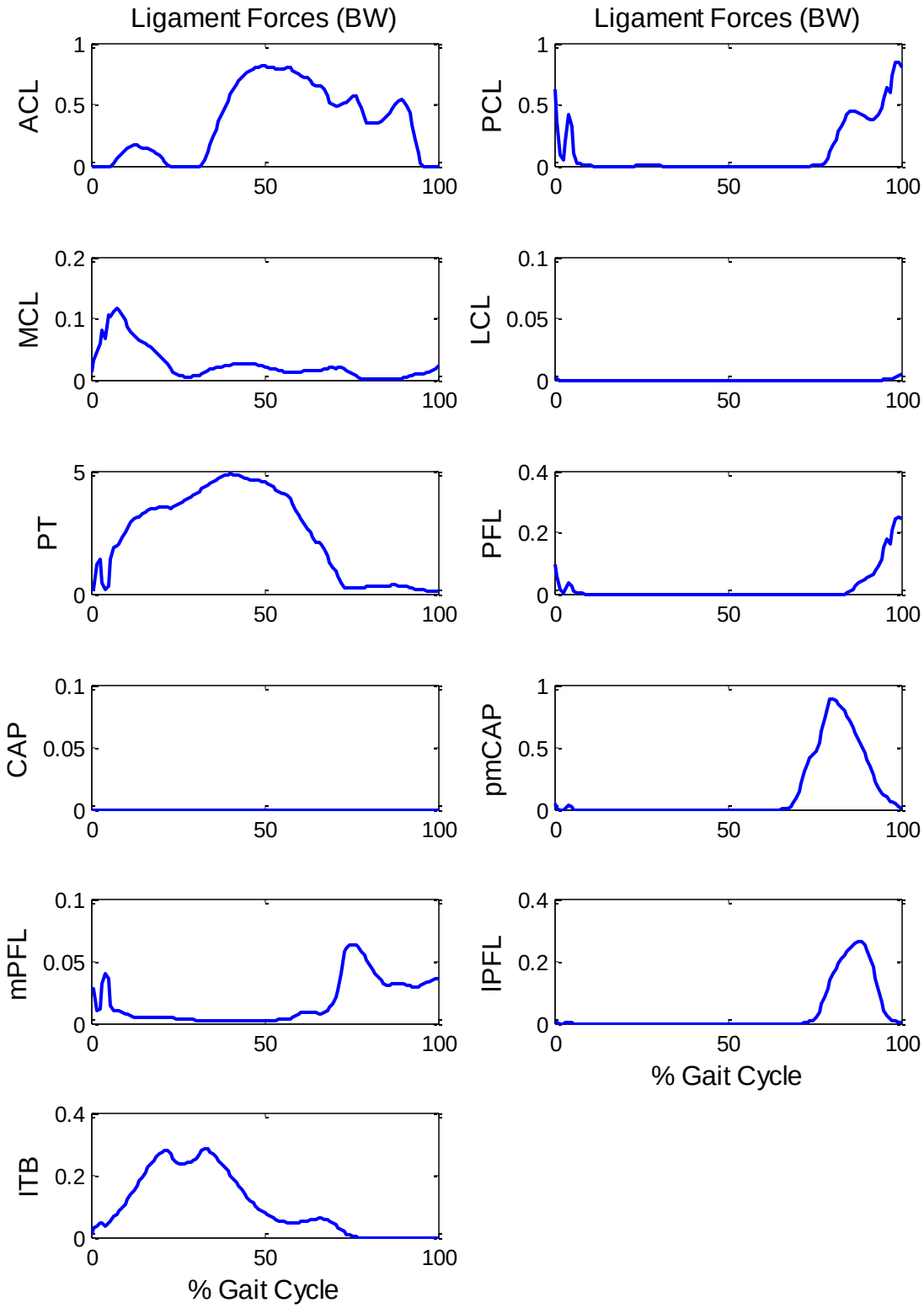
Ligament Forces (BW)
Ligament Forces (BW)
ACL
PCL
MCL
LCL
PT
PFL
CAP
pmCAP
mPFL
lPFL
ITB
% Gait Cycle
% Gait Cycle

Appendix D

Random Forest Potential Predictors

Abbreviations: c_= categorical variable, curr_ = current, t_ = time of, uppercase = from physical exam

Variables considered for inclusion:

'c_curr_SEMLSsurg'
'c_curr_SDRsurg'
'c_curr_Botox'
'c_curr_Baclofen'
'c_curr_NeuralOther'
'c_curr_ADDsurg'
'c_curr_FASoftsurg'
'c_curr_GASsurg'
'c_curr_Psoassurg'
'c_curr_Hamssurg'
'c_curr_RFXsurg'
'c_curr_SoftCombosurg'
'c_curr_SoftOthersurg'
'c_curr_SoftUnknownsurg'
'c_curr_FDOsurg'
'c_curr_TDOsurg'
'c_curr_FABonesurg'
'c_curr_LegLensurg'
'c_curr_Spinesurg'
'c_curr_BoneOthersurg'
'c_curr_BoneUnknownsurg'
'c_curr_CastShort'
'c_curr_CastLong'
'c_curr_CastUnknown'
'c_curr_ExploratorySurg'
'c_curr_HardwarePlacementSurg'
'c_curr_HardwareRemovalSurg'
'c_curr_UnknownSurg'
'c_curr_UpperExtremitySurg'
'c_curr_NoCurrentSurg'
'c_prior_HadPriorSurg'
'c_prior_SDR'
'c_prior_Botox'
'c_prior_Baclofen'
'c_prior_NeuralOther'
'c_prior_FDOsurg'
'c_prior_TDOsurg'
'c_prior_FABonesurg'
'c_prior_DFEOsurg'
'c_prior_FDODFEOsurg'
'c_prior_LegLensurg'
'c_prior_Spinesurg'
'c_prior_ADDsurg'
'c_prior_FASoftsurg'
'c_prior_GASsurg'
'c_prior_Psoassurg'
'c_prior_Hamssurg'
'c_prior_PTAsurg'
'c_prior_RFXsurg'
'c_prior_SoftCombosurg'
'c_prior_SoftOthersurg'
'c_prior_SoftUnknownsurg'
'c_prior_CastShort'
'c_prior_CastLong'
'c_prior_CastUnknown'
'c_prior_Exploratory'
'c_prior_HardwarePlacement'
'c_prior_HardwareRemoval'
'c_prior_Unknown'
'c_prior_UpperExtremity'
'age'
'leglenL'
'leglenR'
'faq'
'gmfcs'
'trialtype2'
'proctype'
'cadence'
'speed'
'steplen'
'strideT'
'footoff'
'oppfootoff'
'oppfootcontact'
'GDI_Pre'
'PHiDI_Pre'
'ABDOM_SEL'
'ABDOM_STR'
'ADDUCTOR_SPAS'
'AGE_AT_DIAG'
'AGE_FIRST_PT'
'ANKLE_DIAM'
'ANKLE_HEEL'
'ANKLE_HEIGHT'
'ANKLE_TOE'
'ANK_DORS_0'
'ANK_DORS_90'
'ANTEVERSION'
'ANT_TIB_SEL'
'ANT_TIB_STR'
'ASIS_ASIS_DIST'
'ASIS_GT_DIST'
'ASIS_GT_DISTL'
'BACK_EXT_SEL'
'BACK_EXT_STR'
'BIMAL'
'BIRTH_WEIGHT'
'DEV_FIRST_STEP'
'DEV_WALK'
'Delivery_ID'
'Delivery_Weeks'
'EXTEN_LAG'
'EXT_HALL_LONG_SEL'
'EXT_HALL_LONG_STR'
'FLEX_HALL_LONG_SEL'
'FLEX_HALL_LONG_STR'
'FOOT_WIDTH'
'HAMSTRING_SPAS'
'HIP_ABD_0'
'HIP_ABD_90'
'HIP_ABD_SEL'
'HIP_ABD_STR'
'HIP_ADD_SEL'
'HIP_ADD_STR'
'HIP_EXT_KN90_SEL'
'HIP_EXT_KN90_STR'
'HIP_EXT_ROT'
'HIP_EXT_SEL'
'HIP_EXT_STR'
'HIP_FLEX'
'HIP_FLEX_SEL'
'HIP_FLEX_SPAS'
'HIP_FLEX_STR'
'HIP_INT_ROT'
'KNEE_DIAM'

'KNEE_EXT'
'KNEE_EXT_SEL'
'KNEE_EXT_STR'
'KNEE_FLEX'
'KNEE_FLEX_SEL'
'KNEE_FLEX_STR'
'KNEE_FLEX_SUP'
'LEG_LENGTH'
'NICU_Weeks'
'NOTICED_PROB'
'NWB_ARCH'
'NWB_FOREFT2_SEVERITY'
'NWB_FOREFT_SEVERITY'
'NWB_HINDFT_SEVERITY'
'NetND_OXYcons'
'NetND_OXYcons_pctSMC'
'NetND_OXYcost'
'NetND_OXYcost_pctSMC'
'O2_ND_Restcons'
'O2_ND_Velocity'
'PERON_BREV_SEL'
'PERON_BREV_STR'
'PERON_LONG_SEL'
'PERON_LONG_STR'
'PLANFLEX_SPAS'
'PLANTFLEX_SEL'
'PLANTFLEX_STR'
'PLANT_FLEX'
'POP_ANG_BI'
'POP_ANG_UNI'
'POST_TIB_SEL'
'POST_TIB_SPAS'
'POST_TIB_STR'
'RECT_FEM_SPAS'
'SEC_TOE'
'TALKED_DOCTOR'
'THIGH_FOOT_ANGLE'
'THOMAS'
'Ventilator_Weeks'
'WB_4FTPOS2_SEVERITY'
'WB_4FTPOS_SEVERITY'
'WB_FTPOS_SEVERITY'
'c_ANKLE_CLONUS'
'c_AssistDev_L_begin'
'c_AssistDev_R_begin'
'c_BUN_DEF'
'c_CONFUSION'
'c_FIR_MTP_DF'
'c_INIT_AMB_DEV'
'c_LIGAM_LAXITY'
'c_MULT_BIRTH'
'c_NICU'
'c_NWB_FOREFT'
'c_NWB_FOREFT2'
'c_NWB_HINDFT'
'c_NWB_HIND_EVER'
'c_NWB_HIND_INVER'
'c_NWB_MID_MOT'
'c_NWB_SUBTAL_NEUT'
'c_OBER'
'c_PATELLA_ALTA'
'c_Side'
'c_VENTILATOR'
'c_WB_4FTPOS'
'c_WB_4FTPOS2'
'c_WB_FTPOS'
'c_WB_MIDFT_POS'
'NDspeed'
'foAnkDor'
'foFooPrg'
'foHipAdd'
'foHipFlx'
'foHipRot'
'foKneFlx'
'foKneRot'
'foKneVar'
'foPelObl'
'foPelRot'
'foPelTlt'
'icAnkDor'
'icFooPrg'
'icHipAdd'
'icHipFlx'
'icHipRot'
'icKneFlx'
'icKneRot'
'icKneVar'
'icPelObl'
'icPelRot'
'icPelTlt'
'maxAnkDor'
'maxFooPrg'
'maxHipAdd'
'maxHipFlx'
'maxHipRot'
'maxKneFlx'
'maxKneRot'
'maxKneVar'
'maxPelObl'
'maxPelRot'
'maxPelTlt'
'maxstaAnkDor'
'maxstaFooPrg'
'maxstaHipAdd'
'maxstaHipFlx'
'maxstaHipRot'
'maxstaKneFlx'
'maxstaKneRot'
'maxstaKneVar'
'maxstaPelObl'
'maxstaPelRot'
'maxstaPelTlt'
'maxswiAnkDor'
'maxswiFooPrg'
'maxswiHipAdd'
'maxswiHipFlx'
'maxswiHipRot'
'maxswiKneFlx'
'maxswiKneRot'
'maxswiKneVar'
'maxswiPelObl'
'maxswiPelRot'
'maxswiPelTlt'
'meanAnkDor'
'meanFooPrg'
'meanHipAdd'
'meanHipFlx'
'meanHipRot'
'meanKneFlx'
'meanKneRot'
'meanKneVar'
'meanPelObl'
'meanPelRot'
'meanPelTlt'
'meanstaAnkDor'
'meanstaFooPrg'
'meanstaHipAdd'
'meanstaHipFlx'
'meanstaHipRot'
'meanstaKneFlx'
'meanstaKneRot'
'meanstaKneVar'
'meanstaPelObl'
'meanstaPelRot'
'meanstaPelTlt'
'meanswiAnkDor'
'meanswiFooPrg'
'meanswiHipAdd'
'meanswiHipFlx'
'meanswiHipRot'

'meanswiKneFlx'
'meanswiKneRot'
'meanswiKneVar'
'meanswiPelObl'
'meanswiPelRot'
'meanswiPelTlt'
'minAnkDor'
'minFooPrg'
'minHipAdd'
'minHipFlx'
'minHipRot'
'minKneFlx'
'minKneRot'
'minKneVar'
'minPelObl'
'minPelRot'
'minPelTlt'
'minstaAnkDor'
'minstaFooPrg'
'minstaHipAdd'
'minstaHipFlx'
'minstaHipRot'
'minstaKneFlx'
'minstaKneRot'
'minstaKneVar'
'minstaPelObl'
'minstaPelRot'
'minstaPelTlt'
'minswiAnkDor'
'minswiFooPrg'
'minswiHipAdd'
'minswiHipFlx'
'minswiHipRot'
'minswiKneFlx'
'minswiKneRot'
'minswiKneVar'
'minswiPelObl'
'minswiPelRot'
'minswiPelTlt'
'romAnkDor'
'romFooPrg'
'romHipAdd'
'romHipFlx'
'romHipRot'
'romKneFlx'
'romKneRot'
'romKneVar'
'romPelObl'
'romPelRot'
'romPelTlt'
'romstaAnkDor'
'romstaFooPrg'
'romstaHipAdd'
'romstaHipFlx'
'romstaHipRot'
'romstaKneFlx'
'romstaKneRot'
'romstaKneVar'
'romstaPelObl'
'romstaPelRot'
'romstaPelTlt'
'romswiAnkDor'
'romswiFooPrg'
'romswiHipAdd'
'romswiHipFlx'
'romswiHipRot'
'romswiKneFlx'
'romswiKneRot'
'romswiKneVar'
'romswiPelObl'
'romswiPelRot'
'romswiPelTlt'
't_maxAnkDor'
't_maxFooPrg'
't_maxHipAdd'
't_maxHipFlx'
't_maxHipRot'
't_maxKneFlx'
't_maxKneRot'
't_maxKneVar'
't_maxPelObl'
't_maxPelRot'
't_maxPelTlt'
't_maxstaAnkDor'
't_maxstaFooPrg'
't_maxstaHipAdd'
't_maxstaHipFlx'
't_maxstaHipRot'
't_maxstaKneFlx'
't_maxstaKneRot'
't_maxstaKneVar'
't_maxstaPelObl'
't_maxstaPelRot'
't_maxstaPelTlt'
't_maxswiAnkDor'
't_maxswiFooPrg'
't_maxswiHipAdd'
't_maxswiHipFlx'
't_maxswiHipRot'
't_maxswiKneFlx'
't_maxswiKneRot'
't_maxswiKneVar'
't_maxswiPelObl'
't_maxswiPelRot'
't_maxswiPelTlt'
't_minAnkDor'
't_minFooPrg'
't_minHipAdd'
't_minHipFlx'
't_minHipRot'
't_minKneFlx'
't_minKneRot'
't_minKneVar'
't_minPelObl'
't_minPelRot'
't_minPelTlt'
't_minstaAnkDor'
't_minstaFooPrg'
't_minstaHipAdd'
't_minstaHipFlx'
't_minstaHipRot'
't_minstaKneFlx'
't_minstaKneRot'
't_minstaKneVar'
't_minstaPelObl'
't_minstaPelRot'
't_minstaPelTlt'
't_minswiAnkDor'
't_minswiFooPrg'
't_minswiHipAdd'
't_minswiHipFlx'
't_minswiHipRot'
't_minswiKneFlx'
't_minswiKneRot'
't_minswiKneVar'
't_minswiPelObl'
't_minswiPelRot'
't_minswiPelTlt'
'device'
'deviceYN'
'BMI'

Variables included at initial stage due to having less than or equal to 5% missing data:
'c_curr_SEMLSsurg'
'c_curr_SDRsurg'
'c_curr_Botox'
'c_curr_Baclofen'
'c_curr_NeuralOther'
'c_curr_ADDsurg'
'c_curr_FASoftsurg'

'c_curr_GASsurg'
'c_curr_Psoassurg'
'c_curr_Hamssurg'
'c_curr_RFXsurg'
'c_curr_SoftCombosurg'
'c_curr_SoftOthersurg'
'c_curr_SoftUnknownsurg'
'c_curr_FDOsurg'
'c_curr_TDOsurg'
'c_curr_FABonesurg'
'c_curr_LegLensurg'
'c_curr_Spinesurg'
'c_curr_BoneOthersurg'
'c_curr_BoneUnknownsurg'
'c_curr_CastShort'
'c_curr_CastLong'
'c_curr_CastUnknown'
'c_curr_ExploratorySurg'
'c_curr_HardwarePlacementSurg'
'c_curr_HardwareRemovalSurg'
'c_curr_UnknownSurg'
'c_curr_UpperExtremitySurg'
'c_curr_NoCurrentSurg'
'c_prior_HadPriorSurg'
'c_prior_SDR'
'c_prior_Botox'
'c_prior_Baclofen'
'c_prior_NeuralOther'
'c_prior_FDOsurg'
'c_prior_TDOsurg'
'c_prior_FABonesurg'
'c_prior_DFEOsurg'
'c_prior_FDODFEOsurg'
'c_prior_LegLensurg'
'c_prior_Spinesurg'
'c_prior_ADDsurg'
'c_prior_FASoftsurg'
'c_prior_GASsurg'
'c_prior_Psoassurg'
'c_prior_Hamssurg'
'c_prior_PTAsurg'
'c_prior_RFXsurg'
'c_prior_SoftCombosurg'
'c_prior_SoftOthersurg'
'c_prior_SoftUnknownsurg'
'c_prior_CastShort'
'c_prior_CastLong'
'c_prior_CastUnknown'
'c_prior_Exploratory'
'c_prior_HardwarePlacement'
'c_prior_HardwareRemoval'
'c_prior_Unknown'
'c_prior_UpperExtremity'
'age'
'leglenL'
'leglenR'
'cadence'
'speed'
'steplen'
'strideT'
'footoff'
'oppfootoff'
'oppfootcontact'
'GDI_Pre'
'PHiDI_Pre'
'ADDUCTOR_SPAS'
'ANKLE_DIAM'
'ANK_DORS_0'
'ANK_DORS_90'
'ANTEVERSION'
'ASIS_ASIS_DIST'
'ASIS_GT_DIST'
'Delivery_ID'
'Delivery_Weeks'
'HAMSTRING_SPAS'
'HIP_ABD_0'
'HIP_ABD_90'
'HIP_EXT_ROT'
'HIP_FLEX'
'HIP_FLEX_SPAS'
'HIP_INT_ROT'
'KNEE_DIAM'
'KNEE_EXT'
'KNEE_FLEX'
'NWB_FOREFT_SEVERITY'
'NWB_HINDFT_SEVERITY'
'PLANFLEX_SPAS'
'PLANT_FLEX'
'POP_ANG_BI'
'POP_ANG_UNI'
'POST_TIB_SPAS'
'RECT_FEM_SPAS'
'THIGH_FOOT_ANGLE'
'WB_4FTPOS_SEVERITY'
'WB_FTPOS_SEVERITY'
'c_ANKLE_CLONUS'
'c_AssistDev_L_begin'
'c_AssistDev_R_begin'
'c_BUN_DEF'
'c_CONFUSION'
'c_INIT_AMB_DEV'
'c_LIGAM_LAXITY'
'c_MULT_BIRTH'
'c_NWB_FOREFT'
'c_NWB_HINDFT'
'c_Side'
'NDspeed'
'foAnkDor'
'foFooPrg'
'foHipAdd'
'foHipFlx'
'foHipRot'
'foKneFlx'
'foKneRot'
'foKneVar'
'foPelObl'
'foPelRot'
'foPelTlt'
'icAnkDor'
'icFooPrg'
'icHipAdd'
'icHipFlx'
'icHipRot'
'icKneFlx'
'icKneRot'
'icKneVar'
'icPelObl'
'icPelRot'
'icPelTlt'
'maxAnkDor'
'maxFooPrg'
'maxHipAdd'
'maxHipFlx'
'maxHipRot'
'maxKneFlx'
'maxKneRot'
'maxKneVar'
'maxPelObl'
'maxPelRot'
'maxPelTlt'
'maxstaAnkDor'
'maxstaFooPrg'
'maxstaHipAdd'
'maxstaHipFlx'
'maxstaHipRot'
'maxstaKneFlx'
'maxstaKneRot'
'maxstaKneVar'
'maxstaPelObl'

'maxstaPelRot'
'maxstaPelTlt'
'maxswiAnkDor'
'maxswiFooPrg'
'maxswiHipAdd'
'maxswiHipFlx'
'maxswiHipRot'
'maxswiKneFlx'
'maxswiKneRot'
'maxswiKneVar'
'maxswiPelObl'
'maxswiPelRot'
'maxswiPelTlt'
'meanAnkDor'
'meanFooPrg'
'meanHipAdd'
'meanHipFlx'
'meanHipRot'
'meanKneFlx'
'meanKneRot'
'meanKneVar'
'meanPelObl'
'meanPelRot'
'meanPelTlt'
'meanstaAnkDor'
'meanstaFooPrg'
'meanstaHipAdd'
'meanstaHipFlx'
'meanstaHipRot'
'meanstaKneFlx'
'meanstaKneRot'
'meanstaKneVar'
'meanstaPelObl'
'meanstaPelRot'
'meanstaPelTlt'
'meanswiAnkDor'
'meanswiFooPrg'
'meanswiHipAdd'
'meanswiHipFlx'
'meanswiHipRot'
'meanswiKneFlx'
'meanswiKneRot'
'meanswiKneVar'
'meanswiPelObl'
'meanswiPelRot'
'meanswiPelTlt'
'minAnkDor'
'minFooPrg'
'minHipAdd'
'minHipFlx'
'minHipRot'
'minKneFlx'
'minKneRot'
'minKneVar'
'minPelObl'
'minPelRot'
'minPelTlt'
'minstaAnkDor'
'minstaFooPrg'
'minstaHipAdd'
'minstaHipFlx'
'minstaHipRot'
'minstaKneFlx'
'minstaKneRot'
'minstaKneVar'
'minstaPelObl'
'minstaPelRot'
'minstaPelTlt'
'minswiAnkDor'
'minswiFooPrg'
'minswiHipAdd'
'minswiHipFlx'
'minswiHipRot'
'minswiKneFlx'
'minswiKneRot'
'minswiKneVar'
'minswiPelObl'
'minswiPelRot'
'minswiPelTlt'
'romAnkDor'
'romFooPrg'
'romHipAdd'
'romHipFlx'
'romHipRot'
'romKneFlx'
'romKneRot'
'romKneVar'
'romPelObl'
'romPelRot'
'romPelTlt'
'romstaAnkDor'
'romstaFooPrg'
'romstaHipAdd'
'romstaHipFlx'
'romstaHipRot'
'romstaKneFlx'
'romstaKneRot'
'romstaKneVar'
'romstaPelObl'
'romstaPelRot'
'romstaPelTlt'
'romswiAnkDor'
'romswiFooPrg'
'romswiHipAdd'
'romswiHipFlx'
'romswiHipRot'
'romswiKneFlx'
'romswiKneRot'
'romswiKneVar'
'romswiPelObl'
'romswiPelRot'
'romswiPelTlt'
't_maxAnkDor'
't_maxFooPrg'
't_maxHipAdd'
't_maxHipFlx'
't_maxHipRot'
't_maxKneFlx'
't_maxKneRot'
't_maxKneVar'
't_maxPelObl'
't_maxPelRot'
't_maxPelTlt'
't_maxstaAnkDor'
't_maxstaFooPrg'
't_maxstaHipAdd'
't_maxstaHipFlx'
't_maxstaHipRot'
't_maxstaKneFlx'
't_maxstaKneRot'
't_maxstaKneVar'
't_maxstaPelObl'
't_maxstaPelRot'
't_maxstaPelTlt'
't_maxswiAnkDor'
't_maxswiFooPrg'
't_maxswiHipAdd'
't_maxswiHipFlx'
't_maxswiHipRot'
't_maxswiKneFlx'
't_maxswiKneRot'
't_maxswiKneVar'
't_maxswiPelObl'
't_maxswiPelRot'
't_maxswiPelTlt'
't_minAnkDor'
't_minFooPrg'
't_minHipAdd'
't_minHipFlx'
't_minHipRot'
't_minKneFlx'
't_minKneRot'
't_minKneVar'

't_minPelObl'
't_minPelRot'
't_minPelTlt'
't_minstaAnkDor'
't_minstaFooPrg'
't_minstaHipAdd'
't_minstaHipFlx'
't_minstaHipRot'
't_minstaKneFlx'
't_minstaKneRot'
't_minstaKneVar'
't_minstaPelObl'
't_minstaPelRot'
't_minstaPelTlt'
't_minswiAnkDor'
't_minswiFooPrg'
't_minswiHipAdd'
't_minswiHipFlx'
't_minswiHipRot'
't_minswiKneFlx'
't_minswiKneRot'
't_minswiKneVar'
't_minswiPelObl'
't_minswiPelRot'
't_minswiPelTlt'
'device'
'deviceYN'
'BMI'